USGS
science for a changing world

Prepared in cooperation with the Santa Barbara County Water Agency

Geology, Water-Quality, Hydrology, and Geomechanics of the Cuyama Valley Groundwater Basin, California, 2008–12

Scientific Investigations Report 2013–5108

U.S. Department of the Interior
U.S. Geological Survey

Cover. View of the Caliente Range, Cuyama Valley area, Santa Barbara and San Luis Obispo Counties, California. (Photography by Joseph Nawikas, U.S. Geological Survey.)

Geology, Water-Quality, Hydrology, and Geomechanics of the Cuyama Valley Groundwater Basin, California, 2008–12

By Rhett R. Everett, Dennis R. Gibbs, Randall T. Hanson, Donald S. Sweetkind, Justin T. Brandt, Sarah E. Falk, and Christopher R. Harich

Prepared in Cooperation with the Santa Barbara County Water Agency

Scientific Investigations Report 2013–5108

U.S. Department of the Interior
U.S. Geological Survey

U.S. Department of the Interior
SALLY JEWELL, Secretary

U.S. Geological Survey
Suzette M. Kimball, Acting Director

U.S. Geological Survey, Reston, Virginia: 2013

Suggested citation:
Everett, R.R., Gibbs, D.R., Hanson, R.T., Sweetkind, D.S., Brandt, J.T., Falk, S.E. and Harich, C.R., 2013, Geology, water-quality, hydrology, and geomechanics of the Cuyama Valley groundwater basin, California, 2008–12: U.S. Geological Survey Scientific Investigations Report 2013–5108, 62 p.

Contents

Figures

Tables

Conversion Factors, Datums, and Abbreviated Water-Quality Units

Inch/Pound to SI

Multiply	By	To obtain
	Length	
inch (in)	2.54	centimeter (cm)
foot (ft)	0.3048	meter (m)
mile (mi)	1.609	kilometer (km)
yard (yd)	0.9144	meter (m)
	Area	
acre	4,047	square meter (m^2)
square foot (ft^2)	0.09290	square meter (m^2)
square mile (mi^2)	2.590	square kilometer (km^2)
	Volume	
ounce, fluid (fl. oz)	0.02957	liter (L)
gallon (gal)	3.785	liter (L)
cubic inch (in^3)	16.39	cubic centimeter (cm^3)
cubic foot (ft^3)	0.02832	cubic meter (m^3)
acre-foot (acre-ft)	1,233	cubic meter (m^3)
	Flow rate	
acre-foot per day (acre-ft/d)	0.01427	cubic meter per second (m^3/s)
acre-foot per year (acre-ft/yr)	1,233	cubic meter per year (m^3/yr)
foot per second (ft/s)	0.3048	meter per second (m/s)
foot per minute (ft/min)	0.3048	meter per minute (m/min)
cubic foot per second (ft^3/s)	0.02832	cubic meter per second (m^3/s)
gallon per minute (gal/min)	0.06309	liter per second (L/s)
	Radioactivity	
picocurie per liter (pCi/L)	0.037	becquerel per liter (Bq/L)
	Specific capacity	
gallon per minute per foot [(gal/min)/ft)]	0.2070	liter per second per meter [(L/s)/m]
	Hydraulic conductivity	
foot per day (ft/d)	0.3048	meter per day (m/d)
	Hydraulic gradient	
foot per mile (ft/mi)	0.1894	meter per kilometer (m/km)
	Transmissivity*	
foot squared per day (ft^2/d)	0.09290	meter squared per day (m^2/d)

Temperature in degrees Celsius (°C) may be converted to degrees Fahrenheit (°F) as follows:

°F=(1.8×°C)+32

Temperature in degrees Fahrenheit (°F) may be converted to degrees Celsius (°C) as follows:

°C=(°F-32)/1.8

Vertical coordinate information is referenced to the North American Vertical Datum of 1988 (NAVD 88).

Horizontal coordinate information is referenced to the North American Datum of 1983 (NAD 83).

Altitude, as used in this report, refers to distance above the vertical datum.

Water-level measurements in this report are given in feet with reference to land-surface datum (lsd). Land-surface datum is a datum plane that is approximately at land surface at each well.

*Transmissivity: The standard unit for transmissivity is cubic foot per day per square foot times foot of aquifer thickness [(ft^3/d)/ft^2]ft. In this report, the mathematically reduced form, foot squared per day (ft^2/d), is used for convenience.

Specific conductance is given in microsiemens per centimeter at 25 degrees Celsius (µS/cm at 25 °C).

Concentrations of chemical constituents in water are given either in milligrams per liter (mg/L) or micrograms per liter (µg/L) which are equivalent to parts per million (ppm) or parts per billion (ppb), respectively.

Activities of radiochemical constituents in water are given in picocuries per liter (pCi/L).

Results for stable isotopes in water are reported in delta notation , *iE*, where the ratio of the rarer isotope of an element (*iE*) is expressed relative to the more common lighter isotope of that element, relative to a standard reference material, and expressed in *per mil*.

Abbreviations and Acronyms

bls	below land surface
CSU	combined standard uncertainty
CUY	Cuyama Valley study well
CVBR	Cuyama Valley Bell Road
CVFR	Cuyama Valley Foothill Road
CVKR	Cuyama Valley Kirschenmann Road
GPS	Global Positioning System
MCL	maximum contaminant level
MCL-US	maximum contaminant level (USEPA)
LSD	land surface datum
NWIS	National Water Information System (USGS)
OEHHA-PHG	Office of Environmental Health Hazard Assessment public health goal
SMCL	secondary maximum contaminant level
SMCL-CA	California Department of Public Health secondary maximum contaminant level
SMCL-US	secondary maximum contaminant level (USEPA)
U.S.	United States
USEPA	United States Environmental Protection Agency
USGS	United States Geological Survey

Acknowledgements

This study could not have been accomplished without the assistance of personnel from the Santa Barbara County Water Agency. In addition, we acknowledge the valuable participation of the residents and well owners of the Cuyama Valley who assisted in the study.

Finally, we acknowledge the valuable guidance of U.S. Geological Survey geologists and geophysicists of the Earth Surface Processes Group, Earthquake Hazards Group, Coastal Marine Geology Group, and Urban Hazards Group and thank them for their efforts supporting the selection of sites, collection of data, and subsequent analysis.

x

Geology, Water-Quality, Hydrology, and Geomechanics of the Cuyama Valley Groundwater Basin, California, 2008–12

By Rhett R. Everett, Dennis R. Gibbs, Randall T. Hanson, Donald S. Sweetkind, Justin T. Brandt, Sarah E. Falk, and Christopher R. Harich

Abstract

To assess the water resources of the Cuyama Valley groundwater basin in Santa Barbara County, California, a series of cooperative studies were undertaken by the U.S. Geological Survey and the Santa Barbara County Water Agency. Between 2008 and 2012, geologic, water-quality, hydrologic and geomechanical data were collected from selected sites throughout the Cuyama Valley groundwater basin.

Geologic data were collected from three multiple-well groundwater monitoring sites and included lithologic descriptions of the drill cuttings, borehole geophysical logs, temperature logs, as well as bulk density and sonic velocity measurements of whole-core samples.

Generalized lithologic characterization from the monitoring sites indicated the water-bearing units in the subsurface consist of unconsolidated to partly consolidated sand, gravel, silt, clay, and occasional cobbles within alluvial fan and stream deposits. Analysis of geophysical logs indicated alternating layers of finer- and coarser-grained material that range from less than 1 foot to more than 20 feet thick. On the basis of the geologic data collected, the principal water-bearing units beneath the monitoring-well sites were found to be composed of younger alluvium of Holocene age, older alluvium of Pleistocene age, and the Tertiary-Quaternary Morales Formation. At all three sites, the contact between the recent fill and younger alluvium is approximately 20 feet below land surface.

Water-quality samples were collected from 12 monitoring wells, 27 domestic and supply wells, 2 springs, and 4 surface-water sites and were analyzed for a variety of constituents that differed by site, but, in general, included trace elements; nutrients; dissolved organic carbon; major and minor ions; silica; total dissolved solids; alkalinity; total arsenic and iron; arsenic, chromium, and iron species; and isotopic tracers, including the stable isotopes of hydrogen and oxygen, activities of tritium, and carbon-14 abundance.

Of the 39 wells sampled, concentrations of total dissolved solids and sulfate from 38 and 37 well samples, respectively, were greater than the U.S. Environmental Protection Agency's secondary maximum contaminant levels. Concentrations greater than the maximum contaminant levels for nitrate were observed in five wells and were observed for arsenic in four wells.

Differences in the stable-isotopic values of hydrogen and oxygen among groundwater samples indicated that water does not move freely between different formations or between different zones within the Cuyama Valley. Variations in isotopic composition indicated that recharge is derived from several different sources. The age of the groundwater, expressed as time since recharge, was between 600 and 38,000 years before present. Detectable concentrations of tritium indicated that younger water, recharged since the early 1950s, is present in parts of the groundwater basin.

Hydrologic data were collected from 12 monitoring wells, 56 domestic and supply wells, 3 surface-water sites, and 4 rainfall-gaging stations. Rainfall in the valley averaged about 8 inches annually, whereas the mountains to the south received between 12 and 19 inches. Stream discharge records showed seasonal variability in surface-water flows ranging from no-flow to over 1,500 cubic feet per second. During periods when inflow to the valley exceeds outflow, there is potential recharge from stream losses to the groundwater system.

Water-level records included manual quarterly depth-to-water measurements collected from 68 wells, time-series data collected from 20 of those wells, and historic water levels from 16 wells. Hydrographs of the manual measurements showed declining water levels in 16 wells, mostly in the South-Main zone, and rising water levels in 14 wells, mostly in the Southern Ventucopa Uplands. Time-series hydrographs showed daily, seasonal, and longer-term effects associated with local pumping. Water-level data from the multiple-well monitoring sites indicated seasonal fluctuations as great as 80 feet and water-level differences between aquifers as great as 40 feet during peak pumping season. Hydrographs from the multiple-well groundwater monitoring sites showed vertical hydraulic gradients were upward during the winter months and downward during the irrigation season. Historic hydrographs showed water-level declines in the Southern-Main, Western Basin, Caliente Northern-Main, and Southern Sierra Madre zone ranging from 1 to 7 feet per year. Hydrographs of wells in the Southern Ventucopa Uplands zone showed several years with marked increases in water levels that corresponded to increased precipitation in the Cuyama Valley.

Investigation of hydraulic properties included hydraulic conductivity and transmissivity estimated from aquifer tests performed on 63 wells. Estimates of horizontal hydraulic

conductivity ranged from about 1.5 to 28 feet per day and decreased with depth. The median estimated hydraulic conductivity for the older alluvium was about five times that estimated for the Morales Formation. Estimates of transmissivity ranged from 560 to 163,400 gallons per day per foot and decreased with depth. The median estimated transmissivity for the younger alluvium was about three times that estimated for the older alluvium.

Geomechanical analysis included land-surface elevation changes at five continuously operating global positioning systems (GPS) and land-subsidence detection at five interferometric synthetic aperture radar (InSAR) reference points. Analysis of data collected from continuously operating GPS stations showed the mountains to the south and west moved upward about 1 millimeter (mm) annually, whereas the station in the center of the Southern-Main zone moved downward more than 7 mm annually, indicating subsidence. It is likely that this subsidence is inelastic (permanent) deformation and indicates reduced storage capacity in the aquifer sediments. Analysis of InSAR data showed local and regional changes that appeared to be dependent, in part, on the time span of the interferogram, seasonal variations in pumping, and tectonic uplift. Long-term InSAR time series showed a total maximum detected subsidence rate of approximately 12 mm per year at one location and approximately 8 mm per year at a second location, while short-term InSAR time series showed maximum subsidence of about 15 mm at one location and localized maximum uplift of about 10 mm at another location.

Introduction

Currently, groundwater is the sole source of water supply in the Cuyama Valley (fig. 1). Groundwater withdrawals, mainly for the irrigation of agricultural crops, have resulted in water-level declines of as much as 300 ft in some areas since the 1940s (California Department of Water Resources, 1998). The Cuyama Valley groundwater basin was identified in 1980 by the California Department of Water Resources (CA DWR) to be in the "critical condition of overdraft," which indicates that a "continuation of present water management practices would probably result in significant adverse overdraft-related environmental, social or economic impact" (California Department of Water Resources, 2003). To provide for sustained beneficial use, it is necessary to define groundwater availability with respect to quantity and quality and to establish tools to allow water users and managers to efficiently utilize the available groundwater resources. The U.S. Geological Survey (USGS), in cooperation with the Santa Barbara County Water Agency, began a study in 2008 to assess the water resources of the Cuyama Valley groundwater basin. The study included a monitoring component (described in this report), a modeling component and a geologic framework component (presented in Sweetkind and others, 2013). As part of this study, the existing monitoring and modeling tools are being updated to provide water managers with the data and resources necessary to address the water-management issues.

Purpose and Scope

The primary purpose of this report is to present selected data that describe current groundwater conditions of the major aquifers in the Cuyama Valley groundwater basin. This report presents a summary of lithologic, geologic, geophysical, water-quality, hydrologic, and land-deformation data collected at three new multiple-well monitoring sites, selected domestic and supply wells (irrigation-supply and municipal-supply), springs, streams and various other sites in the Cuyama Valley during 2008–12. In addition to a summary of data collection, this report includes initial interpretations from these data. Geologic interpretation includes the depths of formation contacts based on lithologic and geophysical data collected at the multi-well monitoring sites. Water-quality interpretations include age dating and isotopic analysis. Hydrologic interpretations include definition of the depths of increased groundwater flow, determination of sources of recharge, and estimation of hydraulic properties. Interpretations of land deformation data include estimating the rate and cause of changes in land-surface elevation.

Description of Study Area

The Cuyama Valley groundwater basin is approximately 40 miles (mi) west of Bakersfield, California, in the southern Coast Ranges physiographic province (fig. 1). The 230 square mile (mi^2) basin lies near the intersection of San Luis Obispo, Santa Barbara, Ventura, and Kern counties. The Coast Ranges province lies west of the Great Valley and north of the west-trending Transverse Ranges. Although within the Coast Ranges, the Cuyama Valley has many of the climatic features of a desert basin, because it is surrounded by relatively high mountains. The Cuyama Valley basin is characterized by hot, dry summers and cold winters. Rainfall averages from 7 to 15 inches per year (in/yr) on the valley floor (California Department of Water Resources, 2003) to about 24 to 30 in/yr in the mountain headwaters of the Cuyama River and along the crest of the Sierra Madre Mountains.

Geologic Units

The Cuyama Valley groundwater basin is underlain by a sequence of unconsolidated to partly consolidated non-marine deposits including the Pliocene to Pleistocene Morales Formation and Pleistocene to recent alluvial and fluvial deposits (Hill and others, 1958; DeLong and others, 2008). These deposits unconformably overlie a late Cretaceous to middle Cenozoic succession of consolidated marine and non-marine sedimentary rocks, which in turn overlie crystalline granitic and gneissic rocks at depth (Hill and others, 1958; Lagoe, 1987). In terms of water-bearing properties, the

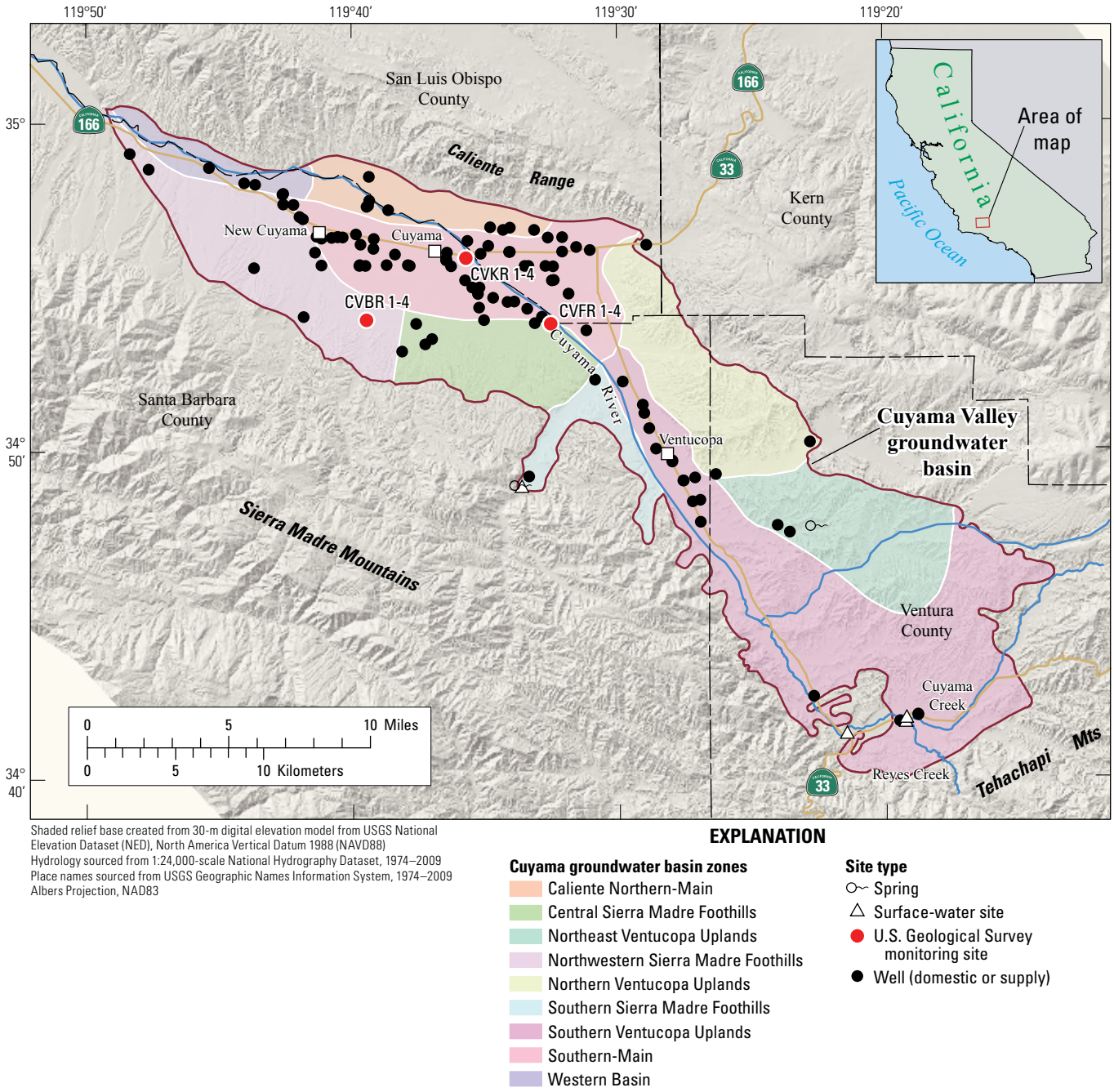

Figure 1. The location of Cuyama Valley, including multiple-well monitoring sites, selected domestic and supply wells, and hydrologic units, Cuyama Valley, Santa Barbara County, California.

geology of the Cuyama Valley can be generalized into four main units: (1) non-water-bearing rocks—the crystalline granitic rocks and all consolidated sedimentary rocks older than the Morales Formation, (2) the Morales Formation, (3) older alluvium of Pleistocene age, and (4) younger alluvium of Holocene age (Upson and Worts, 1951; Singer and Swarzenski, 1970). The aquifer system that is made up of the water-bearing portions of units 2–4 is described in more detail in the "Aquifer System" section.

The Morales Formation (QTm, fig. 2) is a Pliocene-Pleistocene fluvial deposit that is up to 5,000 feet thick and consists of massive- to thick-bedded, partly consolidated deposits of clay, silt, sand, and gravel (Hill and others, 1958; Ellis and others, 1993). The Morales Formation is widely exposed as badland topography to the east of the Cuyama River in the Ventucopa area (Dibblee, 1982; Dibblee and Minch, 2006; Kellogg and others, 2008). The geologic mapping of Dibblee (Dibblee, 1973; Dibblee and Minch, 2005 and 2006) included all young, deformed, non-marine

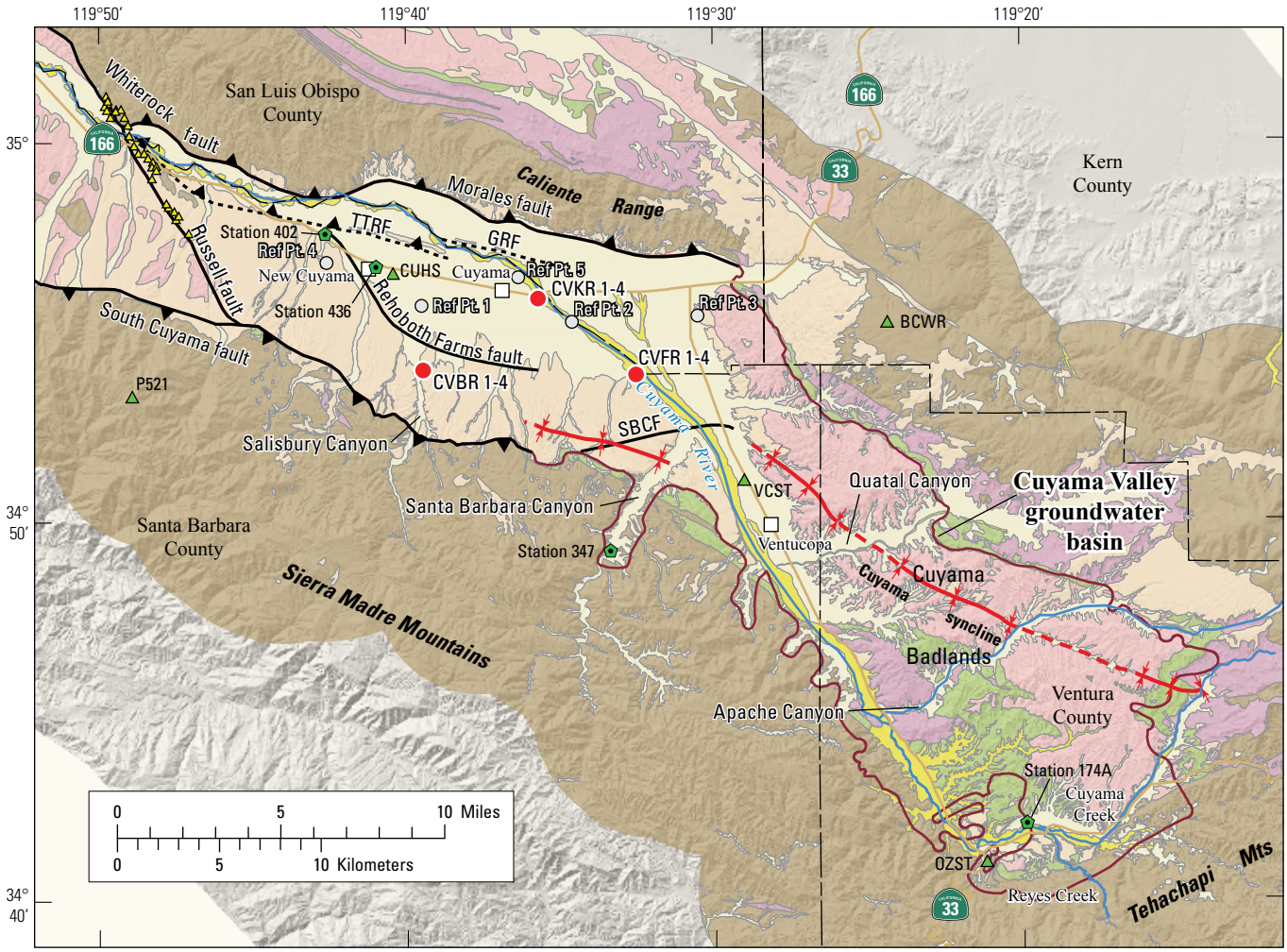

Shaded relief base created from 30-m digital elevation model from USGS National Elevation Dataset (NED); North America Vertical Datum 1988 (NAVD88)
Hydrology sourced from 1:24,000-scale National Hydrography Dataset, 1974–2009
Place names sourced from USGS Geographic Names Information System, 1974–2009
Albers Projection, NAD83

Geology from: Kellogg and others, 2008, and Graham and others, 1999

EXPLANATION

Geologic unit (age)

- Qc: fluvial channel deposits associated with the Cuyama River (Holocene)
- Qya: Younger (inactive) alluvium (Holocene and late Pleistocene)
- Qoa: Older alluvium (late and middle-Pleistocene)
- QTm: Morales Formation, undivided (Pleistocene and upper Pliocene)
- Tq: Quatal Formation, undivided (Pliocene)
- BR1: Caliente Formation (upper and middle Miocene)
- BR2: Miocene and older consolidated rocks

- Normal fault
- Thrust fault
- Thrust fault, concealed
- Syncline
- Syncline, concealed

GRF, Graveyard fault
SBCF, Santa Barbara Canyon fault
TTRF, Turkey Trap Ridge fault

- Russel Ranch oil well
- Cuyama continuous-GPS site
- USGS-monitoring site
- Rainfall station

Figure 2. Geologic formation outcrops, faults, folds, InSAR reference points, continuously operating GPS stations, oil wells, and rainfall stations, Cuyama Valley, Santa Barbara County, California.

sediments of the Cuyama area in the Morales Formation; these maps portray the piedmont upland area along the south edge of the Cuyama Valley as being composed of exposed outcrops of Morales Formation. Subsequent workers (Vedder, 1968; Vedder and Repenning, 1975; Schwing, 1984; Spitz, 1986) classified the upper part of Dibblee's Morales Formation as "deformed older Quaternary alluvium." Using this classification, the Morales Formation is hundreds to greater than 1,000 ft below the surface on the south side of Cuyama Valley, rather than exposed at the surface.

Older alluvium (Qoa, fig. 2) consists of unconsolidated to partly consolidated sand, gravel, and boulders, with some clay (Vedder and Repenning, 1975; DeLong and others, 2008). The percentage of clay increases in the western part of the valley (Singer and Swarzenski, 1970; DeLong and others, 2008). Interpretation of geophysical logs from oil exploration wells indicated that this unit is typically 400 to 600 feet thick, but is as thick as 1,000 feet near the axis of Cuyama Valley (Schwing, 1984; Spitz, 1986). In the study area, older alluvium includes dissected alluvial fans, colluvial deposits, and sediments on multiple terraces and alluvial surfaces (Hill and others, 1958; DeLong and others, 2008). Older alluvial deposits are slightly deformed and are probably of late Pleistocene age, although in some places they could be Holocene (Vedder, 1968; DeLong and others, 2008). Older alluvium is exposed on the piedmont uplands along the south side of Cuyama Valley and locally at two fault-bounded ridges in the center of the valley (Vedder and Repenning, 1975; DeLong and others, 2008).

Younger alluvium (Qya, fig. 2) consists of unconsolidated sand, gravel, and boulders, with some clay deposited as alluvium in stream channels, floodplains, alluvial fans, and stream terraces. The unit is mainly Holocene in age, but locally can be late Pleistocene in part. Active stream deposits consist of river-bed gravels of the Cuyama River and other active channels (Vedder and Repenning, 1975; DeLong and others, 2008).

Geologic Structure

During Miocene and older time, the Cuyama Valley groundwater basin was the site of extensional and strike-slip deformation; older, inactive faults were buried by the Morales Formation and younger units (Yeats and others, 1989; fig. 2). During the Pliocene-Pleistocene, structural deformation of the Cuyama Valley changed to a predominantly compressional mode, resulting in the formation of folds and folding and thrust faults (Davis and others, 1988).

As a result of compression, the Cuyama Valley is currently a downfolded basin bounded to the north and south by faults. Miocene rocks of the Caliente Range to the north of Cuyama Valley are being thrust southward over older and younger alluvium on the Morales and Whiterock thrusts; similar-aged rocks in the Sierra Madre to the south of Cuyama Valley are being thrust northward over older alluvium on the South Cuyama fault (Vedder and Repenning, 1975; Davis and others, 1988; fig. 2).

The Morales Formation and older alluvium are deformed into tight synclines along the north and south margins of the basin near the bounding thrust faults (Spitz, 1986; Kellogg and others, 2008). The eastern part of the basin is underlain by the Cuyama syncline; its strike is parallel to the valley axis and the fold plunges toward the northwest (Ellis, 1994; Dibblee and Minch, 2006; Kellogg and others, 2008). The fold is exposed in outcrops in the Ventucopa area and the Cuyama Badlands to the east; beneath the central part of the valley, it is buried but known to be present from subsurface data from oil exploration wells (Spitz, 1986; Ellis, 1994).

Several ridges of older alluvium are mapped in the center of the Cuyama Valley, north of Highway 166 (Vedder and Repenning, 1975), on the north side on the Turkey Trap Ridge and Graveyard faults (fig. 2). These ridges trend slightly north-northwest and are oriented in a right-stepping, en echelon pattern. Upson and Worts (1951) suggested that these ridges were fault-related on the basis of their orientation and the presence of springs along the ridges. Vedder and Repenning (1975) mapped inferred reverse faults associated with these ridges; the faults cut alluvium and bring older alluvium to the surface. Seismic profiles collected across these ridges indicate that these faults cut the Morales Formation (Ellis, 1994), although their ultimate downdip projection is unknown.

Other faults, not obviously related to the overall compressional tectonics that affect the basin, have been inferred in the subsurface, primarily, on the basis of marked differences in water levels over short distances. One such fault (SBCF on fig. 2) is inferred to trend northeast-southwest near the mouth of the Santa Barbara Canyon (Singer and Swarzenski, 1970); similarly aligned structures are mapped in the piedmont upland to the west of Santa Barbara Canyon (Dibblee and Minch, 2007). Another fault (Rehoboth Farms fault on fig. 2) inferred to exist on the basis of water-level changes is in the west-central part of the valley; the inferred fault trends northwest-southeast near the town of New Cuyama and projects southeastward beneath the Salisbury Canyon drainage (Lane-Western Company, written commun., 1982).

Aquifer System

The main water-bearing deposits in the study area are the saturated portions of the younger and older alluvium and the Morales Formation (fig. 2). All rocks that are older than the Morales Formation were considered by previous investigators to be non-water-bearing (Upson and Worts, 1951; Singer and Swarzenski, 1970). The regional flow pattern of groundwater under natural conditions is northwestward, parallel to the central axis of the basin, similar to the orientation of the overlying Cuyama River, with a substantial component of flow northward from the Sierra Madre Mountains (Singer and Swarzenski, 1970). Historically, most of the water pumped from the study area was from the younger and older alluvium. Inspection of available geologic and geophysical logs indicated that the hydraulic conductivity, in general, decreases with depth.

Large-capacity wells perforated in the alluvium yield 1,000–3,000 gallons per minute (gpm) and have specific capacities of that range from 100 to 200 gpm per foot (Singer and Swarzenski, 1970). Yield and specific capacities generally tend to decrease with depth. Wells perforated in the younger alluvium have a median yield of 1,800 gpm and median specific capacity of 60 gpm per foot. Wells perforated in both the younger and older alluvium have a median yield of 1,200 gpm and median specific capacity of 40 gpm per foot. Wells perforated in the older alluvium have a median yield of 620 gpm and median specific capacity of 20 gpm per foot. Yield and specific capacities are less on the western half of the valley compared to the eastern half, indicating a spatial trend; however, a greater percentage of wells in the western part are perforated in the older alluvium.

The water-bearing properties of the Morales Formation are not well defined, but available data indicate that the hydraulic conductivity of the formation varies greatly both areally and with depth.

Wells perforated in the Morales Formation in the western part of the valley have specific capacities of 5–25 gpm per foot, whereas those in the north-central part of the valley have specific capacities of 25–50 gpm per foot (Singer and Swarzenski, 1970). Inspection of available geologic and geophysical logs indicated that the hydraulic conductivity of the Morales Formation decreases with depth.

Several faults that offset the basin-fill deposits, associated with measured water-level offsets, are inferred to impede groundwater movement (Upson and Worts, 1951; Singer and Swarzenski, 1970; fig. 2). Because the faults do not intersect land surface and are not readily apparent in the unconsolidated surface sediments, their locations have been inferred from well data and topographic features. The Graveyard and Turkey Trap Ridges faults on the northern side of the Cuyama Valley (fig. 2) are postulated from groundwater data by Upson and Worts (1951) and shown on the geologic map of Vedder and Repenning (1975). A fault on the south side of the basin, here called the Santa Barbara Canyon fault (fig. 2), was suggested by Singer and Swarzenski (1970) to be the cause of a steep hydraulic gradient in this part of Cuyama Valley, where water levels in the vicinity of Ventucopa were observed to be 100 feet higher than water levels 2 miles to the north. The fault is mapped in the uplifted piedmont older alluvium to the west of Santa Barbara Canyon (Dibblee and Minch, 2007) and is visible in outcrops to the west of the Cuyama River, but is not readily projected to the eastern side of the Cuyama River on the basis of geologic data. Water-level offsets along the valley were used to infer the location of the fault in the sediment (Sweetkind, 2013).

Historically, flowing springs were found along the trace of faults that parallel Graveyard and Turkey Trap Ridges (Santa Barbara County Planning and Development Department, 1994), and other springs have been reported along the South Cuyama and Santa Barbara fault. While many of the springs and seeps that flowed in 1946 have since dried up (Singer and Swarzenski, 1970), several springs still have seasonal flow. Two springs, one in the Southern Sierra Madre Foothills zone and another in the Northern Ventucopa Uplands zone (fig. 1), were sampled during the study.

This study required a better delineation of the groundwater basin than previously available. The basin was divided into nine groundwater subregional hydrologic zones (fig. 1). These zones separate the aquifers into regions that are fault bounded and where the response to the use, movement, and consumption of water is similar in specific parts of the aquifers, but differs from the other zones. In this context, Cuyama Valley can be considered a collection of zones that are partially connected, but have different geologic boundaries, hydrologic features and hydraulic properties, water quality and age of groundwater, and dominant aquifers that respond to natural and anthropogenic stresses differently.

Accessing Data

Users of the data presented in this report are encouraged to access information through the USGS National Water Information System (NWIS) web page (NWIS Web) at *http://waterdata.usgs.gov/nwis/*. NWIS Web serves as an interface to a database of site information and groundwater, surface-water, and water-quality data collected throughout the 50 states and elsewhere. NWIS Web is updated from the database on a regularly scheduled basis. Data can be retrieved by category and geographic area, and the retrieval can be selectively refined by a specific location or parameter field. NWIS Web can output water-level and water-quality graphs, site maps, and data tables (in HTML and ASCII format) and can be used to develop site-selection lists. Updates to data presented in this report after publication will be made to the NWIS. Additional data could be available on the project web site at *http://ca.water.usgs.gov/projects/cuyama/*. Formal requests for specific data may be directed to the U.S. Geological Survey California Water Science Center, Public Information Officer in Sacramento, California.

Description of the Monitoring Network

Most information presented in this report focuses on three multiple-well monitoring sites installed between December 2008 and October 2009 within the study area (fig. 1). Data collected from the monitoring sites provided information on vertical differences in hydraulic properties, water levels, and water chemistry at the same location; these data can be used to characterize the three-dimensional groundwater system. Existing wells (domestic and supply) were incorporated into the monitoring network to help meet additional needs (fig. 1). Table 1 lists all wells referenced in this report, including information on the well location by zone, and data collected from each well site. Well-identification and well-construction information for groundwater wells in the monitoring network are presented in table 2. Supporting data were collected from four surface-water sites and two springs; related site-identification information and available data for these sites are presented in table 3.

Table 1. Selected characteristics and data availability for wells in the Cuyama Valley groundwater basin, Santa Barbara County, California.

[See figures 1, 8, 15, and 25 for well locations. **Abbreviations**: CVKR, Cuyama Valley Kirschenmann Road; CVBR, Cuyama Valley Bell Road, CVFR, Cuyama Valley Foothill Road; CUY, Cuyama Valley study well; PT, Pump test well; x, data are available; —, data not available]

Common well name	Site identification number	Cuyama groundwater-basin zones	Water-quality data	Discrete (manual) water-level measurements	Time-series (automated) water-level measurements	Aquifer-test data
CVKR-1	345552119354201	Southern-Main	x	x	x	x
CVKR-2	345552119354202	Southern-Main	x	x	x	x
CVKR-3	345552119354203	Southern-Main	x	x	x	x
CVKR-4	345552119354204	Southern-Main	x	x	x	x
CVBR-1	345359119392701	Northwestern Sierra Madre Foothills	x	x	x	x
CVBR-2	345359119392702	Northwestern Sierra Madre Foothills	x	x	x	x
CVBR-3	345359119392703	Northwestern Sierra Madre Foothills	x	x	x	x
CVBR-4	345359119392704	Northwestern Sierra Madre Foothills	x	x	x	x
CVFR-1	345351119323101	Central Sierra Madre Foothills	x	x	x	x
CVFR-2	345351119323102	Central Sierra Madre Foothills	x	x	x	x
CVFR-3	345351119323103	Central Sierra Madre Foothills	x	x	x	x
CVFR-4	345351119323104	Central Sierra Madre Foothills	x	x	x	x
CUY-01	345838119452001	Western Basin	x	x	—	—
CUY-02	345603119411901	Northwestern Sierra Madre Foothills	x	x	x	—
CUY-03	345100119290001	Southern Ventucopa Uplands	x	x	—	—
CUY-04	345602119362401	Southern-Main	x	x	x	—
CUY-05	345600119400001	Southern-Main	x	x	x	—
CUY-06	345300119310001	Southern-Main	x	x	—	—
CUY-07	345538119332201	Southern-Main	x	x	x	—
CUY-08	345405119325101	Southern-Main	x	x	—	—
CUY-11	344143119193001	Southern Ventucopa Uplands	x	x	—	—
CUY-12	345100119290002	Southern Ventucopa Uplands	x	x	x	—
CUY-13	344910119270501	Southern Ventucopa Uplands	x	x	—	—
CUY-14	345338119324801	Central Sierra Madre Foothills	x	—	—	—
CUY-16	345540119410901	Northwestern Sierra Madre Foothills	x	x	—	—
CUY-17	344729119233501	Northeast Ventucopa Uplands	x	x	—	—
CUY-18	344859119280801	Southern Ventucopa Uplands	x	x	—	—
CUY-19	345003119283501	Southern Ventucopa Uplands	x	x	—	—
CUY-20	345615119285501	Outside basin boundary	x	x	—	—
CUY-21	345359119350201	Central Sierra Madre Foothills	x	x	—	—
CUY-22	345552119362901	Southern-Main	x	x	—	—
CUY-23	345539119393901	Southern-Main	x	x	—	—
CUY-24	345325119365603	Central Sierra Madre Foothills	x	x	—	—
CUY-25	345302119380701	Central Sierra Madre Foothills	x	x	—	—
CUY-26	345753119421701	Western Basin	x	x	—	—
CUY-27	345539119394001	Southern-Main	—	x	—	—
CUY-28	344900119332201	Southern Sierra Madre Foothills	x	—	—	—
CUY-30	344156119184801	Southern Ventucopa Uplands	—	x	—	—
CUY-31	344154119184801	Southern Ventucopa Uplands	—	x	—	—
CUY-32	344231119224101	Southern Ventucopa Uplands	—	x	—	—
CUY-33	344828119265301	Southern Ventucopa Uplands	—	x	—	—
CUY-34	344843119272401	Southern Ventucopa Uplands	—	x	—	—
CUY-35	344825119271001	Southern Ventucopa Uplands	—	x	x	—

Table 1. Selected characteristics and data availability for wells in the Cuyama Valley groundwater basin, Santa Barbara County, California.—Continued

[See figures 1, 8, 15, and 25 for well locations. **Abbreviations**: CVKR, Cuyama Valley Kirschenmann Road; CVBR, Cuyama Valley Bell Road, CVFR, Cuyama Valley Foothill Road; CUY, Cuyama Valley study well; PT, Pump test well; x, data are available; —, data not available]

Common well name	Site identification number	Cuyama groundwater-basin zones	Water-quality data	Discrete (manual) water-level measurements	Time-series (automated) water-level measurements	Aquifer-test data
CUY-36	344742119240201	Northeast Ventucopa Uplands	—	x	—	—
CUY-38	345040119285101	Southern Ventucopa Uplands	—	x	—	—
CUY-39	344944119275701	Southern Ventucopa Uplands	—	x	—	—
CUY-40	344939119275901	Southern Ventucopa Uplands	—	x	—	—
CUY-42	344904119273101	Southern Ventucopa Uplands	—	x	—	—
CUY-43	344904119273401	Southern Ventucopa Uplands	—	x	—	—
CUY-44	344915119262001	Northern Ventucopa Uplands	—	x	—	—
CUY-45	345209119304901	Southern Sierra Madre Foothills	—	x	—	—
CUY-46	345206119294701	Southern Ventucopa Uplands	—	x	—	—
CUY-47	344940119330501	Southern Sierra Madre Foothills	—	x	—	—
CUY-48	345315119371501	Central Sierra Madre Foothills	—	x	—	—
CUY-49	345353119373601	Central Sierra Madre Foothills	—	x	—	—
CUY-50	345600119351001	Southern-Main	—	x	—	—
CUY-51	345606119310301	Southern-Main	—	x	—	—
CUY-52	345511119322801	Southern-Main	—	x	—	—
CUY-53	345447119315101	Southern-Main	—	x	—	—
CUY-54	345512119354101	Southern-Main	—	x	—	—
CUY-55	345631119402901	Southern-Main	—	x	x	—
CUY-56	345709119415501	Southern-Main	—	x	—	—
CUY-57	345618119393701	Southern-Main	—	x	—	—
CUY-58	345540119394301	Southern-Main	—	x	—	—
CUY-59	345538119374601	Southern-Main	—	x	—	—
CUY-60	345808119433501	Western Basin	—	x	x	—
CUY-61	345604119340201	Southern-Main	x	—	—	—
CUY-62	345822119391801	Caliente Northern-Main	—	x	—	—
CUY-63	345721119383401	Caliente Northern-Main	x	—	—	—
CUY-64	345540119384201	Southern-Main	x	—	—	—
CUY-73	345014119224901	Northern Ventucopa Uplands	—	x	—	—
CUY-74	344749119265301	Southern Ventucopa Uplands	—	x	—	—
CUY-75	345637119394701	Southern-Main	—	x	—	—
PT-01	—	Southern-Main	—	—	—	x
PT-02	—	Southern-Main	—	—	—	x
PT-03	—	Caliente Northern-Main	—	—	—	x
PT-04	—	Caliente Northern-Main	—	—	—	x
PT-05	—	Caliente Northern-Main	—	—	—	x
PT-07	—	Southern-Main	—	—	—	x
PT-08	—	Southern-Main	—	—	—	x
PT-09	—	Southern-Main	—	—	—	x
PT-10	—	Southern-Main	—	—	—	x
PT-11	—	Southern-Main	—	—	—	x
PT-12	—	Southern-Main	—	—	—	x
PT-13	—	Southern-Main	—	—	—	x
PT-14	—	Southern-Main	—	—	—	x
PT-15	—	Southern-Main	—	—	—	x

Table 1. Selected characteristics and data availability for wells in the Cuyama Valley groundwater basin, Santa Barbara County, California.—Continued

[See figures 1, 8, 15, and 25 for well locations. **Abbreviations**: CVKR, Cuyama Valley Kirschenmann Road; CVBR, Cuyama Valley Bell Road, CVFR, Cuyama Valley Foothill Road; CUY, Cuyama Valley study well; PT, Pump test well; x, data are available; —, data not available]

Common well name	Site identification number	Cuyama groundwater-basin zones	Water-quality data	Discrete (manual) water-level measurements	Time-series (auto-mated) water-level measurements	Aquifer-test data
PT-16	—	Southern-Main	—	—	—	x
PT-17	—	Southern-Main	—	—	—	x
PT-18	—	Southern-Main	—	—	—	x
PT-19	—	Southern-Main	—	—	—	x
PT-20	—	Southern-Main	—	—	—	x
PT-21	—	Southern-Main	—	—	—	x
PT-22	—	Southern-Main	—	—	—	x
PT-23	—	Southern-Main	—	—	—	x
PT-24	—	Southern-Main	—	—	—	x
PT-25	—	Central Sierra Madre Foothills	—	—	—	x
PT-26	—	Southern-Main	—	—	—	x
PT-27	—	Caliente Northern-Main	—	—	—	x
PT-28	—	Caliente Northern-Main	—	—	—	x
PT-30	—	Southern-Main	—	—	—	x
PT-31	—	Southern-Main	—	—	—	x
PT-32	—	Southern-Main	—	—	—	x
PT-34	—	Southern-Main	—	—	—	x
PT-35	—	Southern-Main	—	—	—	x
PT-36	—	Southern-Main	—	—	—	x
PT-37	—	Southern-Main	—	—	—	x
PT-38	—	Southern-Main	—	—	—	x
PT-39	—	Southern-Main	—	—	—	x
PT-40	—	Southern-Main	—	—	—	x
PT-41	—	Southern-Main	—	—	—	x
PT-42	—	Southern-Main	—	—	—	x
PT-43	—	Southern-Main	—	—	—	x
PT-44	—	Southern-Main	—	—	—	x
PT-45	—	Southern-Main	—	—	—	x
PT-46	—	Northwestern Sierra Madre Foothills	—	—	—	x
PT-47	—	Northwestern Sierra Madre Foothills	—	—	—	x
PT-48	—	Northwestern Sierra Madre Foothills	—	—	—	x
PT-49	—	Western Basin	—	—	—	x
PT-50	—	Western Basin	—	—	—	x
PT-51	—	Western Basin	—	—	—	x
PT-52	—	Western Basin	—	—	—	x
PT-53	—	Northwestern Sierra Madre Foothills	—	—	—	x
PT-54	—	Northwestern Sierra Madre Foothills	—	—	—	x

Each of the multiple-well monitoring sites consists of four 2-inch diameter wells installed at different depths in the same borehole. Individual wells are screened over a specific 20-foot interval and isolated from other wells by a low-permeability bentonite grout. The construction of these wells enables the collection of depth-specific water-quality, water-level, and aquifer hydraulic-property data. Well-construction information for the three multiple-well monitoring sites is summarized in table 2.

Boreholes at each site were drilled by the USGS Western Region Research Drilling Unit using the mud-rotary method. Borehole diameter decreased with depth, ranging in diameter from 14-3/4 to 4-1/2 inches. After total hole depth was attained, geophysical log surveys were completed, and the

Table 2. Summary of well completion for selected wells, Cuyama Valley, Santa Barbara County, California.

[See figures 1, 8, 15, and 25 for well locations. **Abbreviations**: CVKR, Cuyama Valley Kirschenmann Road; CVBR, Cuyama Valley Bell Road, CVFR, Cuyama Valley Foothill Road; CUY, Cuyama Valley study well; ft bls, feet below land surface; —, data not available; * denotes data that were reported to the U.S. Geological Survey from various sources and are not stored in the National Water Information System database. Qya, Younger alluvium; Qoa, Older alluvium; QTm, Morales]

Common well name	Site identification number	Depth to bottom of well (ft bls)	Depth to top of perforations (ft bls)	Depth to bottom of perforations (ft bls)	Depth to top of sand pack (ft bls)	Depth to bottom of sand pack (ft bls)	Formation at top of screen	Formation at bottom of screen
CVKR-1	345552119354201	980	960	980	944	1,000	Qoa	Qoa
CVKR-2	345552119354202	780	760	780	728	800	Qoa	Qoa
CVKR-3	345552119354203	620	600	620	575	627	Qoa	Qoa
CVKR-4	345552119354204	460	440	460	417	471	Qoa	Qoa
CVBR-1	345359119392701	850	830	850	807	858	QTm	QTm
CVBR-2	345359119392702	750	730	750	702	767	QTm	QTm
CVBR-3	345359119392703	560	540	560	518	581	Qoa	Qoa
CVBR-4	345359119392704	380	360	380	303	403	Qoa	Qoa
CVFR-1	345351119323101	980	960	980	935	1,000	QTm	QTm
CVFR-2	345351119323102	830	810	830	787	839	QTm	QTm
CVFR-3	345351119323103	700	680	700	660	720	QTm	QTm
CVFR-4	345351119323104	610	590	610	568	625	QTm	QTm
CUY-01	345838119452001	188	45	125	—	—	Qoa	Qoa
CUY-02	345603119411901	790	340	790	—	—	Qoa	QTm
CUY-03	345100119290001	—	75*	200*	—	—	Qya	Qya
CUY-04	345602119362401	720	420	720	—	—	Qya	Qoa
CUY-05	345600119400001	—	100*	300*	—	—	Qya	Qya
CUY-06	345300119310001	800	640	800	—	—	QTm	QTm
CUY-07	345538119332201	750	250	750	—	—	Qya	Qoa
CUY-08	345405119325101	550	100*	400*	—	—	Qya	Qoa
CUY-11	344143119193001	357	100*	357*	—	—	Below QTm	Below QTm
CUY-12	345100119290002	93	50*	150*	—	—	Qya	Qya
CUY-13	344910119270501	233	100*	233*	—	—	Qya	QTm
CUY-14	345338119324801	1,100	580	1,100	—	—	Qya	Qoa
CUY-16	345540119410901	880	380	880	—	—	Qoa	QTm
CUY-17	344729119233501	400	300	400	—	—	Below QTm	Below QTm
CUY-18	344859119280801	—	100*	212*	—	—	Undetermined	Undetermined
CUY-19	345003119283501	198	87*	198*	—	—	Qya	Qya
CUY-20	345615119285501	155	100*	155*	—	—	Undetermined	Undetermined
CUY-21	345359119350201	805	620	800	—	—	QTm	QTm
CUY-22	345552119362901	1,000	401	1,000	—	—	Qya	Qoa
CUY-23	345539119393901	2,120	400	2,120	—	—	Qya	Qoa
CUY-24	345325119365603	500	300	500	—	—	Qoa	Qoa
CUY-25	345302119380701	750	325*	400*	—	—	Qoa	Qoa
CUY-26	345753119421701	—	100*	215*	—	—	Qya	Qoa
CUY-27	345539119394001	993	144	993	—	—	Qya	QTm
CUY-28	344900119332201	—	—	—	—	—	Undetermined	Undetermined
CUY-30	344156119184801	73	100*	500*	—	—	Undetermined	Undetermined
CUY-31	344154119184801	140	40	140	—	—	Undetermined	Undetermined
CUY-32	344231119224101	125	65	125*	—	—	Undetermined	Undetermined
CUY-33	344828119265301	360	50*	372*	—	—	Qya	QTm
CUY-34	344843119272401	284	120	302	—	—	Qya	QTm

Table 2. Summary of well completion for selected wells, Cuyama Valley, Santa Barbara County, California.—Continued

[See figures 1, 8, 15, and 25 for well locations. **Abbreviations**: CVKR, Cuyama Valley Kirschenmann Road; CVBR, Cuyama Valley Bell Road, CVFR, Cuyama Valley Foothill Road; CUY, Cuyama Valley study well; ft bls, feet below land surface; —, data not available; * denotes data that were reported to the U.S. Geological Survey from various sources and are not stored in the National Water Information System database. Qya, Younger alluvium; Qoa, Older alluvium; QTm, Morales]

Common well name	Site identification number	Depth to bottom of well (ft bls)	Depth to top of perforations (ft bls)	Depth to bottom of perforations (ft bls)	Depth to top of sand pack (ft bls)	Depth to bottom of sand pack (ft bls)	Formation at top of screen	Formation at bottom of screen
CUY-35	344825119271001	220	100*	175*	—	—	Qya	Qya
CUY-36	344742119240201	435	255	435	—	—	Undetermined	Undetermined
CUY-38	345040119285101	200	120	200	—	—	Qya	Qya
CUY-39	344944119275701	212	100*	212*	—	—	Qya	Qya
CUY-40	344939119275901	200	50*	200*	—	—	Qya	Qya
CUY-42	344904119273101	160.7	100*	174*	—	—	Qya	Qoa
CUY-43	344904119273401	225	125	225	—	—	Qya	Qoa
CUY-44	344915119262001	230	100*	235*	—	—	QTm	QTm
CUY-45	345209119304901	230	100*	300*	—	—	Qya	Qoa
CUY-46	345206119294701	175	120*	175*	—	—	Qya	Qya
CUY-47	344940119330501	151	31	151	—	—	Undetermined	Undetermined
CUY-48	345315119371501	—	425*	500*	—	—	Qoa	Qoa
CUY-49	345353119373601	750	425*	500*	—	—	Qoa	Qoa
CUY-50	345600119351001	—	50*	300*	—	—	Qya	Qya
CUY-51	345606119310301	800	50*	800*	—	—	Qya	QTm
CUY-52	345511119322801	1,008	484	1,008	—	—	Qoa	QTm
CUY-53	345447119315101	—	50*	500*	—	—	Qya	Qoa
CUY-54	345512119354101	239	124*	370*	—	—	Qya	Qoa
CUY-55	345631119402901	425	100*	441*	—	—	Qya	Qoa
CUY-56	345709119415501	240	58*	237*	—	—	Qya	Qoa
CUY-57	345618119393701	1,004	160	1,004	—	—	Qya	QTm
CUY-58	345540119394301	—	150*	500*	—	—	Qya	Qoa
CUY-59	345538119374601	—	306	620	—	—	Qya	Qoa
CUY-60	345808119433501	215	100*	215*	—	—	Qya	Qoa
CUY-61	345604119340201	—	50*	745*	—	—	Qya	Qoa
CUY-62	345822119391801	238	108	232	—	—	Qya	Qoa
CUY-63	345721119383401	634	200	628	—	—	Qya	Qoa
CUY-64	345540119384201	—	150*	425*	—	—	Qya	Qoa
CUY-73	345014119224901	232	100*	232*	—	—	Qoa	Qoa
CUY-74	344749119265301	—	100*	290*	—	—	Qya	QTm
CUY-75	345637119394701	646	166	640	—	—	Qya	Qoa
PT-01	—	392	50*	392*	—	—	Qya	Qoa
PT-02	—	194	97*	319*	—	—	Qya	Qya
PT-03	—	346	50*	346*	—	—	Qya	Qya
PT-04	—	288	50*	288*	—	—	Qya	Qya
PT-05	—	203.5	50*	304*	—	—	Qya	Qya
PT-07	—	316	112*	310*	—	—	Qya	Qya
PT-08	—	—	110*	371*	—	—	Qya	Qya
PT-09	—	656	108*	656*	—	—	Qya	Qoa
PT-10	—	298.5	50*	337*	—	—	Qya	Qya
PT-11	—	623	94*	623*	—	—	Qya	Qoa
PT-12	—	—	50*	600*	—	—	Qya	Qoa
PT-13	—	660	108	660*	—	—	Qya	Qoa

Table 2. Summary of well completion for selected wells, Cuyama Valley, Santa Barbara County, California.—Continued

[See figures 1, 8, 15, and 25 for well locations. **Abbreviations**: CVKR, Cuyama Valley Kirschenmann Road; CVBR, Cuyama Valley Bell Road, CVFR, Cuyama Valley Foothill Road; CUY, Cuyama Valley study well; ft bls, feet below land surface; —, data not available; * denotes data that were reported to the U.S. Geological Survey from various sources and are not stored in the National Water Information System database. Qya, Younger alluvium; Qoa, Older alluvium; QTm, Morales]

Common well name	Site identification number	Depth to bottom of well (ft bls)	Depth to top of perforations (ft bls)	Depth to bottom of perforations (ft bls)	Depth to top of sand pack (ft bls)	Depth to bottom of sand pack (ft bls)	Formation at top of screen	Formation at bottom of screen
PT-14	—	810	175	810	—	—	Qya	Qoa
PT-15	—	666	119*	665*	—	—	Qya	Qoa
PT-16	—	239	124*	370*	—	—	Qya	Qoa
PT-17	—	186	120*	369*	—	—	Qya	Qya
PT-18	—	417	50*	417*	—	—	Qya	Qya
PT-19	—	—	50*	400*	—	—	Qya	Qya
PT-20	—	—	100*	359*	—	—	Qoa	Qoa
PT-21	—	370	100*	370*	—	—	Qya	Qoa
PT-22	—	400	100*	400*	—	—	Qya	Qya
PT-23	—	—	156*	351*	—	—	Qya	Qya
PT-24	—	333	100*	204*	—	—	Qya	Qya
PT-25	—	390	190*	390*	—	—	Qoa	Qoa
PT-26	—	204	100*	204*	—	—	Qya	Qoa
PT-27	—	222	42*	218*	—	—	Qoa	Qoa
PT-28	—	380	33*	212*	—	—	Qoa	Qoa
PT-30	—	508	226	—	—	—	Qya	Qoa
PT-31	—	409	108*	308*	—	—	Qya	Qya
PT-32	—	240	58*	237*	—	—	Qya	Qoa
PT-34	—	465	173	465*	—	—	Qya	Qoa
PT-35	—	350	128	350*	—	—	Qya	Qoa
PT-36	—	441	100*	441*	—	—	Qya	Qoa
PT-37	—	407	133*	407*	—	—	Qya	Qya
PT-38	—	514	133*	514*	—	—	Qya	Qoa
PT-39	—	—	166*	454*	—	—	Qya	Qoa
PT-40	—	371	50*	190*	—	—	Qya	Qya
PT-41	—	—	150*	310*	—	—	Qya	Qya
PT-42	—	—	130*	322*	—	—	Qya	Qya
PT-43	—	278	130*	278*	—	—	Qya	Qya
PT-44	—	720	420	720	—	—	Qya	Qoa
PT-45	—	298	53*	275*	—	—	Qya	Qya
PT-46	—	1,006	196	1003*	—	—	Qoa	QTm
PT-47	—	603	224*	560*	—	—	Qoa	Qoa
PT-48	—	404	100	404*	—	—	Qoa	QTm
PT-49	—	215	100*	215*	—	—	Qya	Qoa
PT-50	—	378	36*	117*	—	—	Qya	Qya
PT-51	—	138	40*	138*	—	—	Qya	Qya
PT-52	—	294	40*	294*	—	—	Qya	Qoa
PT-53	—	110	57*	128*	—	—	Qoa	Qoa
PT-54	—	700	125	625*	—	—	Qoa	Qoa

Table 3. Site identification and data availability for selected springs and surface-water sites in the Cuyama Valley groundwater basin, Santa Barbara County, California

[See figure 8 for locations. An "x" denotes data are available. **Abbreviations**: mm/dd/yyyy, month, day, year; SP, spring site; SW, surface water site; —, data not available]

Common site name	Site type	Site identification number	Sub-region	Site description	Water-chemistry data	Discharge data	Discharge data start (mm/dd/yyyy)
SP-01	Spring	344740119224801	Northeast Ventucopa Uplands	Quail Creek Spring	x	—	—
SP-02	Spring	344857119334701	Southern Sierra Madre Foothills	Reyes Creek Spring	x	—	—
SW-01	Surface water	344143119191701	Southern Ventucopa Uplands	Reyes Creek at Lockwood Valley Road near Ventucopa	x	—	—
SW-02	Surface water	344147119191601	Southern Ventucopa Uplands	Cuyama River at Lockwood Valley Road near Ventucopa	x	—	—
SW-03	Surface water	11136600	Southern Sierra Madre Foothills	Santa Barbara Canyon Creek near Ventucopa	x	x	9/30/2009
SW-04	Surface water	11136500	Outside basin boundary	Cuyama River near Ventucopa	x	x	5/15/2009
SW-05	Surface water	11136800	Outside basin boundary	Cuyama River below Buckhorn Canyon near Santa Maria	—	x	2/10/1962

monitoring wells were installed. The monitoring wells were constructed by using flush-threaded, 2-inch-diameter, schedule 80 polyvinyl chloride (PVC) casing. The screened interval for each monitoring well typically consisted of a 20-foot section of slotted PVC (slot size is 0.020 inch) at the bottom. Once the well was lowered to the desired depth, a filter pack was tremied around the screened interval using No. 3 Monterey sand. A low-permeability bentonite grout was then tremied in place to seal the borehole and effectively isolate the screened interval of the monitoring well. The process was repeated for each successive well. Well-construction diagrams for each multiple-well monitoring site are presented in figures 3–5.

After completion, drilling fluid was evacuated from each monitoring well by using compressed air. Extensive airlifting and a surging technique with compressed air were employed to further develop the filter pack surrounding the well. Specific conductance, pH, temperature, apparent color, and turbidity, along with the discharge rate and total volume, were recorded during this process. Development was continuous until no discernible drilling mud was present and field measurements had stabilized.

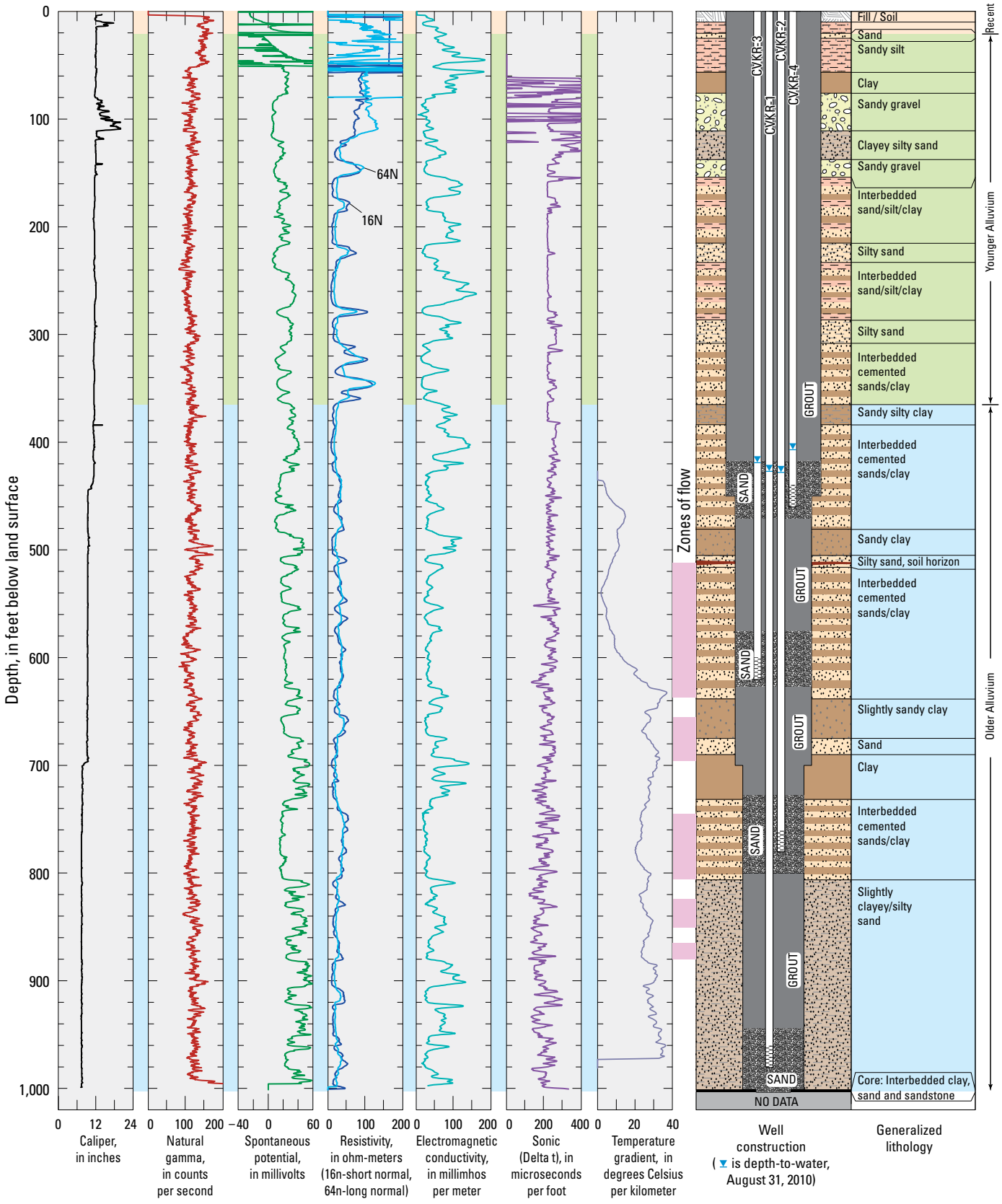

Figure 3. Geophysical logs, well-construction diagram, and generalized lithologic description for multiple-well monitoring site Cuyama Valley Kirschenmann Road (CVKR), Cuyama Valley, Santa Barbara County, California.

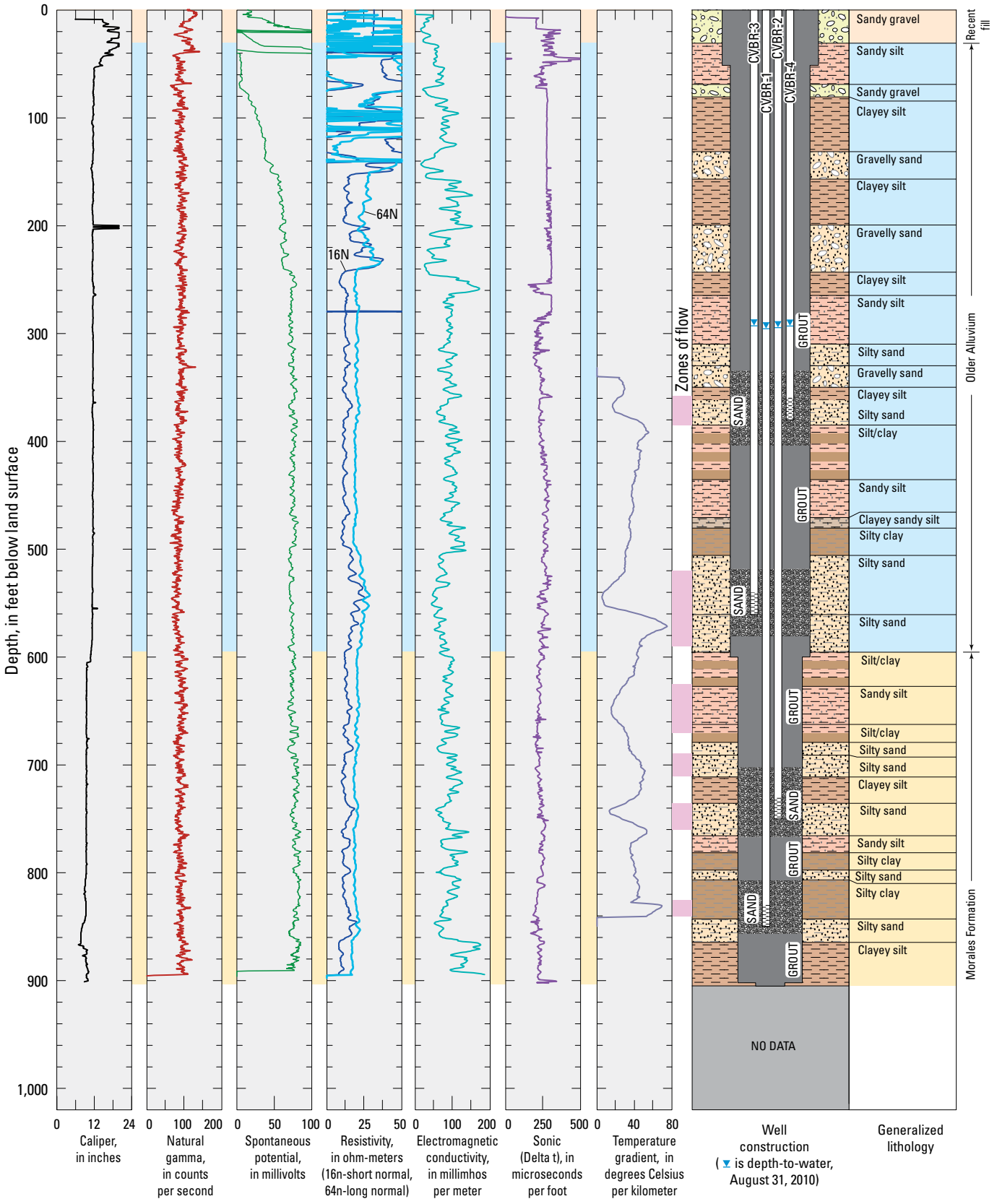

Figure 4. Geophysical logs, well-construction diagram, and generalized lithologic description for multiple-well monitoring site Cuyama Valley Bell Road (CVBR), Cuyama Valley, Santa Barbara County, California.

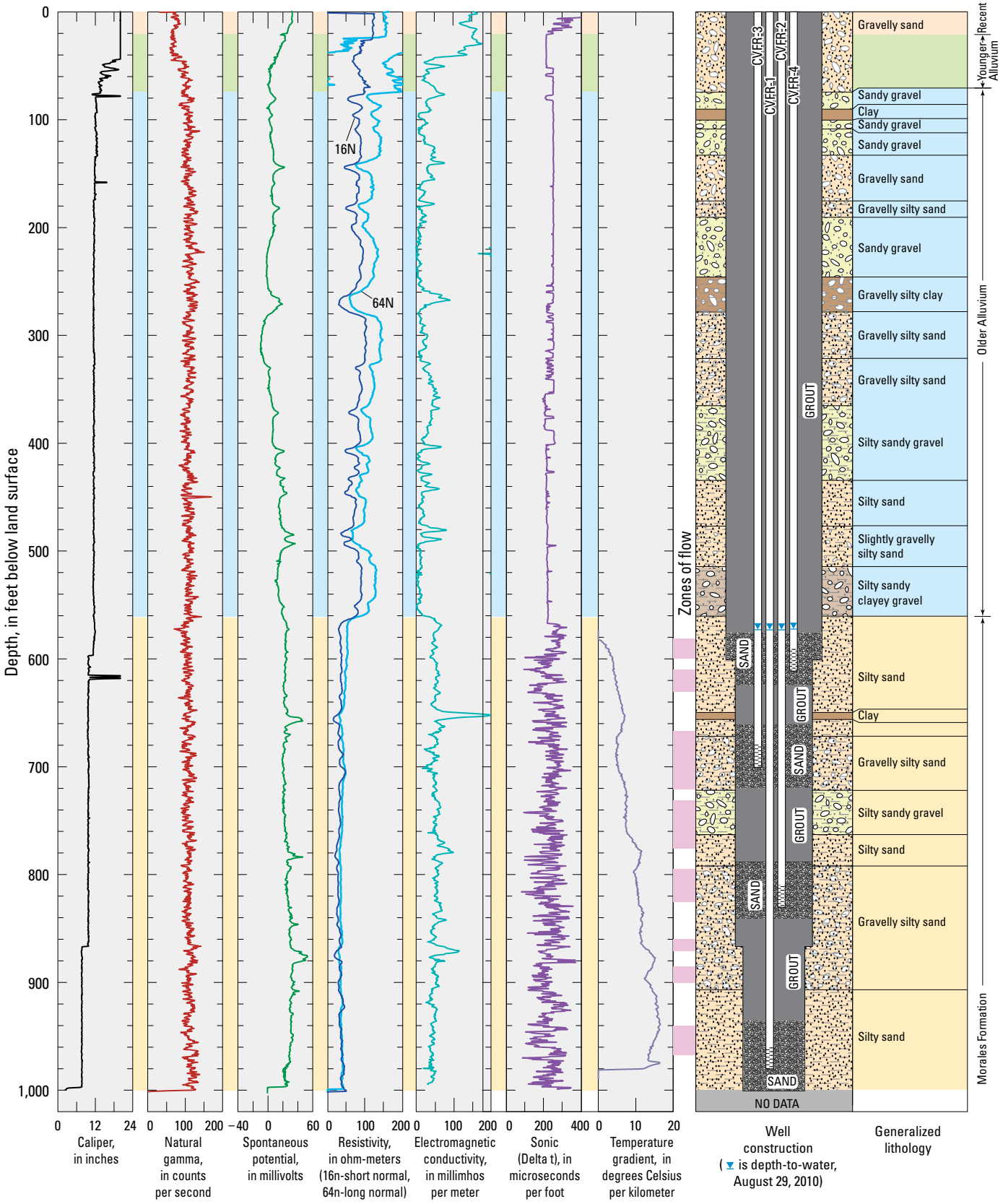

Figure 5. Geophysical logs, well-construction diagram, and generalized lithologic description for multiple-well monitoring site Cuyama Valley Foothill Road (CVFR), Cuyama Valley, Santa Barbara County, California.

Geology

Geologic information was collected to characterize and correlate stratigraphic units and boundaries associated with the aquifer system. Geologic information for each multiple-well monitoring site included lithologic cutting descriptions and a suite of geophysical logs. At two locations, CVKR and CVBR, whole core samples were collected.

Lithologic Descriptions

Detailed lithologic logs were compiled from descriptions of drill cuttings or whole core samples collected at each borehole site and from observations recorded during drilling. Cuttings samples (tables 4–6), termed "sieved drill cuttings," were composited from 20-foot depth intervals and sieved at the borehole surface by using a No. 120 sieve (0.125-mm screen opening). Additional cutting samples, termed "shaker cuttings," were collected at 10-ft depth intervals from a No. 60 screen (0.250-mm screen opening) mounted on the drill rig's shaker tank.

Sieve and shaker cuttings were first described in the field. Subsequently, samples were examined in greater detail in the office by using a microscope and characterized by grain size, texture, sorting, rounding, color, and other features.

Texture descriptions followed the National Research Council (National Research Council, 1947) grain-size classification shown in figure 6. This classification allows for correlation of grain-size terms (such as "sand") to size limits in millimeters or inches. For samples containing gravel, the terms "silt" and "clay" are used in lieu of "mud." Color, determined on moist samples, followed the numerical color designations in Munsell Soil Color Charts (Munsell Color, 1994). Lithologic logs from the sieved drill cuttings are presented in tables 4–6.

The generalized lithology next to each monitoring site diagram (figs. 3–5) was compiled by grouping similar lithologic units, as determined from the detailed lithologic logs from the sieved and shaker samples. The lithologic units were categorized into textural groups, such as gravels or sands (fig. 6), on the basis of estimated percentages of gravel and sand and the ratios of sand, silt, and clay present following the nomenclature of Folk (1954). Information collected from borehole geophysical logs also was used to help identify contact depths between major lithologic units.

Geophysical Logs

Borehole geophysical surveys provided information about the nature of the lithologic units and the water chemistry and flow patterns of groundwater. Geophysical log surveys were done shortly after attaining total hole depth in the uncased, fluid-filled borehole. These surveys included caliper, bulk-natural gamma, spontaneous potential, 16- and 64-inch normal resistivity, electromagnetic induction, and acoustic logs. High-resolution temperature logs were performed in the deepest completed well at each site at a later date. Geophysical logs for each multiple-well monitoring site are presented in figures 3–5.

Calipers were used to measure the diameter of the borehole. The caliper log can be used to identify the depth intervals of consolidated layers, washed-out sand, or the presence of swelling clay. Caliper logs also are useful in the construction of multiple-well sites by providing accurate borehole-volume calculations for placement of sand filter packs and environmental sealing materials.

Bulk natural-gamma logs measure the intensity of gamma-rays emitted from the natural decay of potassium-40 and of the daughter products of uranium and thorium (Schlumberger, 1972). Gamma logs are used primarily to define lithology indicators and for correlation of geologic units among boreholes within the same region. Typically, increases in gamma-ray emissions are observed in clay, feldspar-rich sand and gravel, and granite.

The spontaneous potential (SP) log measures the difference in electrical potentials, as a voltage, that develops at the contacts between different formations, such as shale or clay beds and a sand aquifer. Spontaneous potential is a function of the chemical activities of fluids in the borehole and adjacent rocks, the temperature, and the type and quantity of clay present; therefore, SP logs are directly influenced by the drilling fluid in undeveloped water wells. If the drilling fluid in the borehole is fresher than the native interstitial water, there is a negative spontaneous potential opposite sand beds—this is the so-called standard response. If the salinities are reversed, the spontaneous-potential response is reversed also (Keys and MacCary, 1983). SP logs are not directly related to porosity or permeability.

Resistivity tools measure the apparent resistivity of a volume of material surrounding the borehole under the direct application of an electric current (Keys and MacCary, 1983). These logs are used to determine formation and fluid resistivity and to estimate formation porosity. In general, low resistivity indicates water with higher concentrations of dissolved solids or fine-grained deposits such as silt, clay, and shale; high resistivity indicates water with lower concentrations of dissolved solids or coarser material, such as sand or gravel.

The 16-in. normal resistivity probe measures the apparent resistivity of material surrounding the borehole that was most likely invaded with drilling fluid. The 64-in. normal resistivity probe measures the apparent resistivity at a greater radius, which is considered to be representative of material that is saturated with formation water beyond the invaded zone. Comparison of the two logs is a useful indicator of aquifer zones with relatively high total dissolved solids.

Electromagnetic (EM) induction logs yield detailed information about the vertical electrical conductivity of the formation and pore water (McNeill, 1986). Electrical conductivity is affected by the porosity, permeability, clay and silt content of the sand-and-gravel aquifers, and the dissolved-solids concentration of the groundwater in the aquifer. EM induction logs can help identify water-bearing units to

Table 4. Lithologic log from sieved drill cuttings (0.125-millimeter screen opening) from multiple-well monitoring site Cuyama Valley Kirschenmann Road (CVKR).

Depth (ft)		Description
From	To	
0	20	Sand (S); fine to coarse sand; well sorted; angular to subangular; very pale brown (10YR 7/4)
20	40	Sand (S); fine to medium sand; well sorted; angular to subangular; yellowish brown (10YR 5/4)
40	60	Clayey sand (cS); fine to coarse sand with clay; well sorted; subangular; yellowish brown (10YR 5/4)
60	80	Slightly gravelly sand ((g)S); medium sand with granules to small pebbles; well sorted; subangular; yellowish brown (10YR 5/4)
80	100	Gravelly sand (gS); fine to coarse sand with granules to medium pebbles; poorly sorted; subrounded to subangular; yellowish brown (10YR 5/4)
100	120	Gravelly sand (gS); very fine to coarse sand with granules to small pebbles; poorly sorted; subrounded to subangular; yellowish brown (10YR 5/4)
120	140	Gravelly sand (gS); fine to coarse sand with granules to medium pebbles; poorly sorted; subrounded to subangular; yellowish brown (10YR 5/4)
140	160	Slightly gravelly sand ((g)S); very fine to very coarse sand with minor small pebbles; poorly sorted; subrounded to subangular; yellowish brown (10YR 5/4)
160	180	Slightly gravelly sand ((g)S); fine to coarse sand with minor granules; poorly sorted; subrounded to subangular; yellowish brown (10YR 5/4)
180	200	Sand (S); medium to very coarse sand; moderately sorted; subrounded to subangular; yellowish brown (10YR 5/4)
200	220	Slightly gravelly sand ((g)S); fine to very coarse sand with granules to small pebbles; poorly sorted; subrounded to subangular; yellowish brown (10YR 5/4)
220	240	Gravelly sand (gS); fine to coarse sand with granules; poorly sorted; subrounded to subangular; yellowish brown (10YR 5/4)
240	260	Slightly gravelly clayey sand ((g)mS); medium to coarse sand with clay and small pebbles; poorly sorted; subrounded to subangular; yellowish brown (10YR 5/4)
260	280	Clayey sand (cS); medium sand with clay; very well sorted; rounded to subrounded; yellowish brown (10YR 5/4)
280	300	Clayey sand (cS); medium sand with clay; very well sorted; rounded to subrounded; yellowish brown (10YR 5/4)
300	320	Sand (S); fine to medium sand; well sorted; subrounded to subangular; yellowish brown (10YR 5/4)
320	340	Sand (S); fine to medium sand; well sorted; subrounded to subangular; yellowish brown (10YR 5/4)
340	360	Sand (S); fine to medium sand; well sorted; subrounded to subangular; yellowish brown (10YR 5/4)
360	380	Slightly gravelly sand ((g)S); medium to coarse sand with minor granules; well sorted; subrounded to subangular; yellowish brown (10YR 5/4)
380	400	Sand (S); medium to coarse sand; well sorted; subrounded to subangular; yellowish brown (10YR 5/4)
400	420	Sand (S); medium to coarse sand; well sorted; subrounded to subangular; yellowish brown (10YR 5/4)
420	440	Sand (S); medium to coarse sand; well sorted; subrounded to subangular; yellowish brown (10YR 5/4)
440	460	Sand (S); medium to very coarse sand; well sorted; rounded to subrounded; yellowish brown (10YR 5/4)
460	480	Sand (S); medium to very coarse sand; well sorted; rounded to subrounded; yellowish brown (10YR 5/4)
480	500	Sand (S); fine to medium sand; well sorted; rounded to subrounded; yellowish brown (10YR 5/4)
500	520	Sand (S); very fine to medium sand; moderately sorted; subrounded to subangular; yellowish brown (10YR 5/4)
520	540	Sand (S); very fine to medium sand; moderately sorted; subrounded to subangular; yellowish brown (10YR 5/4)
540	560	Sand (S); very fine to medium sand; moderately sorted; subrounded to subangular; yellowish brown (10YR 5/4)
560	580	Sand (S); very fine to medium sand; moderately sorted; subrounded to subangular; yellowish brown (10YR 5/4)
580	600	Sand (S); very fine to medium sand; moderately sorted; subrounded to subangular; yellowish brown (10YR 5/4)
600	620	Sand (S); fine to medium sand; well sorted; subangular; yellowish brown (10YR 5/4)
620	640	Sand (S); fine to coarse sand; well sorted; subangular; yellowish brown (10YR 5/4)
640	660	Sand (S); fine to coarse sand; well sorted; subangular; yellowish brown (10YR 5/4)
660	680	Sand (S); fine to coarse sand; moderately sorted; subangular; yellowish brown (10YR 5/4)
680	700	Sand (S); fine to coarse sand; moderately sorted; subangular; yellowish brown (10YR 5/4)
700	720	Sand (S); fine to coarse sand; moderately sorted; subangular; yellowish brown (10YR 5/4)
720	740	Sand (S); fine to coarse sand; moderately sorted; subangular; yellowish brown (10YR 5/4)
740	760	Sand (S); fine to coarse sand; moderately sorted; subangular; yellowish brown (10YR 5/4)
760	780	Sand (S); fine to coarse sand; moderately sorted; subangular; yellowish brown (10YR 5/4)
780	800	Sand (S); fine to coarse sand; moderately sorted; subangular; yellowish brown (10YR 5/4)
800	820	Sand (S); fine to coarse sand; moderately sorted; subrounded to subangular; yellowish brown (10YR 5/4)
820	840	Sand (S); fine to coarse sand; moderately sorted; subrounded to subangular; yellowish brown (10YR 5/4)
840	860	Sand (S); fine to medium sand; well sorted; subangular; yellowish brown (10YR 5/4)
860	880	Sand (S); fine to coarse sand; moderately sorted; angular to subangular; yellowish brown (10YR 5/4)
880	900	Sand (S); fine to coarse sand; moderately sorted; angular to subangular; yellowish brown (10YR 5/4)
900	920	Sand (S); fine to coarse sand; moderately sorted; angular to subangular; yellowish brown (10YR 5/4)
920	940	Sand (S); fine to coarse sand; moderately sorted; subangular; yellowish brown (10YR 5/4)
940	960	Sand (S); fine to coarse sand; moderately sorted; subangular; yellowish brown (10YR 5/4)
960	980	Sand (S); fine to coarse sand; well to moderately sorted; subangular; yellowish brown (10YR 5/4)
980	1,000	Sand (S); fine to coarse sand; well to moderately sorted; subangular; yellowish brown (10YR 5/4)
980	1,000	Sand (S); medium to coarse sand with trace granules; well sorted; angular to subangular; yellowish brown (10YR 5/4)

Table 5. Lithologic log from sieved drill cuttings (0.125-millimeter screen opening) from multiple-well monitoring site Cuyama Valley Bell Road (CVBR).

Depth (ft)		Description
From	To	
0	19	Slightly gravelly sand ((g)S); medium to coarse sand with minor small pebbles; well to moderately sorted; subrounded to subangular; light yellowish brown (2.5Y 6/4)
19	39	Gravelly sand (gS); medium to very coarse sand with granules to medium pebbles; moderately sorted; subrounded to subangular; light yellowish brown (2.5Y 6/4)
39	60	Sand (S); fine to medium sand; well sorted; subrounded to subangular; light yellowish brown (2.5Y 6/4)
60	80	Sand (S); fine to coarse sand; moderately sorted; subrounded to subangular; light yellowish brown (2.5Y 6/4)
80	100	Sand (S); fine to coarse sand; moderately sorted; subrounded to subangular; light yellowish brown (2.5Y 6/4)
100	120	Sand (S); fine to coarse sand; moderately sorted; subrounded to subangular; light yellowish brown (2.5Y 6/4)
120	140	Sand (S); fine to coarse sand; moderately to poorly sorted; subrounded to subangular; light yellowish brown (2.5Y 6/4)
140	160	Sand (S); fine to very coarse sand with minor clay; poorly sorted; subrounded to subangular; light yellowish brown (2.5Y 6/4)
160	180	Sandy clay (sC); clay with very fine to medium sand; moderately sorted; light yellowish brown (2.5Y 6/4)
180	200	Sandy clay (sC); clay with fine to medium sand and trace coarse sand; moderately sorted; light yellowish brown (2.5Y 6/4)
200	220	Sand (S); fine to coarse sand; moderately to poorly sorted; subrounded to subangular; light yellowish brown (2.5Y 6/4)
220	240	Sand (S); fine to very coarse sand; poorly sorted; subrounded to subangular; light yellowish brown (2.5Y 6/4)
240	260	Silty sand (zS); medium to coarse sand with silt; moderately sorted; subrounded to subangular; light yellowish brown (2.5Y 6/4)
260	280	Slightly gravelly sand ((g)S); fine to very coarse sand with small amounts of medium pebbles; poorly sorted; subrounded to subangular; light yellowish brown (2.5Y 6/4)
280	300	Sand (S); fine to coarse sand; moderately to poorly sorted; subrounded to subangular; light yellowish brown (2.5Y 6/4)
300	320	Sand (S); fine to coarse sand; moderately sorted; rounded to subrounded; light yellowish brown (2.5Y 6/4)
320	340	Silty sand (zS); fine to coarse sand with silt; moderately to poorly sorted; rounded to subrounded; light yellowish brown (2.5Y 6/4)
340	360	Slightly gravelly silty sand ((g)mS); fine to coarse sand with silt and small pebbles; poorly to very poorly sorted; subrounded to subangular; light yellowish brown (2.5Y 6/4)
360	380	Sand (S); very fine to coarse sand; moderately to poorly sorted; subrounded to subangular; light yellowish brown (2.5Y 6/4)
380	400	Silty sand (zS); very fine to coarse sand with silt; moderately to poorly sorted; subrounded to subangular; light yellowish brown (2.5Y 6/4)
400	420	Silty sand (zS); very fine to coarse sand with silt; moderately to poorly sorted; subrounded to subangular; light yellowish brown (2.5Y 6/4)
420	440	Silty sand (zS); very fine to coarse sand with silt; moderately to poorly sorted; subrounded to subangular; light yellowish brown (2.5Y 6/4)
440	460	Silty sand (zS); very fine to coarse sand with silt; moderately to poorly sorted; subrounded to subangular; light yellowish brown (2.5Y 6/4)
460	480	Sand (S); fine to coarse sand; moderately sorted; rounded to subrounded; light yellowish brown (2.5Y 6/4)
480	500	Sand (S); fine to medium sand; well sorted; rounded to subrounded; light yellowish brown (2.5Y 6/4)
500	520	Sand (S); fine to coarse sand; well sorted; rounded to subrounded; light yellowish brown (2.5Y 6/4)
520	540	Sand (S); fine to coarse sand; well sorted; rounded to subrounded; light yellowish brown (2.5Y 6/4)
540	560	Sand (S); fine to coarse sand; moderately sorted; subrounded to subangular; light yellowish brown (2.5Y 6/4)
560	580	Sand (S); fine to coarse sand; moderately sorted; subrounded to subangular; light yellowish brown (2.5Y 6/4)
580	600	Sand (S); fine to very coarse sand; moderately to poorly sorted; subrounded to subangular; light yellowish brown (2.5Y 6/4)
600	620	Sand (S); very fine to medium sand; well to moderately sorted; subrounded to subangular; light yellowish brown (2.5Y 6/4)
620	640	Sand (S); very fine to medium sand; well to moderately sorted; subrounded to subangular; light yellowish brown (2.5Y 6/4)
640	660	Sand (S); very fine to medium sand; well to moderately sorted; subrounded to subangular; light yellowish brown (2.5Y 6/4)
660	680	Sand (S); fine to coarse sand; moderately sorted; subrounded to subangular; light yellowish brown (2.5Y 6/4)
680	700	Sand (S); fine to coarse sand; moderately sorted; subrounded to subangular; light yellowish brown (2.5Y 6/4)
700	720	Sand (S); fine to coarse sand; moderately sorted; subrounded to subangular; light yellowish brown (2.5Y 6/4)
720	740	Sand (S); fine to coarse sand; moderately sorted; subrounded to subangular; light yellowish brown (2.5Y 6/4)
740	760	Sand (S); medium to coarse sand; well sorted; subrounded to subangular; light yellowish brown (2.5Y 6/4)
760	780	Sand (S); fine to coarse sand; moderately sorted; subrounded to subangular; light yellowish brown (2.5Y 6/4)
780	800	Sand (S); fine to coarse sand; moderately sorted; subrounded to subangular; light yellowish brown (2.5Y 6/4)
800	820	Sand (S); fine to coarse sand; moderately sorted; subrounded to subangular; light yellowish brown (2.5Y 6/4)
820	840	Sand (S); fine to medium sand; well sorted; subrounded to subangular; light yellowish brown (2.5Y 6/4)
840	860	Sand (S); fine to coarse sand; moderately sorted; subrounded to subangular; light yellowish brown (2.5Y 6/4)
860	880	Sand (S); fine to coarse sand; moderately sorted; subrounded to subangular; light yellowish brown (2.5Y 6/4)

Table 6. Lithologic log from sieved drill cuttings (0.125-millimeter screen opening) from multiple-well monitoring site Cuyama Valley Foothill Road (CVFR).

Depth (ft)		Description
From	To	
0	20	Sand (S); medium to coarse sand; well sorted; angular to subangular; light yellowish brown (2.5Y 6/3)
20	40	Slightly gravelly sand ((g)S); fine to coarse sand with minor amounts of medium pebbles; moderately sorted; angular to subangular; light olive brown (2.5Y 5/4)
40	60	Slightly gravelly sand ((g)S); fine to very coarse sand with minor amounts of granules; poorly sorted; subangular; light olive brown (2.5Y 5/3)
60	80	Sandy gravel (sG); small to medium pebbles with medium to very coarse sand; poorly sorted; subrounded to subangular; light olive brown (2.5Y 5/4)
80	100	Gravelly sand (gS); fine to coarse sand with granules to medium pebbles; poorly sorted; angular to subangular; light olive brown (2.5Y 5/4)
100	120	Sandy gravel (sG); small to medium pebbles with very fine to coarse sand; very poorly sorted; angular to subangular; light olive brown (2.5Y 5/4)
120	140	Gravelly sand (gS); very fine to coarse sand with granules to medium pebbles; very poorly sorted; angular to subangular; light olive brown (2.5Y 5/4)
140	160	Sandy gravel (sG); small to large pebbles with very fine to coarse sand; very poorly sorted; subrounded to subangular; yellowish brown (10YR 5/4)
160	180	Gravelly sand (gS); very fine to coarse sand with small to medium pebbles; poorly sorted; angular to subangular; yellowish brown (10YR 5/4)
180	200	Sandy gravel (sG); granules to very large pebbles with very fine to coarse sand; very poorly sorted; angular; yellowish brown (10YR 5/4)
200	220	Sandy gravel (sG); granules to medium pebbles with very fine to medium sand; poorly sorted; angular to very angular; yellowish brown (10YR 5/4)
220	240	Gravelly silty sand (gmS); fine to coarse sand with silt and small to medium pebbles; poorly sorted; subrounded to subangular; yellowish brown (10YR 5/4)
240	260	Gravelly silty sand (gmS); fine to coarse sand with silt and small pebbles; poorly sorted; subrounded to subangular; yellowish brown (10YR 5/4)
260	280	Gravelly sand (gS); medium to coarse sand with small pebbles; moderately sorted; subrounded to subangular; yellowish brown (10YR 5/4)
280	300	Sand (S); fine to medium sand; well sorted; subangular to subrounded; yellowish brown (10YR 5/4)
300	320	Sand (S); very fine to coarse sand; moderately sorted; rounded to subrounded; yellowish brown (10YR 5/4)
320	340	Sand (S); very fine to coarse sand; moderately sorted; angular to subangular; yellowish brown (10YR 5/4)
340	360	Slightly gravelly sand ((g)S); very fine to coarse sand with minor granules to small pebbles; poorly sorted; subrounded to subangular; yellowish brown (10YR 5/4)
360	380	Slightly gravelly sand ((g)S); very fine to very coarse sand with minor granules and clay; poorly sorted; angular to subangular; yellowish brown (10YR 5/4)
380	400	Sand (S); very fine to coarse sand; moderately to poorly sorted; subangular to subrounded; yellowish brown (10YR 5/4)
400	420	Gravelly sand (gS); very fine to coarse sand with granules; moderately sorted; angular to subangular; yellowish brown (10YR 5/4)
420	440	Gravelly sand (gS); very fine to coarse sand with granules; moderately sorted; angular to subangular; yellowish brown (10YR 5/4)
440	460	Sand (S); fine to coarse sand; moderately sorted; angular to subangular; yellowish brown (10YR 5/4)
460	480	Slightly gravelly sand ((g)S); fine to coarse sand with small amounts of granules; moderately sorted; angular to subangular; yellowish brown (10YR 5/4)
480	500	Sand (S); fine to coarse sand; moderately sorted; angular to subangular; yellowish brown (10YR 5/4)
500	520	Sand (S); fine to coarse sand; moderately sorted; angular to subangular; yellowish brown (10YR 5/4)
520	540	Sand (S); fine to coarse sand; moderately sorted; angular to subangular; yellowish brown (10YR 5/4)
540	560	Sand (S); fine to coarse sand; moderately sorted; angular to subangular; yellowish brown (10YR 5/4)
560	580	Sand (S); fine to coarse sand; moderately sorted; angular to subangular; yellowish brown (10YR 5/4)
580	600	Sand (S); fine to coarse sand; moderately sorted; angular to subangular; yellowish brown (10YR 5/4)
600	620	Sand (S); fine to coarse sand; moderately sorted; subrounded to subangular; yellowish brown (10YR 5/4)
620	640	Sand (S); fine to very coarse sand; moderately to poorly sorted; angular; yellowish brown (10YR 5/4)
640	660	Gravelly sand (gS); fine to very coarse sand with granules; poorly sorted; angular; yellowish brown (10YR 5/4)
660	680	Sand (S); fine to very coarse sand; poorly sorted; angular; yellowish brown (10YR 5/4)
680	700	Gravelly sand (gS); medium to very coarse sand with granules; moderately sorted; angular to subangular; yellowish brown (10YR 5/4)
700	720	Gravelly sand (gS); medium to very coarse sand with granules; moderately sorted; angular to subangular; yellowish brown (10YR 5/4)
720	740	Gravelly sand (gS); fine to very coarse sand with granules; poorly sorted; angular to subangular; yellowish brown (10YR 5/4)
740	760	Gravelly sand (gS); fine to very coarse sand with granules; poorly sorted; angular to subangular; yellowish brown (10YR 5/4)
760	780	Gravelly sand (gS); medium to very coarse sand with granules; moderately sorted; angular to subangular; yellowish brown (10YR 5/4)
780	800	Sand (S); fine to very coarse sand; moderately sorted; subrounded to subangular; yellowish brown (10YR 5/4)
800	820	Sand (S); fine to coarse sand; moderately sorted; subrounded to subangular; yellowish brown (10YR 5/4)
820	840	Gravelly sand (gS); fine to very coarse sand with granules to small pebbles; poorly sorted; subrounded to subangular; yellowish brown (10YR 5/4)

Table 6. Lithologic log from sieved drill cuttings (0.125-millimeter screen opening) from multiple-well monitoring site Cuyama Valley Foothill Road (CVFR).—Continued

Depth (ft)		Description
From	To	
840	860	Gravelly sand (gS); fine to coarse sand with granules; moderately to poorly sorted; subrounded to subangular; yellowish brown (10YR 5/4)
860	879	Sand (S); fine to very coarse sand; moderately to poorly sorted; subrounded to subangular; yellowish brown (10YR 5/4)
879	899	Slightly gravelly sand ((g)S); fine to medium sand with minor small pebbles; moderately sorted; subrounded to subangular; yellowish brown (10YR 5/4)
899	919	Sand (S); very fine to very coarse sand; poorly sorted; subrounded to subangular; yellowish brown (10YR 5/4)
919	939	Sand (S); very fine to medium sand; well to moderately sorted; subrounded to subangular; yellowish brown (10YR 5/4)
939	959	Sand (S); very fine to medium sand; well to moderately sorted; subrounded to subangular; yellowish brown (10YR 5/4)
959	979	Sand (S); fine to coarse sand; well to moderately sorted; subrounded to subangular; yellowish brown (10YR 5/4)
979	1,000	Sand (S); medium sand; very well sorted; subrounded to subangular; yellowish brown (10YR 5/4)

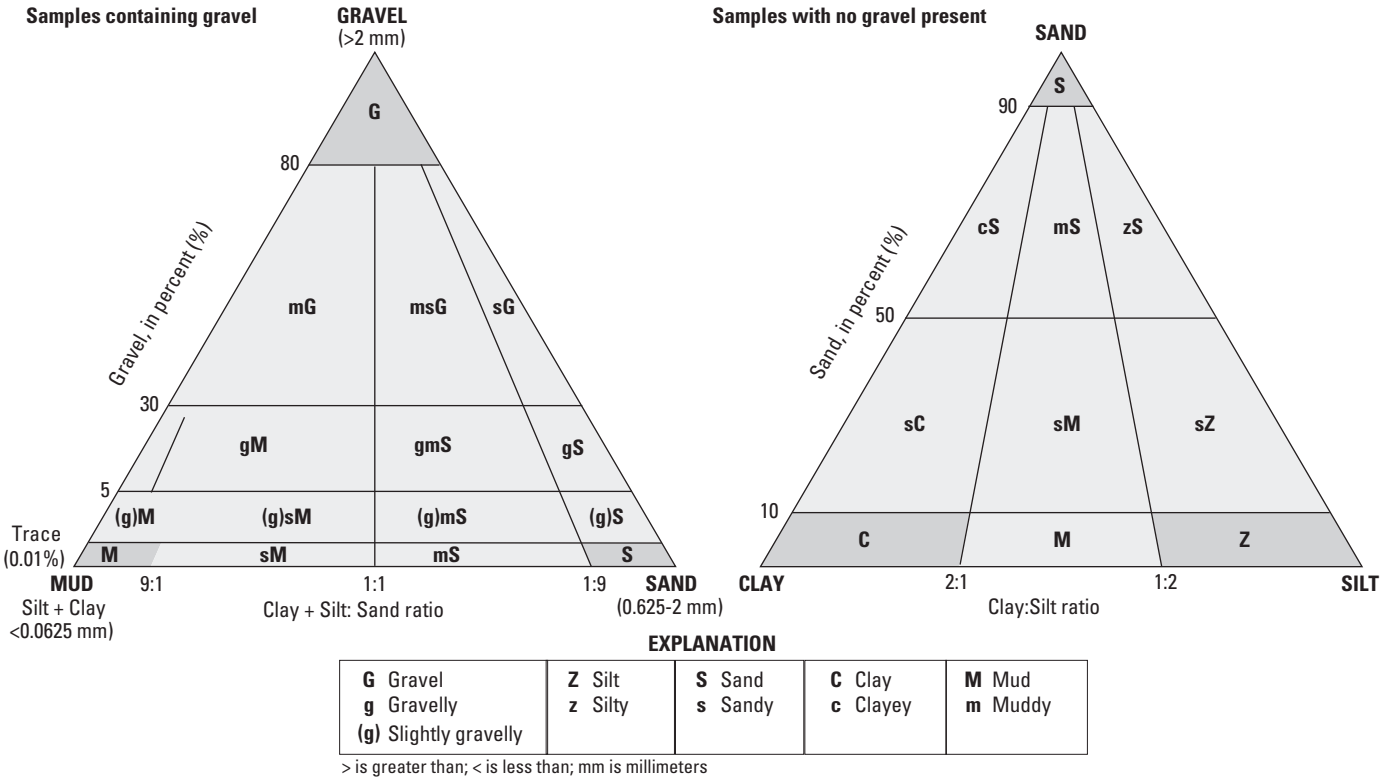

Figure 6. Rock-type nomenclature used for lithologic-log descriptions.

determine optimum depths for the placement of monitoring well screens and can help identify temporal changes in water quality through sequential logging (Williams and others, 1993).

An acoustic (sonic) log measures the time it takes for a pulsed compressional sound wave to travel from a downhole source to downhole receivers. The sonic tool used has two receivers, near and far, that recorded the arrival time of the compressional sound wave. The difference in arrival times between the receivers, or delta t, can be related to the physical properties of the adjacent material. In unconsolidated material, sonic logs principally are used to identify contacts between lithologic units that were penetrated by the borehole.

Temperature Logs

High-resolution borehole temperature logs were collected in the deepest well at each multiple-well monitoring site on June 24, 2010. To ensure that the water temperature was characteristic of ambient groundwater conditions, logging was performed several months after the site had been constructed, developed, and sampled for water-quality to allow sufficient time for the water column in the well to equilibrate with the surrounding material. Generally, groundwater temperature increases with depth, and the global average is about 25 degrees Celsius (°C) per kilometer. The geothermal gradient in sedimentary basins generally exceeds this average because of the relatively low thermal conductivity of sedimentary

materials (Ingebritsen and Sanford, 1998). Perturbations in the geothermal gradient in temperature logs can provide information about geologic formations as well as horizontal and vertical groundwater-flow patterns. Groundwater temperature is related to factors such as lithology (which affects thermal conductance), depth, recharge source, and residence time within the aquifer. Measured temperature logs, when expressed as a measured vertical temperature gradient and compared with the geothermal gradient, can be used to identify potential zones of groundwater flow. Depth intervals where the temperature gradient is concave upward, or increases more quickly than the geothermal gradient, are consistent with the cooling influence of groundwater flow through relatively permeable units. Depth intervals exhibiting greater temperature perturbation (relatively large increases in temperature gradient with depth) can be interpreted as zones of greater flow.

Changes in the temperature gradients were used, in conjunction with other logs, to identify discrete flow zones at each monitoring site (see figs. 3, 4 and 5). At the CVKR site (fig. 3), five flow zones were identified: (1) 513–637 ft, (2) 655–695 ft, (3) 745–804 ft, (4) 823–850 ft, and (5) 865–880 ft below land surface. A comparison of the magnitude of the vertical change in temperature gradient with depth among flow zones indicated a general decrease in flow with increasing depth and that the majority of flow at the CVKR site is in the shallowest zone. This zone not only is the thickest, but also showed the greatest temperature perturbation. At the CVBR site (fig. 4), six flow zones were identified: (1) 357–385 ft, (2) 520–590 ft, (3) 625–670 ft, (4) 690–710 ft, (5) 735–760 ft, and (6) 825–840 ft below land surface. A comparison of the flow zones indicated a general decrease in flow with increasing depth and that a majority of the flow is in zone 2. Similar in nature to the zone of greatest flow at CVKR site, zone 2 is the thickest at CVBR and also showed the greatest temperature perturbation. At the CVFR site (fig. 5), eight flow zones were identified: (1) 580–600 ft, (2) 610–630 ft, (3) 667–720 ft, (4) 730–775 ft, (5) 795–825 ft, (6) 860–870 ft, (7) 885–900 ft, and (8) 940–967 ft below land surface. Overall, differences in flow among zones at CVFR were less apparent than at the other sites, as was indicated by a relatively small perturbation in the gradient. The majority of flow at CVFR could be in the deepest zones (7 and 8), unlike the CVKR and CVBR sites. Although the deeper zones at CVFR are not as thick as some of the shallower zones, they exhibited greater fluctuations in the temperature gradient.

Core Measurements

Core samples were collected from the bottom of the borehole at the CVKR and CVBR sites. The cores were collected in 3-inch-diameter thin-walled metal tubes. Each coring “push” retrieved a cylinder of sediment as long as 3 feet. The locations, depths, and the total recovery of these core samples are given in table 7. The CVKR core was analyzed for bulk density and sonic velocity (fig. 7) by using a multi-sensor core log scanner (Kayen and others, 1999). The CVKR core varied in density from approximately 1.5–2.7 grams per cubic centimeter. Density changes indicated seven distinct layers within the 2.8 feet of recovered sediment. On the basis of a visual inspection of the top and bottom of the core, and the density measurements, the core was characterized as interbedded clay, sand, and sandstone. The CVBR core was not analyzed with a multi-sensor core log scanner. The top of the core contained clay and minor fine sands, and the bottom of the core contained a silty very fine to medium sand. For any future use, the cores were sealed and are stored under refrigerated conditions at the USGS core storage facility in Menlo Park, California.

Geology at the Monitoring Well Sites

Geologic maps of the Cuyama Valley (Vedder and Repenning, 1975; Kellogg and others, 2008) show two units of Holocene and Pleistocene-aged alluvial deposits, termed younger and older alluvium, underlying the three monitoring-well sites. Interpretive geologic cross sections, which were based in part on deep oil and gas exploration wells, showed that these alluvial deposits extend to a depth of approximately 1,000 ft bls beneath the monitoring-well sites (Vedder and Repenning, 1975). These alluvial deposits are underlain by the weakly to moderately indurated arkosic Morales Formation of Pleistocene to upper Pliocene age. The three multiple-well monitoring sites test different sections of the basin-fill alluvial stratigraphy relative to their locations within the basin (fig. 1). The CVKR site is in the main axis of Cuyama Valley in younger alluvium, west of the active alluvial channel of the Cuyama River. The CVFR site, 3.8 miles to the southeast of CVKR at the northern edge of the Central Sierra Madre Foothills zone, is also west of the active alluvial channel of the Cuyama River, but is close to the mapped contact between

Table 7. Summary of cores collected from multiple-well monitoring sites, Cuyama Valley groundwater basin, Santa Barbara County, California.

[See table 1 for definitions of common well names. **Abbreviations**: —, data not available; ft bls, feet below land surface; %, percent; F, fine; VF, very fine; M, medium; C, coarse]

Common well name	Core ID (site-core#-section)	Top of core interval (ft bls)	Bottom of core interval (ft bls)	Total core-interval length (ft)	Total recovery (%)	Description
CVKR	CVKR-1C-1	1,000.5	1,003.5	3	93	Interbedded clay, sand, and sandstone throughout
CVBR	CVBR-1C-1	903	906	3	88	Top: clay with minor sand (F); Bottom: Silty sand (VF-M with trace C)
CVFR	—	—	—	—	—	No core collected

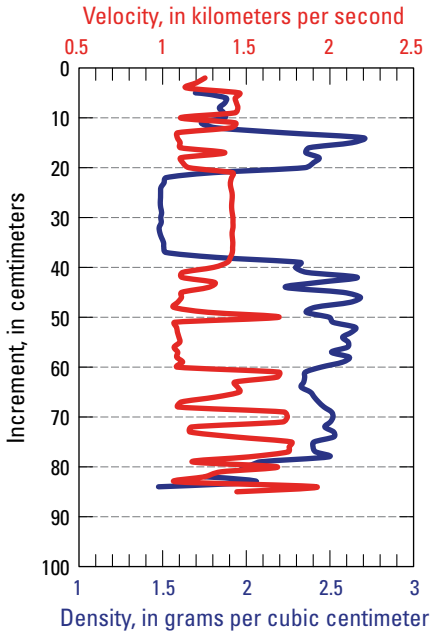

Figure 7. Sonic velocity and bulk density of core CVKR-1C-1 collected from the bottom of the Cuyama Valley Kirschenmann Road (CVKR) borehole, Cuyama Valley, Santa Barbara County, California.

younger and older alluvium. The CVBR site is in the alluvial uplands that lie to the north of the Sierra Madre Mountains and south of Cuyama Valley, next to the Salisbury Canyon drainage. The well site is in older alluvium; the site is above and to the west of the young alluvial fill in the main part of the valley.

Lithologic and borehole geophysical logs aided distinguishing among the younger and older alluvium and the underlying Morales Formation. Younger alluvium in Cuyama Valley tends to be the coarsest-grained deposit, typically consisting of unconsolidated sand, gravel, and boulders, with some clay. These coarse-grained deposits tended to yield the greatest response on borehole resistivity logs and, where thin clays were present, indicated large SP-log deflections as well. By contrast, the relatively fine-grained, massively bedded Morales Formation typically yielded a subdued response on SP and resistivity logs. The older alluvium produced an intermediate response on borehole geophysical logs. Similar to the younger alluvium, the older alluvium contains unconsolidated to partly consolidated sand, gravel, and boulders, but the older alluvium also contains a significant amount of fine-grained arkosic sands and clays that are derived from erosional reworking of the underlying Morales Formation.

The CVKR borehole penetrated terrestrial siliciclastic sediments that are alluvial fan and stream deposits. The geophysical logs indicated a distinct drop-off in resistivity at about 365 ft bls, which was interpreted as the contact of younger alluvium overlying more consolidated older alluvium. Sediments encountered in the CVKR borehole at depths of 365–620 ft bls, correlating to the top of the Older Alluvium, were much more consolidated than expected from the descriptions of these units published on the geologic maps. A paleosol (buried soil horizon) was encountered at the CVKR site at approximately 505 ft bls, further subdividing the sequence of consolidated older alluvium (fig. 3). The highest level of natural gamma radioactivity was observed within, and just above, this paleosol. This paleosol was not encountered at the other drill sites.

On the basis of an absence of distinctive changes in either the geophysical logs or mineralogy of the sediments, the CVKR wellbore did not reach the Morales Formation. The core collected from the bottom of the borehole contained interbedded clay, sand, and sandstone. Two oil and gas exploration holes drilled 1,500 ft and 4,300 ft to the northwest of the CVKR borehole have geophysical logs that begin about 1,400 ft bls (California Division of Oil, Gas and Geothermal Resources, accessed in July 2009, at *http://owr.conservation.ca.gov/WellSearch/WellSearch.aspx*). Geophysical logs from these wells showed they were both in Morales Formation at this depth. If similar conditions exist beneath the CVKR site, this places a lower bound on the thickness of older alluvium at the CVKR site.

The CVBR borehole penetrated terrestrial siliciclastic sediments that are alluvial fan and stream deposits (fig. 4). The well penetrated an upper 30-ft thick section of sandy gravel with high and variable resistivity on borehole geophysical logs that can be interpreted as recent deposits (fig. 4). This thin layer of younger alluvium, consistent with the position of this well, is in the uplands on the southern edge of the valley, which are mapped as underlain by older alluvial deposits. The geophysical logs had an interval of moderate resistivity response between 30 ft bls and 240 ft bls that we interpreted as more consolidated older alluvium (fig. 4). The interval between 260 ft bls and 595 ft bls is characterized by silty sands, with some intervals of gravelly sands, and generally low-resistivity values on borehole geophysical logs. This interval was interpreted to be part of the older alluvium; it could correlate to the older, deformed alluvium of Vedder and Repenning (1975). This interval appeared to be lithologically similar to the underlying Morales Formation and could be composed, in large part, from sediments derived from erosion of the Morales Formation.

The contact between the older alluvium and the Morales Formation at CVBR was interpreted to be at about 595 ft bls and was below the deepest elevated resistivity values (fig. 4). Below this point, resistivity values were generally low, and the lithology is uniformly silty clay. No distinctive changes in the mineralogy of the sediments were observed at this site. The core collected from the bottom of the borehole contained a clay with minor fine sand and a silty very fine to medium sand. An oil and gas exploration well 2,900 ft to the northwest of CVBR was reported to have an electric-log response interpreted as Morales Formation at 840 ft bls,

where the geophysical logging of this hole began (California Division of Oil, Gas and Geothermal Resources, accessed on July, 2009, at *http://owr.conservation.ca.gov/WellSearch/WellSearch.aspx*). The top of the Morales Formation in this oil and gas exploration well is shallower than 840 ft bls, which is generally consistent with the interpreted top of the Morales in CVBR.

The CVFR borehole penetrated terrestrial siliciclastic sediments that are alluvial fan and stream deposits (fig. 5). The upper 75 ft of the hole are characterized by sandy gravel, granules to medium pebbles, and medium to very coarse sand with relatively high values of resistivity; this interval can be interpreted as recent deposits and younger alluvium. Deposits below 75 ft bls are also coarse-grained, but contain minor amounts of silt and clay and had less resistivity on geophysical logs; these deposits were interpreted as older, more consolidated alluvium. The relatively thin interval of younger alluvium is consistent with the location of this well near the mapped surface expression of the contact between younger and older alluvium.

The contact between the older alluvium and the underlying Morales Formation at CVFR was interpreted to be at 560 ft bls on the basis of the lack of pebbles and gravel and overall drop in resistivity values to consistently low values below this depth (fig. 5). No distinctive changes in the mineralogy of the sediments were observed at this site.

Geophysical logs from well CUY-06, on the east side of the Cuyama River 1.25 mi east-southeast of the CVFR site, showed a similar drop in resistivity at about 600 ft bls, which was interpreted as the depth of the contact between the older alluvium and the Morales Formation. Geophysical logs from an oil and gas exploration hole drilled 1-mi east-southeast of the CVFR borehole (California Division of Oil, Gas and Geothermal Resources, accessed on July, 2009, at *http://owr.conservation.ca.gov/WellSearch/WellSearch.aspx*) showed high resistivity values typical of younger alluvium to a depth of 1,100 ft bls, below which an abrupt drop in resistivity values to low values typical of the Morales Formation was observed. This well, very close to the active channel of the Cuyama River, could record the local presence of a channel scoured through the older alluvium, placing young alluvial channel fill directly on the Morales Formation.

Water-Quality

Groundwater samples were collected from the 12 monitoring wells (4 wells at each of the 3 multiple-well monitoring sites), 27 selected domestic and supply wells, and 2 springs (fig. 8). In addition, four surface-water samples were collected (fig. 8). Samples were analyzed for as many as 53 constituents, including field parameters (water temperature, specific conductance, pH, dissolved oxygen, and alkalinity); major and minor ions; nitrate; trace elements; stable isotopes of hydrogen and oxygen; tritium and carbon-14 activities; and species of arsenic, iron, and chromium. Selected water-quality constituents results are presented. Water-quality results not presented in this report are available through the USGS NWIS web site.

Field and Laboratory Methods

Sampling was done by USGS personnel, and all samples were collected, handled, and preserved following written USGS field procedures (U.S. Geological Survey, variously dated). Prior to sampling, water-level measurements were made, and at least three well-casing volumes were purged from the well. For monitoring wells, a portable submersible pump was used for purging and sampling the well; for domestic and supply wells, samples were collected from the discharge of the installed pump before it entered a storage tank or any treatment. Specific conductance, pH, and temperature were monitored during the purging process. Samples were collected only after these parameters had stabilized. Stability was attained when three successive measurements taken at intervals of 5 minutes or more differed by less than 5 percent for specific conductance, 0.1 units for pH, and 0.2°C for temperature. Purge logs, field measurements, and other information related to sample collection are on file at the USGS office in San Diego, California.

During sample collection, water from the pump was diverted into a special sample-collection chamber designed to minimize contamination. Most water samples intended for routine analyses (major and minor ions, nutrients, and trace elements) were pressure-filtered in the field through a polyethersulfone (PES) membrane capsule filter having a pore size of 0.45 µm. Laboratory samples intended for the analysis of pH, specific conductance, and acid-neutralizing capacity were not filtered. Polyethylene bottles were used to contain most samples and were rinsed three times with filtered native water prior to filling. Samples for nutrient determinations were collected in dark, opaque polyethylene bottles and preserved on ice to inhibit bacterial growth. Samples for cations and selected trace element determinations were collected in acid-rinsed polyethylene bottles and preserved by acidifying the sample to a pH less than 2 with a small volume of concentrated nitric acid. Samples for anion determination were collected in a natural polyethylene bottle and did not require preservation. Samples were shipped to the USGS National Water Quality Laboratory (NWQL) in Lakewood, Colorado, for analysis following standard methods outlined by Fishman and Friedman (1989), Fishman (1993), Struzeski and others (1996), Garbarino (1999), and Garbarino and others (2006).

Water samples for analysis of stable isotopes of hydrogen and oxygen (δ^2H and $\delta^{18}O$) were collected in 60-mL glass bottles. These samples were not filtered. The bottles were not rinsed, but were sealed with a special polyseal (conical) cap to minimize exchange with the atmosphere. These samples were shipped to the USGS Stable Isotope Laboratory in Reston, Virginia, for analysis according to methods outlined by Coplen

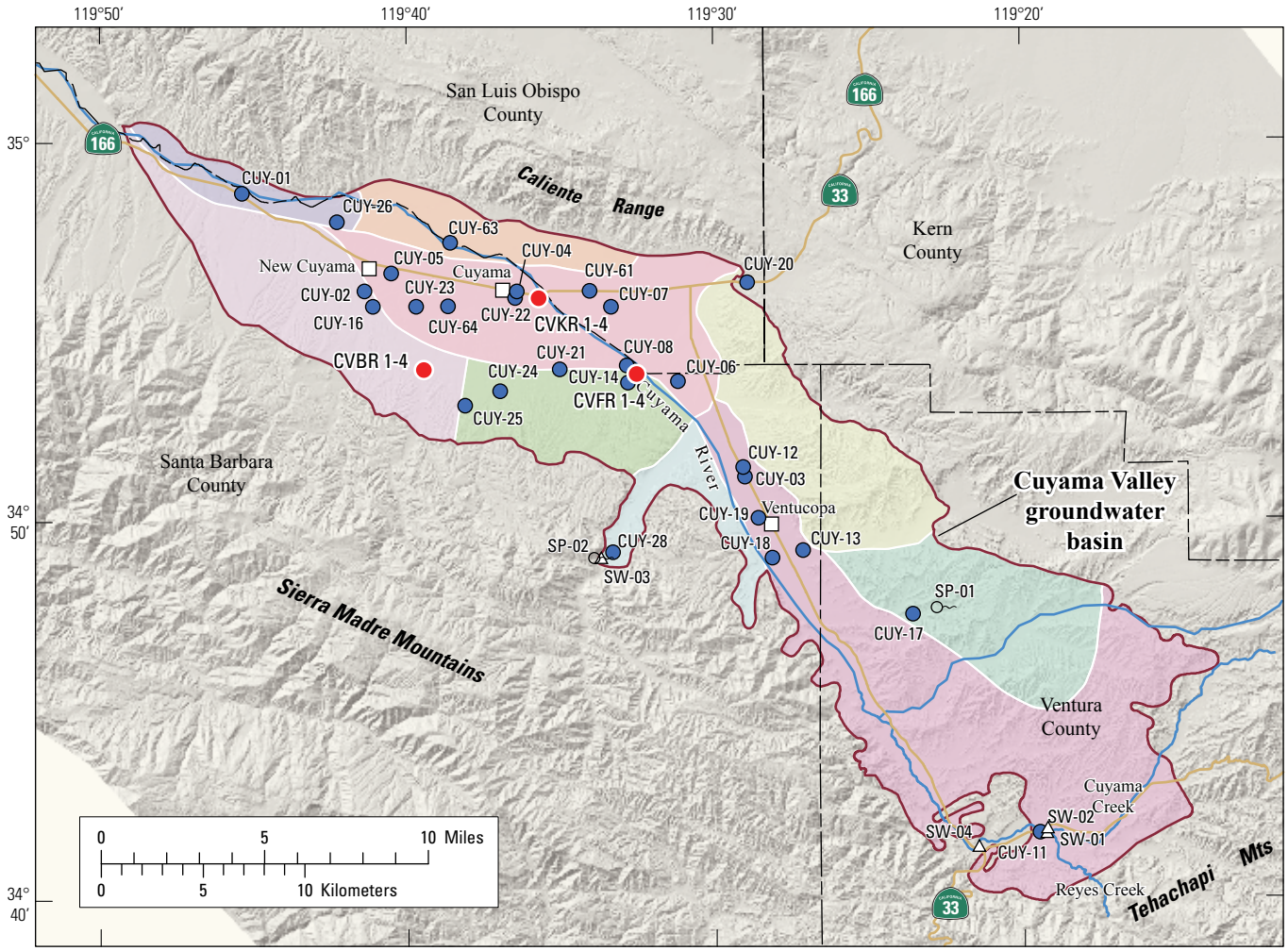

Shaded relief base created from 30-m digital elevation model from USGS National Elevation Dataset (NED), North America Vertical Datum 1988 (NAVD88)
Hydrology sourced from 1:24,000-scale National Hydrography Dataset, 1974–2009
Place names sourced from USGS Geographic Names Information System, 1974–2009
Albers Projection, NAD83

EXPLANATION

Cuyama groundwater basin zones
- Caliente Northern-Main
- Central Sierra Madre Foothills
- Northeast Ventucopa Uplands
- Northwestern Sierra Madre Foothills
- Northern Ventucopa Uplands
- Southern Sierra Madre Foothills
- Southern Ventucopa Uplands
- Southern-Main
- Western Basin

Site type
- Spring
- Surface-water site
- U.S. Geological Survey monitoring site
- Water-quality site

Figure 8. The location of multiple-well monitoring sites, domestic and supply wells, springs, and surface water sites with available water-quality data, Cuyama Valley, Santa Barbara County, California.

and others (1991). The results of these determinations are expressed in terms of per mil relative to Vienna Standard Mean Ocean Water (Gonfiantini, 1984). The estimates of precision (two-sigma) for δ^2H and $\delta^{18}O$ are 2 are 0.2 per mil, respectively.

Water samples intended for the analysis of tritium were collected in one-L polyethylene bottles. The samples were not filtered. Bottles were not rinsed and care was taken not to aerate the sample during collection. Samples were sealed with a polyseal (conical) cap to minimize exchange with the atmosphere. These samples were analyzed at the USGS Isotope Tracers Laboratory in Menlo Park, California, or at the University of Miami (through arrangements with the NWQL), by gas counting (or liquid scintillation) after electrolytic enrichment as described by Ostlund and Dorsey (1977) and Ostlund and others (1987). The activity of tritium is reported in terms of picocuries per liter (pCi/L) plus or minus the 1 sigma combined standard uncertainty (CSU). Tritium values less than the sample-specific critical level (ssLC) are reported as non-detections.

Water samples for analysis of $\delta^{13}C$ and carbon-14 isotopes were collected in either a 500-milliliter (mL) or one-liter (L) plastic coated glass bottle fitted with a polyseal cone cap. Samples were filtered in the field through PES membrane

capsule filter having a pore size of 0.45 micrometer (µm). The bottle was bottom-filled and allowed to overflow to several times the bottle volume, then sealed with a special Teflon-septa cap and held on ice. $\delta^{13}C$ and carbon-14 of the dissolved inorganic carbon were analyzed by the National Ocean Sciences Accelerator Mass Spectrometry Facility (NOSAMS) in Woods Hole, Mass., by accelerator mass spectrometry (through arrangements with the NWQL). Results of the $\delta^{13}C$ determination are reported in per mil relative to the Vienna PeeDee belemnite standard (Coplen, 1994). The activity of carbon-14 expressed as percent modern carbon (pmc) is reported with a 1-sigma estimate of precision relative to the 1950 National Bureau of Standards (NBS) oxalic acid standard (Stuiver and Polach, 1977; Wigley and Muller, 1981).

Water samples intended for analysis of chromium species were collected by using a 10-mL syringe with an attached 0.45-µm disk filter. After the syringe was thoroughly rinsed and filled with native water, 4 mL were forced through the disk filter; the next 2 mL of native water was slowly filtered into a small centrifuge vial and analyzed for total chromium. Hexavalent chromium, Cr (VI), was then collected by attaching a small cation-exchange column to the syringe filter, and after conditioning the column with 2 mL of sample water, two mL were collected in a second centrifuge vial. Vials for both constituents were preserved with 7.5 Normal (N) nitric acid (Ball and McCleskey, 2003a and 2003b). Water samples intended for analysis of arsenic and iron species were filtered into 250-mL polyethylene bottles that were covered with tape to prevent light exposure and preserved with 6 N hydrochloric acid. Total chromium, total arsenic, total iron, and the dissolved concentration of either the reduced or the oxidized species of the element were analyzed at the USGS National Research Program (NRP) Trace Metal Laboratory (TML) in Boulder, Colorado, by using various techniques of ultraviolet visible (UV-VIS) spectrophotometer and atomic absorbance spectroscopy (Stookey, 1970; Ball and McCleskey, 2003a and 2003b; McCleskey and others, 2003).

Comparison Benchmarks

Concentrations of constituents detected in groundwater samples were compared with U.S Environmental Protection Agency (USEPA) and California Department of Public Health (CDPH) regulatory and non-regulatory drinking-water health-based benchmarks and benchmarks established for aesthetic purposes (California Department of Public Health, 2012a and 2012b; U.S. Environmental Protection Agency, 2012a and 2012b). The chemical data presented in this report are meant to characterize the quality of the untreated groundwater within the primary aquifer system of the Cuyama Valley groundwater basin and are not intended to represent the treated drinking water delivered to consumers by water purveyors. The chemical composition of treated drinking water can differ from untreated groundwater because treated drinking water can be subjected to disinfection, filtration, mixing with other waters or exposure to the atmosphere prior to its delivery to consumers. Comparisons of untreated groundwater to benchmarks are for illustrative purposes only and are not indicative of compliance or non-compliance with drinking-water regulations. Three benchmarks—maximum contaminant level, secondary maximum contaminant level, and public health goal—are used for comparisons. The maximum contaminant level (MCL) is a legally enforceable standard that applies to public-water systems and is designed to protect public health by limiting the levels of contaminants in drinking water. MCLs established by the USEPA are the minimum standards with which states are required to comply, and individual states may choose to set more stringent standards. The CDPH has established MCLs for additional constituents not regulated by the USEPA, as well as lowered the benchmark concentrations for a number of constituents with MCLs established by the USEPA. In this report, a benchmark set by the USEPA is labeled "MCL-US," and one set by the CDPH that is more stringent than the MCL-US is labeled "MCL-CA." The secondary maximum contaminant level (SMCL) is a non-enforceable standard applied to constituents that affect the aesthetic qualities of drinking water, such as taste, odor, and color, or the technical qualities of drinking water, such as scaling and staining. Both the USEPA and the CDPH define SMCLs, but unlike MCLs, SMCLs established by the CDPH are not required to be at least as stringent as those established by USEPA. In this report, the USEPA SMCLs (SMCL-US) are used unless the SMCLs established by the CDPH (SMCL-CA) have a lower value. The public health goal (PHG) is a non-enforceable standard set by the California Office of Environmental Health Hazard Assessment (OEHHA). In this report, the public health goal (OEHHA-PHG) is listed for hexavalent chromium (Cr-VI), which does not have a MCL or SMCL; for constituents that have a MCL, the OEHHA-PHG is typically orders of magnitude lower than the MCL. The benchmark type and benchmark level are included in all tables with water-quality data.

Selected Chemical Attributes

Water-quality data indicated that the groundwater in the alluvial aquifer system generally has high concentrations of total dissolved solids and sulfate. Concentrations greater than the SMCL-US for total dissolved solids (greater than 500 mg/L) were observed in samples collected from 38 of 39 wells (97 percent); concentrations greater than the SMCL-US for sulfate (greater than 250 mg/L) were observed in samples collected from 37 of 39 wells (95 percent; table 8).

Table 8. Results for analyses of major and minor ions, silica, and total dissolved solids in samples collected from selected sites, Cuyama Valley groundwater basin, Santa Barbara County, California.

Table available separately as Microsoft Excel® at http://pubs.usgs.gov/sir/2013/5108.

Concentrations greater than the MCL-US for nitrate were observed in 5 of the 39 wells (13 percent; table 9). Concentrations greater than the MCL-US for arsenic were observed in 4 of 33 wells (12 percent; table 10). Concentrations of fluoride greater than the MCL-CA of 2 mg/L were observed in one well (CUY-20; table 8).

Table 9. Results for analyses of stable isotopes, tritium and carbon-14, estimated age since recharge, and nitrate in samples collected from selected sites, Cuyama Valley groundwater basin, Santa Barbara County, California.

Table available separately as Microsoft Excel® at http://pubs.usgs.gov/sir/2013/5108.

Table 10. Results for analyses of arsenic, iron, and chromium speciation and dissolved oxygen in samples collected from selected well sites, Cuyama Valley, Santa Barbara County, California.

Table available separately as Microsoft Excel® at http://pubs.usgs.gov/sir/2013/5108.

Five wells (CVKR-2, CVBR-1, CVBR-2, CVBR-3, CUY21) had concentrations of manganese greater than the SMCL-US of 50 µg/L; one of these wells (CUY-21) also had concentrations of iron greater than the SMCL-US of 300 µg/L (table 10). One well (CUY-20) had concentrations of chloride greater than the SMCL-US of 250 mg/L (table 8), and one well (CVKR-4) had concentrations of aluminum greater than the SMCL-US of 50 mg/L (table 10).

Major Ions

Piper diagrams show the relative abundance of major cations and anions (on a charge equivalent basis) as a percentage of the total ion content of the water (Piper, 1944). Piper diagrams often are used to define groundwater type (Hem, 1992). In this report, the dominant cation and anion species are used to describe the water type of a water sample when a single cation or anion composes more than 60 percent of the total cations or anions, respectively. Where no one cation or anion exceeds 60 percent, the first and second most abundant cations or anions are given for description purposes.

The samples from CVKR were characterized as calcium-magnesium sulfate waters (fig. 9*A*) and had total dissolved-solids concentrations ranging from 1,480 to 1,930 mg/L (table 8). The samples from CVBR were calcium-magnesium sulfate waters and had total dissolved-solids concentrations ranging from 772 to 1,560 mg/L. The samples from CVFR also were calcium-magnesium sulfate waters and had total dissolved-solids concentrations ranging from 1,140 to 1,480 mg/L. At the CVFR site, total dissolved-solids increased with depth, but the highest concentrations were observed in samples collected from the shallowest wells at the CVKR and CVBR sites. The majority of the other groundwater samples also were calcium-magnesium sulfate waters (fig. 9*B*). A few samples had a lesser abundance of calcium and magnesium and a greater abundance of sodium (fig.9*B*), which is consistent with loss of calcium and magnesium from solution by means of ion exchange with sodium attached to clays; this process is commonly observed in groundwater with longer residence times and abundant clays in the subsurface.

Nitrate

Samples from all 12 monitoring wells, 27 additional wells, 2 springs, and 2 surface-water sites were analyzed for nitrate. Nitrate concentrations reported as nitrogen (NO_3-N) ranged from less than 0.02 to 45.3 mg/L (table 9). Five of the samples (CVKR-4, CUY-04, -07, -20, and -61) had concentrations greater than the MCL-US of 10 mg/L.

At the CVKR site, nitrate concentrations ranged from 0.45 to 15.2 mg/L and decreased with depth. At the CVBR site, nitrate concentrations were 1.01 mg/L in the shallowest well and were below the detection limit of 0.04 in the three deeper wells. At the CVFR site, nitrate concentrations ranged from estimated values of 0.53 to 1.37 mg/L and, generally, increased with depth.

Irrigation return flows are a possible source of the high nitrate concentrations detected in the Cuyama Valley groundwater basin. A majority of the agricultural activity within the Cuyama Groundwater basin lies within the Caliente Northern-Main and Southern-Main zones and within the northern half of the Southern Ventucopa Uplands. Four of the wells (CVKR-4, CUY-4, -07, -61) where the nitrate levels were greater than the MCL were in the Southern-Main zone (fig. 8) in the center of the agricultural land-use area. A decrease in concentrations with depth at the CVKR site, in the center of the Southern-Main zone, indicated the source of higher nitrate concentrations is likely to be near the surface. Four wells (CUY-2, -16, -21, -28), where the observed nitrate levels were the lowest, below 0.15 mg/L, were south of the Southern-Main zone, outside of the agricultural-use area. Low concentrations of nitrate, less than 0.02 mg/L, in the surface-water samples indicated that surface-water recharge was not a source of high nitrate.

Isotope Analyses

Oxygen-18 (^{18}O) and deuterium (^{2}H) are naturally occurring stable isotopes of oxygen and hydrogen. The isotopic ratios are expressed in delta notation (δ) as per mil (parts per thousand) differences relative to the standard known as Vienna Standard Mean Ocean Water (VSMOW) (Gonfiantini, 1978). The $\delta^{2}H$ and $\delta^{18}O$ composition of precipitation throughout the world is linearly correlated because most of the world's precipitation is derived from the evaporation of seawater. This linear relationship is known as the global meteoric water line (Craig, 1961). The stable isotope ratios of oxygen and hydrogen in groundwater reflect the altitude, latitude, and temperature of recharge and the extent of evaporation before the water entered the groundwater system. Isotope ratios were analyzed from water samples collected from all of the monitoring sites, 21 selected wells, 4 surface-water collection sites, and 2 springs.

The isotope samples from the three deeper CVKR wells became progressively lighter (more negative), indicating that groundwater does not move freely between the different flow paths of the older alluvium and that the units within the

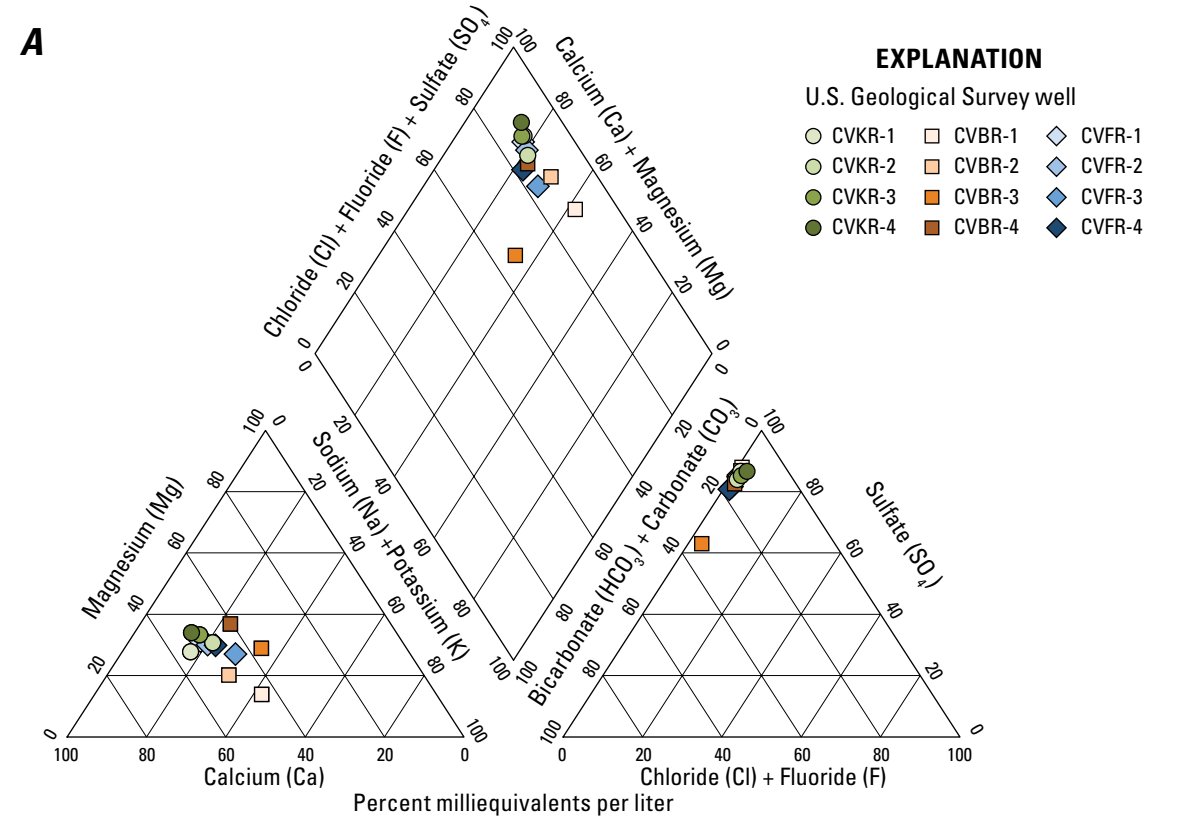

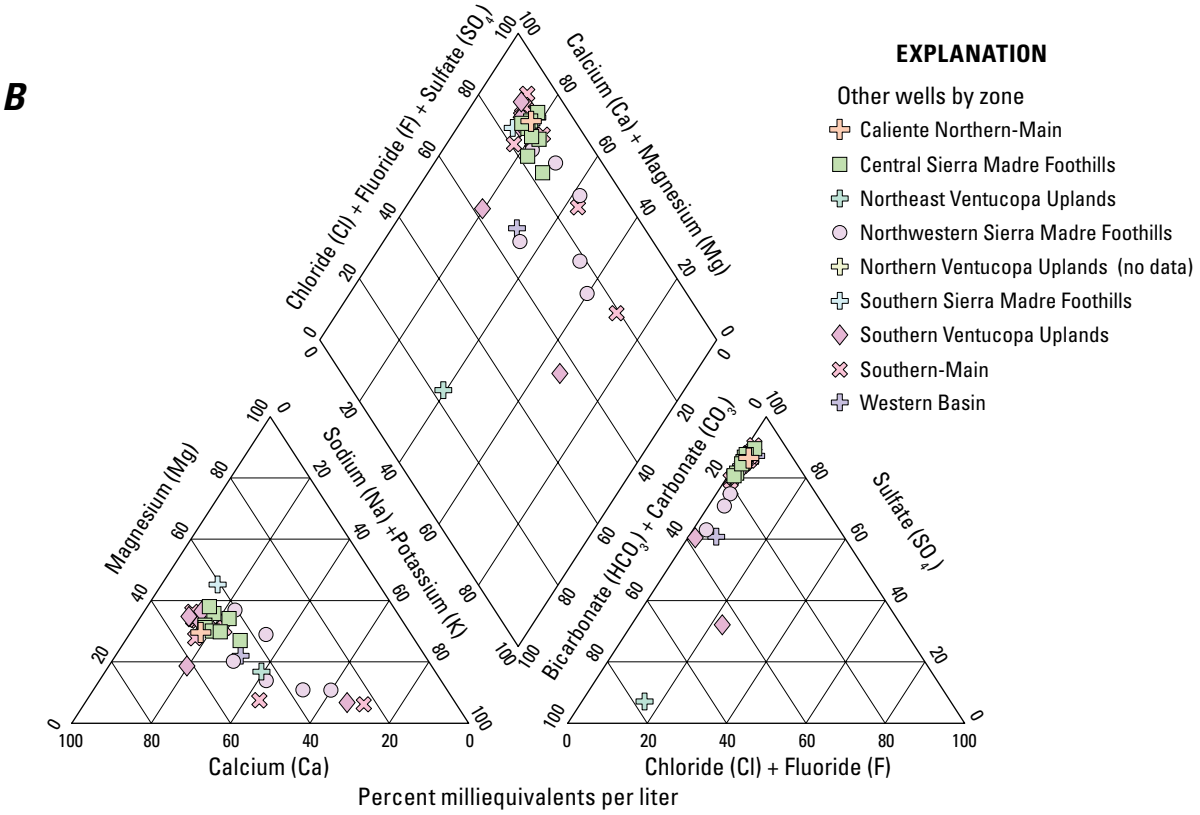

Figure 9. Piper diagrams depicting major-ion composition for groundwater samples, Cuyama Valley, California, collected from *A*, the selected multiple-well monitoring sites; and *B*, multiple-well monitoring sites, domestic and supply wells grouped by zone.

formations could have different sources of recharge (fig. 10*A*). The isotopic composition of the sample from the shallow well (CVKR-4) was similar to the composition of a surface-water sample collected from the nearby Cuyama River (SW-02), indicating a larger contribution from surface-water sources to this shallower depth interval than to the deeper wells at this site.

The isotope samples from the four CVBR wells were, in general, lighter in deuterium than the CVKR wells (fig. 10*A*). The range in values among the four wells also indicated that groundwater does not move freely between the older alluvium and the Morales Formation and that the units could have different sources of recharge.

The isotope samples from the four CVFR wells were the heaviest (least negative) from the three multiple-well monitoring sites (fig. 10*A*). The slightly different isotopic composition of the sample from the deep well (CVFR-1) indicated that groundwater might not move freely between units within the Morales Formation. The isotopic compositions of the four samples were between the compositions of the two surface-water samples collected from the nearby Cuyama River (SW-02 and SW-04), indicating the source of recharge could be the Cuyama River. The substantial difference in isotopic values between the SW-02 and SW-04 sites, which were relatively near each other on the Cuyama River, could reflect that SW-04 was sampled in late August, when evaporative effects on surface water would be expected to be greatest; in contrast, SW-02 was sampled in early April. Evaporation causes isotopic values to move to the right of the meteoric water line, and the isotopic composition of SW-04 is consistent with evaporative modification (fig. 10*A*). Because streamflow is higher in the spring, when evaporative effects are less, it is logical that recharge from Cuyama River water would have an isotopic composition closer to SW-02, a spring value, than SW-04, a summer value.

Restricted movement of water between units was also supported by the wide variability among the isotope samples from the other supply wells in the basin (fig. 10*B*). Samples from the Central Sierra Madre Foothills tended to be heavier (less negative) than most of the other samples. Samples from the Southern Ventucopa Uplands were similar to each other, indicating the same source of recharge. Samples from the Southern-Main and Northwestern Sierra Madre zone were typically lighter than samples from the Southern Ventucopa Uplands zone and trended along or below the meteoric water line, with the latter zone being lighter in deuterium. Isotope ratios for most samples from the Southern-Main zone were between the lightest samples from the Central Sierra Madre Foothills and most of the samples from the Southern Ventucopa Uplands, indicating that water in most of the Southern-Main zone could include a mixture of sources of recharge from the other two zones. Samples from the Southern-Main zone showed greater variation in isotope values than the other zones (fig. 10*B*), which is consistent with groundwater in this zone being derived from a variety of upgradient recharge sources.

Age Dating

Water samples from all of the wells at the CVKR, CVBR, and CVFR sites were analyzed for tritium and carbon-14. Ten other wells (CUY-01 through -08,-11, and -12) were analyzed for tritium, and twenty wells (CUY-01 through -08,-11, -12, and -17 through 26) and one spring (SP-01) were analyzed for carbon-14 (table 9). Tritium and carbon-14 activities provide information about the age (time since recharge) of groundwater. Tritium is a short-lived radioactive isotope of hydrogen; therefore, tritium concentrations above the detection level (0.3 picocuries per liter) indicate the presence of water recharged since the early 1950s, or recent recharge (Plummer and others, 1993; Clark and Fritz, 1997).

Samples from CVKR-3, CVKR-4, and CVBR-3 contained tritium concentrations near the detection level of 0.3 pCi/L, indicating recent recharge. Samples from CVKR-1, CVKR-2, CVBR-1, CVBR-2 and CVBR-4 contained concentrations less than 0.3 pCi/L, indicating that the water from these wells was recharged prior to the early 1950s. Post-1950s recharge in CVKR-3 and CVKR-4 was supported by relatively high NO_3-N concentrations in samples from these wells (table 9). Samples from all four wells at the CVFR site contained relatively high concentrations of tritium, indicating that the water from these wells contains water recharged since the 1950s. Tritium concentrations at the CVFR site increased with depth. The presence of modern water throughout the depth profile is most likely caused by local pumping. Pumping at depth can alter the natural flow paths and draw younger water from the edges of the basin under the shallower, non-pumped units or can draw younger water down to the pumped depths from above. Greater groundwater flows in the deeper depth intervals are consistent with the measured temperature gradients at CVKR and CVBR; however, fluctuations in temperature gradients at CVFR were greatly subdued relative to these sites, indicating lateral groundwater fluxes at CVFR are relatively modest. However, the isotopic data from CVFR were consistent with recharge derived from Cuyama River water at all depths. Because the CVFR site has an unsaturated zone that is nearly 570 ft thick with some clay layers (fig. 5), it is most likely that recharge from the Cuyama River followed horizontal and vertical flow paths through the saturated aquifer between the river and CVFR to reach these monitoring wells.

Tritium was detected in 14 of the 20 water samples collected from other wells (table 9). Tritium concentrations in these samples ranged from 0.43 to 9.0 pCi/L. The presence of tritium in most of the wells indicated that recent recharge contributes to the water resources in all zones in the Cuyama Valley groundwater basin.

Carbon-14 is a radioactive isotope of carbon with a half-life of about 5,700 years (Godwin, 1962). Carbon-14 activities are used to determine the age (time since recharge) of groundwater on time scales ranging from recent to more than 20,000 years before present (Izbicki and Michel, 2003). Carbon-14 ages presented in this report do not account for changes in carbon-14 activities resulting from chemical

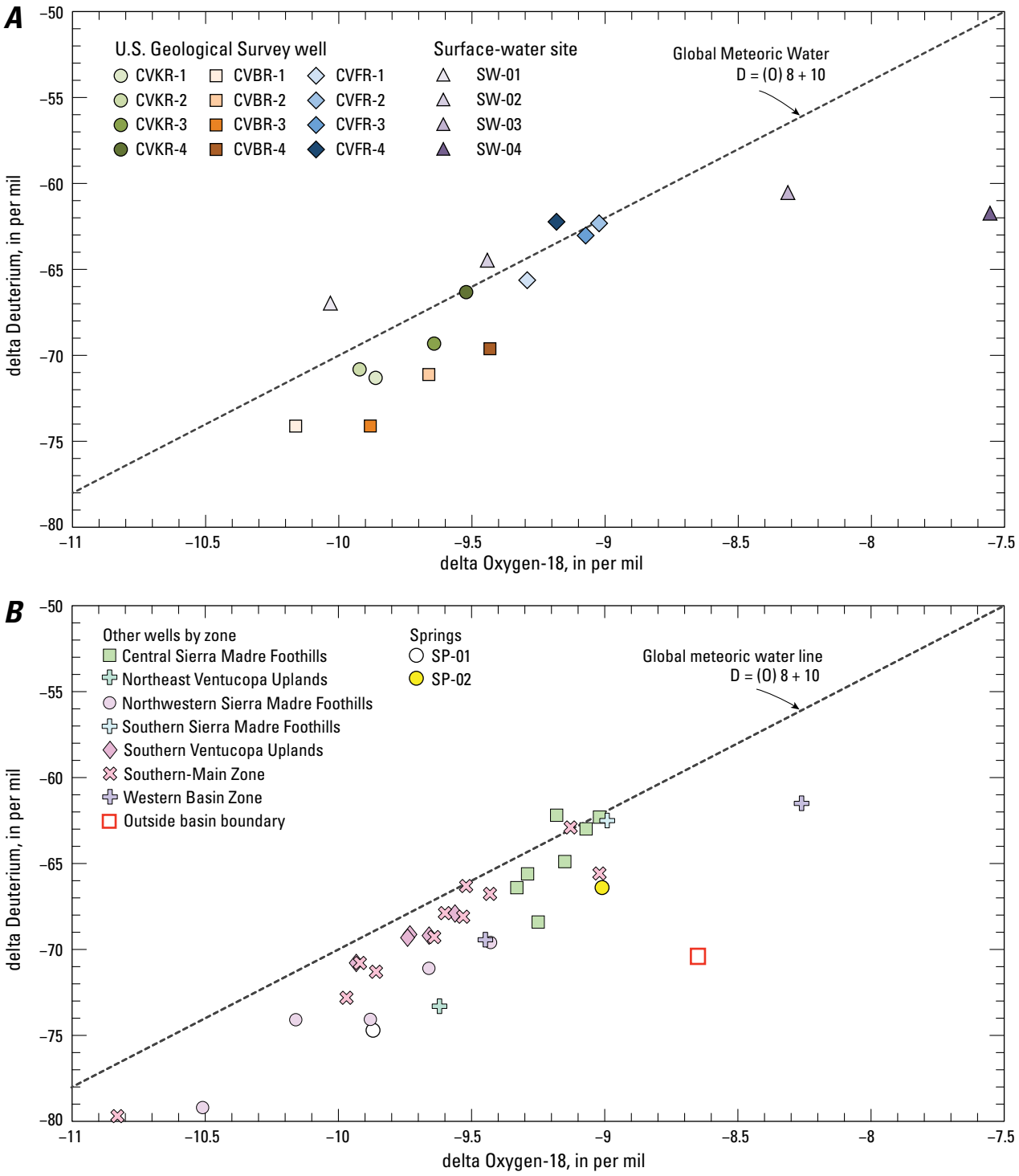

Figure 10. Isotopic composition of water samples, Cuyama Valley, California, collected from *A*, selected multiple-well monitoring sites and surface-water sites, and *B*, multiple-well monitoring sites, domestic and supply wells, grouped by zone and springs.

reactions or mixing and, therefore, are considered uncorrected ages. In general, uncorrected carbon-14 ages are older than the actual ages of the water after correction. Uncorrected ages (in years before present) were calculated by multiplying 8,033 by the natural log (ln) of the percent modern carbon expressed as a decimal as shown in the following equation (Stuiver and Polach, 1977):

Estimated age = 8,033 * ln (percent modern carbon/100 percent)

Uncertainties in the initial value of carbon-14 in recharge waters add uncertainties to the groundwater-age estimations using carbon-14; without more comprehensive geochemical modeling, the carbon-14 ages are to be treated as relative estimates of age rather than accurate, absolute estimates of age. Water from the CVKR and CVFR monitoring wells (near the Cuyama River) was found to be younger than the water from the CVBR monitoring wells (4 miles away from the Cuyama River). Estimated carbon-14 ages for the CVKR, CVBR, and CVFR sites ranged from 3,600 to 6,400, 20,900 to 31,200, and 2,700 to 3,100 years before present, respectively. Estimated ages increased with depth at the CVKR and CVBR sites. The samples from CVKR-3 and -4, CVBR-3, and CVFR-1, -2, -3, and -4 contained water with detectable tritium (recent recharge) and an uncorrected carbon-14 age of more than 2,700 years before present, indicating that these wells receive groundwater of different ages that are mixed in the sampled groundwater. In these mixed samples, tritium activities were less than 0.55 pCi/L in CVKR-3, and -4, and CVBR-3; these samples could contain relatively small amounts of modern water. The carbon-14 value in CVBR-3 was an order of magnitude less than in CVKR-3, -4; this comparison indicated that the water at CVBR-3 is primarily very old with a small fraction of modern water and that CVKR-3 and -4 could contain mixtures of water that do not span as wide a range of ages. The samples from CVFR had tritium activities that were an order of magnitude higher than CVKR-3, and -4, and CVBR-3; consequently, fractions of modern water in CVFR wells are likely to be much larger than in CVKR-3, and -4, and CVBR-3.

Estimated carbon-14 ages for the other 20 sites ranged from 600 (CUY-03) to 38,300 (CUY-23) years before present (table 9). In general, the youngest water was found in wells in the Southern Ventucopa Uplands; this zone is a source of recharge for the Cuyama Valley and the presence of younger water is expected. The oldest water was found in wells in the Southern-Main, Northwestern Sierra Madre Foothills, and Central Sierra Madre Foothills zones. This is in contrast to the observation of Singer and Swarzenski (1970) that a substantial component of regional flow was northward from the Sierra Madre Mountains. If a significant portion of the flow is from the Sierra Madres, water in this flow path would be expected to be younger than what was observed, unless formations deeper than the Morales Formation, previously thought to be non-water-bearing, are contributing to groundwater discharge from the Sierra Madres toward the Southern-Main zone.

Arsenic, Iron, and Chromium Species

Arsenic, chromium, and iron can be different species depending on the oxidation-reduction state of the groundwater. The oxidized and reduced species have different solubilities in groundwater and can have different effects on human health. The relative proportions of the oxidized and reduced species of each element can be used to aid in interpretation of the oxidation–reduction conditions of the aquifer, which affect the mobility of many constituents. Concentrations of dissolved arsenic, chromium, and iron, and the dissolved concentration of either the reduced or the oxidized species of the element are reported in table 10. The concentration of the other species can be calculated by difference. The concentrations measured by the NWQL are considered to be more accurate determinations of dissolved arsenic, iron, and chromium. For some samples, the concentrations of total arsenic, total iron, and total chromium were measured by the TML and the NWQL using different sample collection and analytical methods; therefore, the total concentrations reported from the TML in table 10 could be different than those reported by the NWQL. The data from TML were primarily used to identify the predominant oxidation-reduction species present in the samples, which is useful for understanding the geochemical environment and processes affecting trace-element concentrations in the system.

Concentrations of total arsenic [As(T)] were greater than the MCL-US of 10 micrograms per liter (µg/L) in well samples analyzed at the NWQL from 4 of 33 wells. The highest concentration of arsenic, 67.1 µg/L, was in well CUY-23, which is in the Southern-Main zone and screened in both the younger and older alluvium; this sample had the oldest groundwater age in the study area, with no detected tritium, and an uncorrected carbon-14 age of 38,300 years before present (table 9), as well as the deepest bottom of perforations at 2,120 ft bls (table 2). Concentrations of arsenic in the CVBR-2 and CVBR-1 samples were 58.1 and 37.7 µg/L, respectively. The CVBR multiple-well monitoring site is in the Northwestern Sierra Madre Foothills zone, and both wells are screened in the Morales Formation and have uncorrected carbon-14 ages older than 25,000 years before present. An arsenic concentration of 44.0 µg/L was observed in well CUY-02, which is in the Northwestern Sierra Madre Foothills, is screened in both the older alluvium and Morales Formation, and contained water that had an uncorrected carbon-14 age of 33,400 years before present. The next highest concentrations of arsenic in groundwater—8.6 and 5.6 µg/L—were measured for CVBR-3, which is in the Northwestern Sierra Madre Foothills and screened in the older alluvium, followed by CUY-21, with a total arsenic concentration of 3.5 ug/L, which is in the Central Sierra Madre Foothills and screened in the Morales. The surface-water sample collected from the Cuyama River at site SW-04 in the southern end of the Southern Ventucopa Uplands contained a total concentration of 0.51 µg/L, indicating that surface-water recharge potentially is not a source of the arsenic. The four highest concentrations of arsenic were found in water that is

older than 25,000 years, indicating that arsenic concentrations are higher in groundwater that has had more time to mobilize the arsenic.

Concentrations of total chromium [Cr(T)] ranged from no detections to 2.2 µg/L, less than the MCL-CA threshold 50 µg/L. The highest concentration of Cr(T), 2.2 µg/L, was observed in well CUY-20, which is outside of the basin boundary (fig. 8). All of the wells inside the basin had concentrations of Cr(T) less than or equal to 1.3 µg/L. Concentrations of hexavalent chromium [Cr(VI)], however, were greater than the OEHHA-PHG of 0.02 µg/L in 20 of the samples. Concentrations of Cr(VI) ranged from 0.1 to 1.7 µg/L. Concentrations of Cr(VI) were greater than the concentrations of Cr(T) in five of the samples. The difference in values can be attributed to the different methods of analysis used and the level of error (0.1 µg/L for each method) in the laboratory analysis. In these five samples, all concentrations of Cr(VI) and Cr(T)) were very near the detection limit (0.1 µg/L), and the laboratory measurement error can account for the differences. The three remaining samples had detections of Cr(VI) below the reporting limit of 0.1 µg/L.

Hydrology

Hydrologic data analyzed as part of this study included rainfall records, stream-discharge records, water-level records, and estimates of hydraulic properties. Rainfall records include monthly and annual rainfall totals and provide information on seasonal and annual variability in precipitation. Stream-discharge records include daily mean discharge measurements from three stream gaging stations and provide information on seasonal variability in surface-water flows and the potential stream losses (recharge) to the groundwater system. Water-level records include quarterly manual depth-to-water measurements collected from the 12 monitoring wells and 55 domestic and supply wells and time-series data collected from the monitoring wells and 8 domestic and supply wells. Water-level measurements, manual and time-series, provide information on the seasonal responses of the aquifer system to pumping. Estimates of hydraulic properties include hydraulic conductivity and transmissivity estimated from aquifer tests performed on the 12 monitoring wells and 51 domestic and supply wells. Estimates of hydraulic properties of the Cuyama Valley aquifer provide insight into the rates of groundwater movement.

Rainfall Gaging Stations

The annual rainfall data in this report are presented by "water year." A water year is defined as the 12-month period from October 1 of any given year through September 30 of the following year. The water year is designated by the calendar year in which it ends. Thus, the year ending September 30, 1999, is called the "water year 1999." Historical yearly and monthly rainfall totals from three rainfall gages operating in Santa Barbara County and one rainfall gage operating in Ventura County are shown in figures 11 and 12, respectively. The Caltrans, New Cuyama gage (Station 402), and the Cuyama Fire Station gage (Station 436) are near the city of New Cuyama; the Santa Barbara Canyon gage (Station 347) is in Santa Barbara County; and the Ozena Guard Station (NWS) gage (Station 174A) is near the Cuyama River in the southern half of the Southern Ventucopa Uplands (fig. 2). Rainfall records for Stations 402 and 436 are available from water-year 1955 to the present. Records for Station 347 are available from water-year 1905 through water-year 1980, and from water-year 1997 to the present. Rainfall records for Station 174A are available from water-year 1980 through July 2008. The official monthly and yearly rainfall records for the Santa Barbara County stations are published by the Santa Barbara County Flood Control District. The data are available for public access at *http://www.countyofsb.org/pwd/*. The monthly and yearly rainfall records for the Ventura County stations are published by the Ventura County Watershed Protection District and are available for public access at *http://www.vcwatershed.net/hydrodata*.

Analysis of the annual rainfall showed that Stations 402 and 436, in the valley, received less rainfall than Stations 347 and 174A in the uplands to the south (fig. 11). Stations 402 and 436 received approximately the same amount of rainfall. Annual totals for the two sites averaged 8 inches and range from less than 2 inches (Station 436) to over 20 inches (Station 402) per year. Station 174A typically received the most rainfall. Annual rainfall totals at Stations 174A averaged almost 19 inches and ranged from about 5 to over 44 inches per year. Annual rainfall totals at Stations 347 averaged over 12 inches and ranged from about 4 to over 32 inches per year.

Averaging the total annual rainfall from all stations since records began at multiple sites in 1954 indicated that the highest annual rainfall in the Cuyama Valley was during water-years 1958, 1969, 1978, 1983, 1995, and 1998 (fig. 11). Records from the only station to exist prior to 1954 (Station 347) showed an annual rainfall of over 32 inches during water year 1941, the highest observed at that station.

Streamflow Gaging Stations

Daily discharge data from three streamflow gaging stations in the Cuyama Valley drainage are available (figs. 13–14). Two gaging stations are on the Cuyama River: one is south of Ventucopa and measures surface-water flow into the valley from the Cuyama River, and the second site is near Buckhorn Canyon, west of the valley, and measures all surface flow out of the valley. The third gaging station is in Santa Barbara Canyon. The station on the Cuyama River near Ventucopa (SW-04) has historic data from October 1945 through September 1958. The site was reestablished on August 24, 2009. The station near Buckhorn Canyon (SW-05) was established on October 1, 1959. The station in Santa Barbara Canyon (SW-03) was established on October 1, 2009.

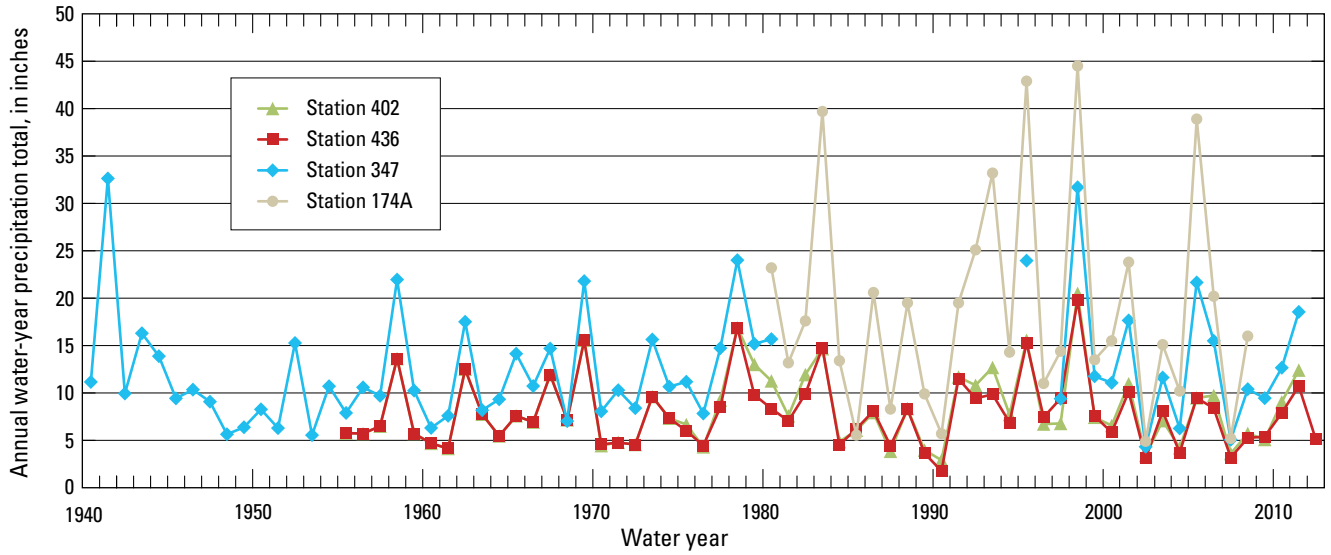

Figure 11. Historic annual rainfall graphs from four rainfall stations in the study area, Cuyama Valley, Santa Barbara County, California.

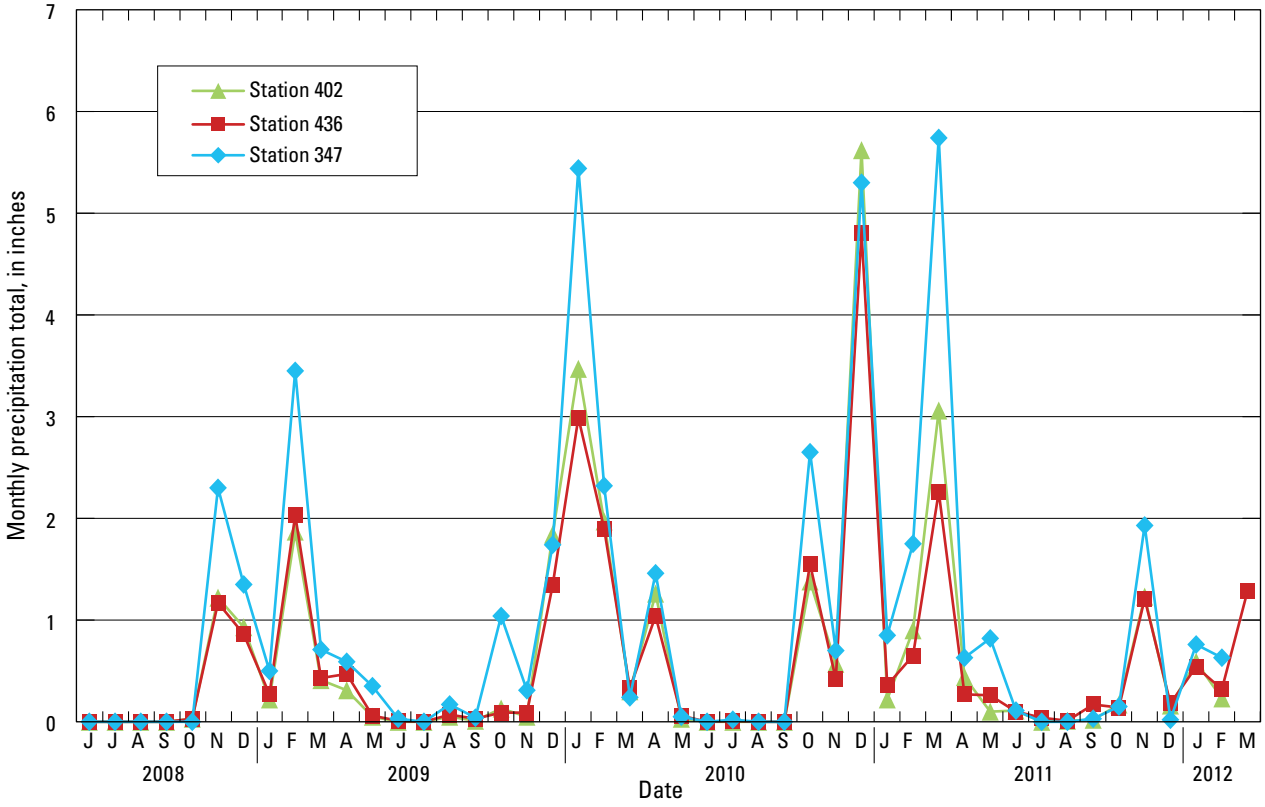

Figure 12. Monthly rainfall graphs for three rainfall stations in the study area from June 2008 to March 2012, Cuyama Valley, Santa Barbara County, California.

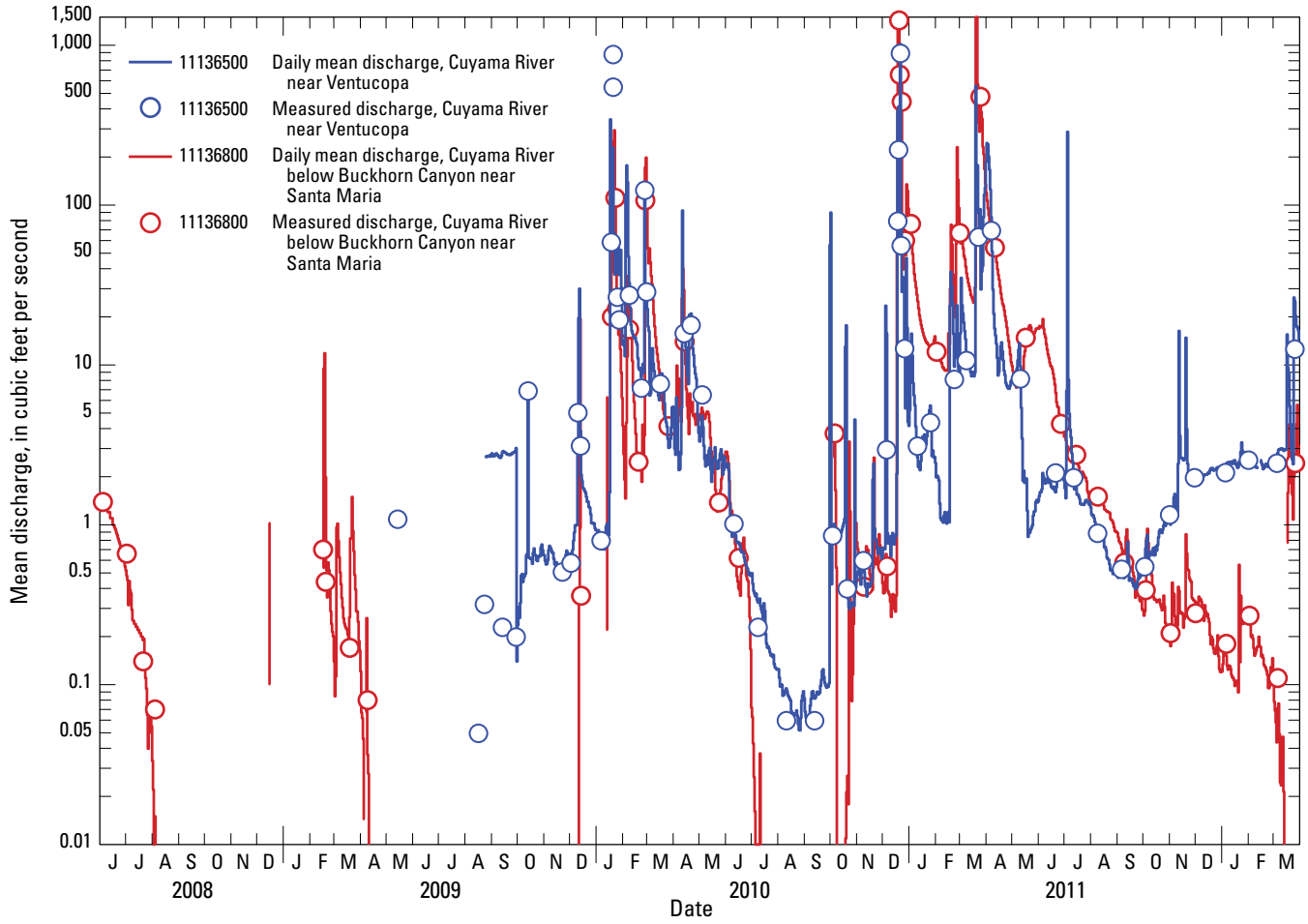

Figure 13. Daily discharge graphs for two streamflow gaging stations (11136500 and 11136800) on the Cuyama River, Cuyama Valley, Santa Barbara County, California.

Locations of these gaging stations, with the exception of SW-05, are shown in figure 1. Data collected from these sites are available online at *http://waterdata.usgs.gov/ca/nwis*.

Cuyama River

Records from the Ventucopa station (fig. 13) showed the streamflow is perennial, but varies seasonally. Higher flow, averaging between 2 and 200 cubic feet per second (cfs), generally is observed during the wet season, or December through May; lower flow, averaging below 2 cfs, is observed during the dry season, or the remainder of the year. Flow observed during the dry season of 2011 was greater than that of 2010. Three flow events exceeding 100 cfs were observed between September 2009 and March 2012. High flows of 875 and 1,020 cfs were observed in January and December of 2010, respectively. A sustained increase in flow was observed between March 20 and April 9, 2011. While four distinct peaks were observed, flows exceeded 30 cfs during the entire period and averaged 136 cfs for the 21-day period.

Records from the Buckhorn Canyon station showed the streamflow is not continuous and varies seasonally. Higher flow, averaging between 2 and 200 cfs is observed through most of the wet season, while flow during the dry season averaged less than 2 cfs, and it is typically dry late in the season. Flows exceeding 1500 cfs were observed during the wet season of 2011, but high flows were typically below 200 cfs.

Periods when the inflow from the Cuyama River (SW-04) was equal to or greater than the Cuyama River outflow (SW-05) indicated that the surface water was recharging the groundwater system. Simplistically, it can be assumed that if the inflow and outflow along the Cuyama River are equal, then the total of all other inflow to the Cuyama Valley, such as from Apache, Quanta, Santa Barbara, and Salisbury Canyon, represents the total amount of potential recharge. In general, surface water flowing into the Cuyama Valley from the Cuyama River is about equal to the amount of water flowing out, indicating that some degree of recharge from streams is typical. There are periods when outflow exceeds inflow, which indicate some combination of significant input

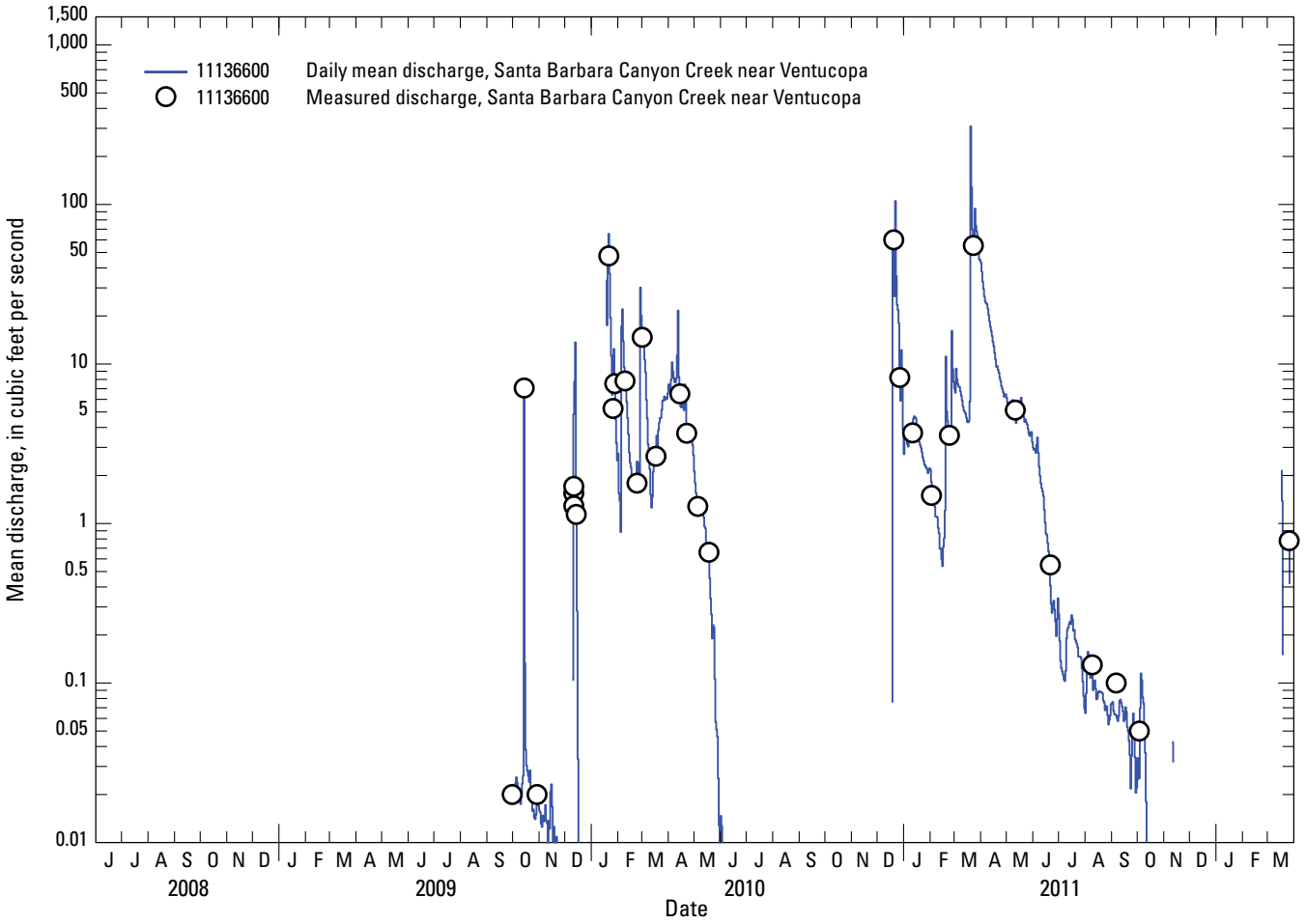

Figure 14. Daily discharge graphs for streamflow gaging stations (11136600) in Santa Barbara Canyon, Cuyama Valley, Santa Barbara County, California.

from tributaries, baseflow, and return flow from bank storage. Periods when inflow exceeds outflow indicate significant recharge from streams; the longest such period was from October 2011 to March 2012 (fig. 13).

Santa Barbara Canyon

Santa Barbara Canyon drains the southwest flanks of the Sierra Madre Mountains and represents the largest of the surrounding watersheds that flow into Cuyama Valley as a tributary to the Cuyama River (fig. 14). Streamflow records showed seasonality, with continuous flow generally ranging between 1 and 20 cfs through most of the wet season and no flow during the dry season. Flow was observed during the dry season of 2011, but was less than 0.5 cfs. The highest flow on record at this site, about 300 cfs, was measured in late March of 2011.

Groundwater Levels

Water levels, measured as depth to water below land surface, were routinely measured in all 12 monitoring wells and in an additional 56 selected wells in the Cuyama Valley (table 1). Thirty-three of the additional wells had water-level records prior to January 1, 2008; some records date as far back as August 1941 (table 11). Twenty of the wells were equipped with instrumentation to automatically measure and record the depth to water at regular time intervals (time-series; table 1). The water-level measurements in this report are given in feet with reference to land-surface datum (LSD). LSD is a datum plane that is approximately at land surface at each well. The elevation of the land-surface datum is given in table 11. Users of the data are encouraged to access site information through the USGS NWIS Web at *http://waterdata.usgs.gov/nwis/*.

Table 11. Summary of sites with manual water-level measurements including period of record, number of observation, and minimum and maximum observed water levels for selected wells, Cuyama Valley, Santa Barbara County, California.

Table available separately as Microsoft Excel® at http://pubs.usgs.gov/sir/2013/5108.

Manual Measurements

Manual water-level measurements were typically taken once every 3 months in all wells shown in figure 15. Water levels were measured and recorded to within 0.01 foot by using a calibrated electric or steel tape. A summary of the available water-level data is presented in table 11, including land-surface elevation, period of record, number of measurements, and the minimum and maximum observed water levels.

Hydrographs for most wells showed seasonal fluctuations in water levels. Water levels generally declined during the summer months, coinciding with the peak of the agricultural season, and recovered during the winter months, when agricultural pumping is at a minimum. Several wells on the outer edges of the basin and in the Southern Ventucopa Uplands showed delayed responses, with the highest levels in the summer and lowest in the winter.

A comparison of the highest annual measured water levels since January 2008 in the 56 domestic and supply wells showed that 16 wells had a declining trend, 7 wells had an upward trend, 8 wells had a reversal from downward to upward trends, 1 well had a reversal from upward to downward trend, and 9 wells showed no trend. Records from the remaining 15 wells were insufficient to determine a trend. Water-level declines in the 16 wells with downward trends ranged from about 6 feet in several wells to over 30 feet (CUY-07). Downward water-level trends were observed in five zones; 7 of the 16 wells were in the Southern-Main zone (CUY-04, -06, -07, -50, -51, -56, and -59), 4 were in the Central Sierra Madre Foothills (CUY-21, -24, -25, and -48), and 3 were in the Southern Ventucopa Uplands (CUY-03, -12, and -46). Water-level increases in the seven wells with upward trends ranged from less than 1 foot in several wells to about 8 feet (CUY-47). Two of the seven wells showing upward trends were in the Southern Ventucopa Uplands (CUY-31, and -35), two were in the Northeast Ventucopa Uplands (CUY-17, and -36), two were in the Southern-Main zone (CUY-08, and -27), and one was in the Southern Sierra Madre Foothills (CUY-47). The eight wells showing a reversal from declining to rising water levels were all in the Southern Ventucopa Uplands (CUY-13, -19, -30, -38, -39, -40, -42, and -43). Water levels declined from 2008 through the summer of 2010, began to rise early in 2012, and continued to rise throughout the summer of 2012. The observed rise in these wells ranged from 5 to 15 feet. The rise in water level indicated that the aquifers receive recharge under certain conditions; this rise only in the Southern Ventucopa Uplands indicates that the water table in this zone could be relatively well-connected with recharge sources.

Time-Series Water Levels

All 12 monitoring wells and 8 additional wells were equipped with instrumentation to automatically measure and record the depth to water at regular time intervals, typically every hour or 15 minutes (fig. 15). The computed unit values, and daily maximum, minimum, and median values for all time-series water-level data for these sites are available through the USGS NWIS Web. Periodic manual measurements of water levels were made to verify the time-series data. Seventeen wells with time-series water-level data are presented as time-series plots. Three wells (CUY-04,-55, and -60) with time-series records shorter than 6 months are not presented in this report.

Time-series data presented in this report are the computed hourly unit values, as opposed to daily statistical values. Including the computed hourly values, even those water levels affected by pumping can cause the hydrograph to appear cluttered or "fuzzy," especially when the x-axis is compressed. The hourly data display the entire range of water levels observed in the well under static and pumping conditions, and indicate when pumping and recovery are occurring. Most data gaps, denoted in grey on the hydrographs, were caused by the water level in the well dropping below the level of the sensor; consequently, the water level during these gaps is known to be deeper than the last measurement before the data gap.

The pumping of nearby irrigation wells directly influenced water levels in all of the CVKR (fig. 16) and CVBR (fig. 17) wells. During the period of record (2009–12), data showed a seasonal pattern, with water levels declining between March and August, coinciding with the peak of the agricultural season, and rising between September and February, when nearby irrigation and related pumping were at a minimum.

At the CVKR site, water levels in the three deeper wells (CVKR-1, -2, and -3) varied as much as 60 feet between March and August, while water levels in the shallowest well (CVKR-4) varied by about 25 ft over the same period (fig. 16). Water levels showed a decline in the seasonally high levels over the period of record. Manual measurements made in late February 2012 showed a decline of over 30 feet compared to those made in early March 2009. Vertical hydraulic gradients were upward during the winter months and reversed to downward gradients during the irrigation season.

Seasonal patterns at the CVBR site were similar to those at the CVKR site. Water levels in the three deeper wells (CVBR-1, -2, and -3) varied by as much as 90 feet between March and August, while water levels in the shallowest well (CVBR-4) varied by about 40 ft over the same period (fig. 17). Water levels showed a decline in the seasonally high levels over the period of record. Manual measurements made in late February of 2011 showed a decline of about 5 feet compared to those made in early March of 2010. Vertical hydraulic gradients were upward during the winter months and reversed to downward gradients during the irrigation season. Short-term fluctuations in water levels were larger at CVBR than CVKR, which is consistent with CVBR being more strongly affected by pumping in close proximity to the monitoring wells than CVKR.

Observations at the CVFR site indicated that water levels did not show short-term (daily) variability from nearby pumping as seen at the other sites, but did show similar

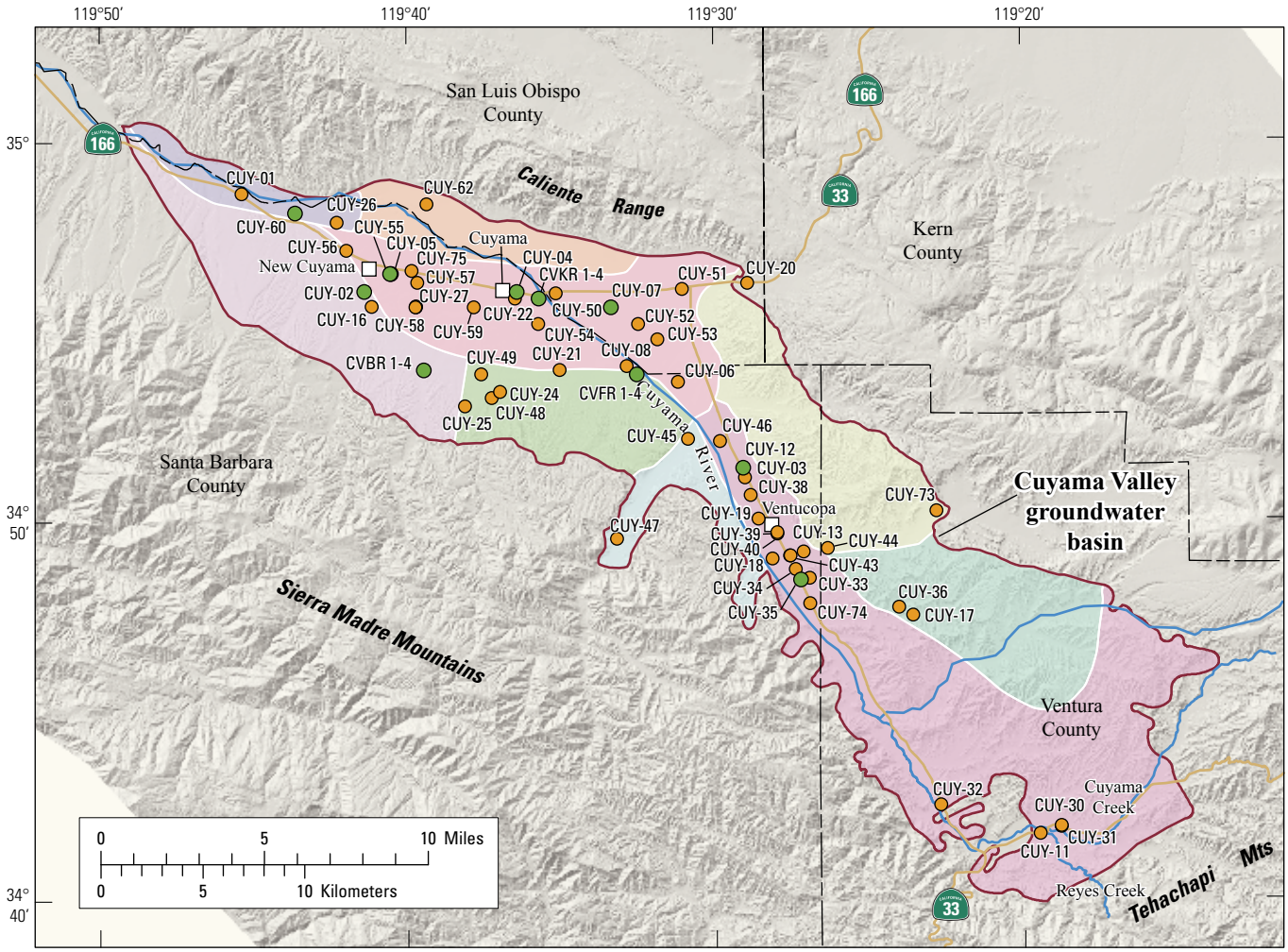

Shaded relief base created from 30-m digital elevation model from USGS National Elevation Dataset (NED), North America Vertical Datum 1988 (NAVD88)
Hydrology sourced from 1:24,000-scale National Hydrography Dataset, 1974–2009
Place names sourced from USGS Geographic Names Information System, 1974–2009
Albers Projection, NAD83

EXPLANATION

Cuyama groundwater basin zones

- Caliente Northern-Main
- Central Sierra Madre Foothills
- Northeast Ventucopa Uplands
- Northwestern Sierra Madre Foothills
- Northern Ventucopa Uplands
- Southern Sierra Madre Foothills
- Southern Ventucopa Uplands
- Southern-Main
- Western Basin

- Time-series site
- Manual water level

Figure 15. The location of multiple-well monitoring sites, domestic, and supply wells with available water-level data, Cuyama Valley, Santa Barbara County, California.

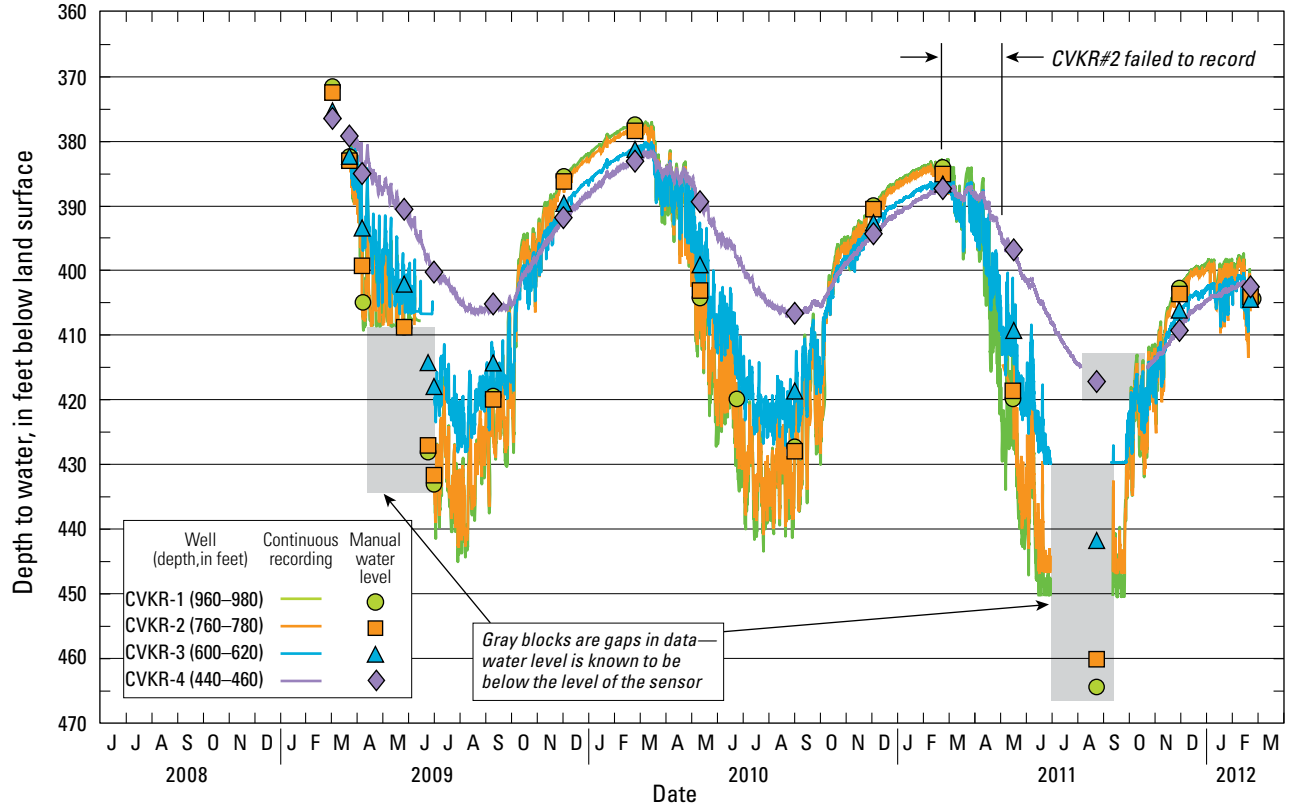

Figure 16. Water-level hydrograph from multiple-well monitoring site Cuyama Valley Kirschenmann Road (CVKR) from April 8, 2009, to February 20, 2012, Cuyama Valley, California.

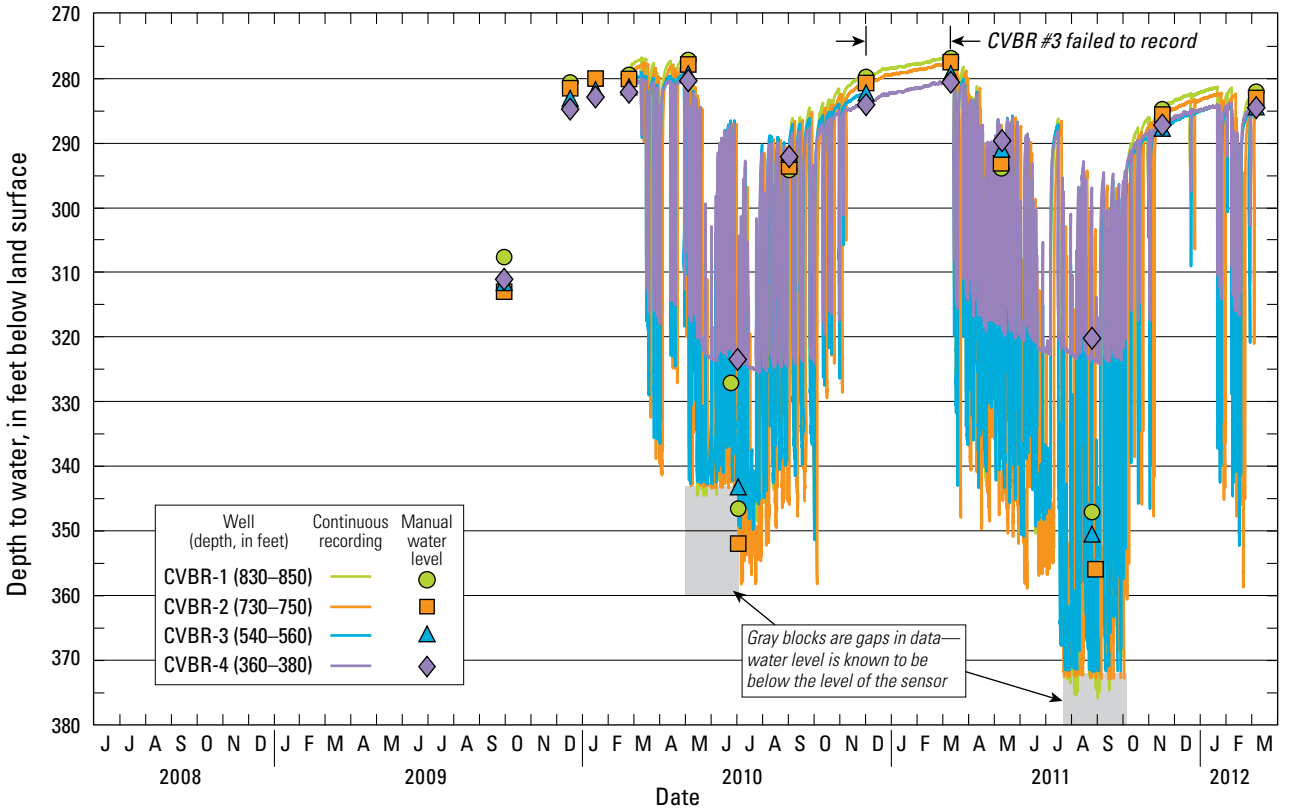

Figure 17. Water-level hydrograph from multiple-well monitoring site Cuyama Valley Bell Road (CVBR) from September 29, 2009, to March 5, 2012, Cuyama Valley, California.

seasonal and longer-term changes. Similar to CVKR and CVBR, the vertical hydraulic gradients were upward during the winter months and reversed to downward gradients during the irrigation season; however, the gradients at the CVFR site were notably smaller. The gradient reversal at this location indicated that water levels at this site were influenced by local pumping but were not as strongly affected as CVKR and CVBR. Seasonal water levels in the wells varied about 15 feet between March and September (fig. 18). Water levels showed a decline in the seasonally high levels over the period of record by about 10 feet per year.

Time-series data from well CUY-02 (fig. 19) in the Northwestern Sierra Madre Foothills zone showed no discernible trend over the period of record. Seasonally high water levels rose slightly between 2009 and 2010, were similar between 2010 and 2011, then declined by almost 25 ft between 2011 and 2012; this pattern correlates to the relative duration of seasonal pumping of the well, which was apparent on the hydrograph (fig. 19). In 2009, daily pumping in this well started in late June and continued for about 5 months. Because of the data gap between early August 2009 and April 2010, caused by a probe failure, the entire pumping season did not show, but manual water-level measurements indicated pumping stopped sometime before mid-November. This pumping cycle correlated with the observed rise. In 2010, daily pumping in this well covered the same period: pumping started in early June and continued until early November. Comparison of the daily records, however, indicated the pump was operated more frequently during the first 30 days of operation in 2010 than in 2009. This pumping cycle correlated with the observed static water levels. In 2011, daily pumping in this well covered a longer time span: pumping started a month earlier, in mid-May, and continued through November. A comparison of the daily records indicated the pump was operated more during 2011 than 2010. This pumping cycle correlated with the observed decrease in water levels. The increased irrigational pumping

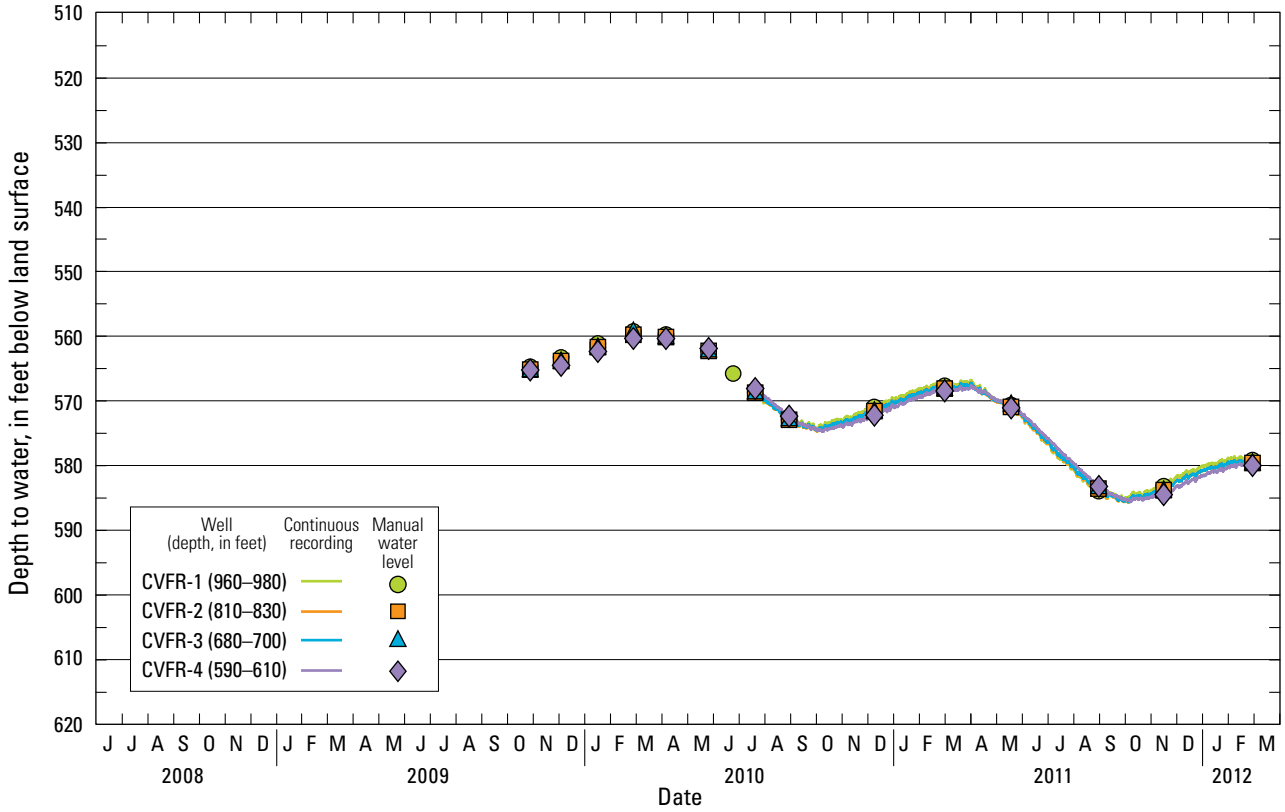

Figure 18. Water-level hydrograph from multiple-well monitoring site Cuyama Valley Foothill Road (CVFR) from October 27, 2009, to February 28, 2012, Cuyama Valley, California.

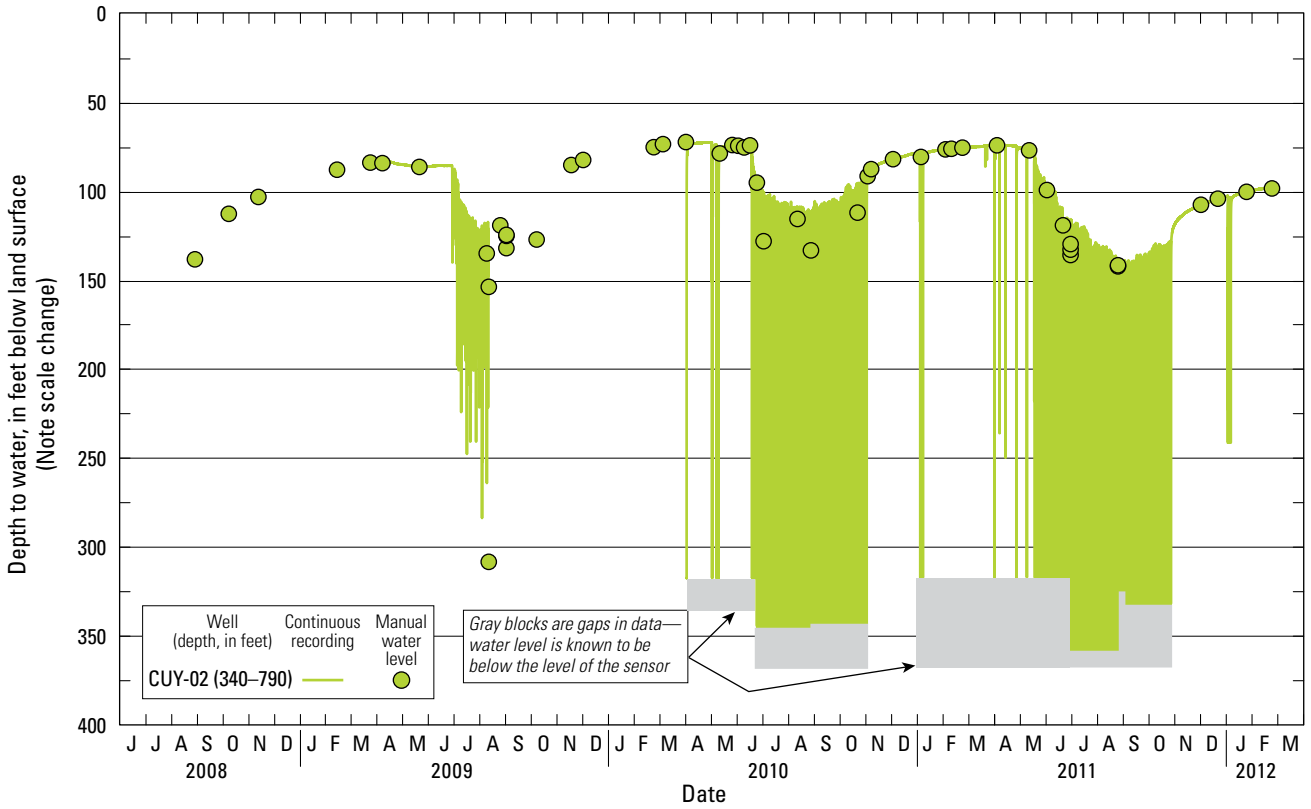

Figure 19. Water-level hydrograph from CUY-02, from January 1, 2008, to March 23, 2012, Cuyama Valley, California.

of other wells in the Northwestern Sierra Madre Foothills zone, reported during the summer of 2011 by several residents, also could have contributed to the observed decline in water levels. Irrespective of cause, the change in the pumping, and possibly recharge, conditions between 2010 and 2011 in the Northwestern Sierra Madre Foothills zone resulted in changes from static and overdraft conditions; these patterns were evident in both CVBR and CUY-02.

Time-series data from wells CUY-05 (fig. 20) and CUY-07 (fig. 21) in the Southern Main zone showed a more detailed record of the steady decline in water level than was observed in the manual measurements. These hydrographs showed the seasonal highs and lows that are expected, and the year-to-year seasonal highs showed a steady decline in water levels. A decline of approximately 2.5 feet per year was observed at CUY-05 (fig. 20) between 2010 and 2012, and a decline of about 7 feet per year was observed at CUY-07 (fig. 21) between 2010 and 2012. Water levels in well CUY-05 showed high daily variability associated with the active pumping during the period of record, while water levels in the non-pumped well CUY-07 showed low daily variability. The lower variability in CUY-07 likely reflected the effects of regional pumping rather than local pumping effects near CUY-07.

Time-series water-level data from two wells, CUY-12 and CUY-35 in the Southern Ventucopa Uplands zone, showed a rise in water levels during the spring of 2012 compared to earlier spring high water levels. At CUY-12 (fig. 22), the 3 to 4 foot per year of decline in water levels observed over the previous 2 years did not continue into 2012. Generally, increasing water levels at CUY-35 (fig. 23) corresponded with the high-flow events observed at the stream gage station on the Cuyama River near Ventucopa (11136500) between December 2009 and February 2012 (fig. 13). At CUY-35 (fig. 23), an increase of approximately 27 feet corresponded with a high-flow event in late March and early April 2011. A water-level increase of over 5 feet was observed at CUY-35 shortly after a December 2010 flow event. The correspondence of rising groundwater and river levels indicates that the Southern Ventucopa Uplands zone is strongly hydraulically connected to the Cuyama River.

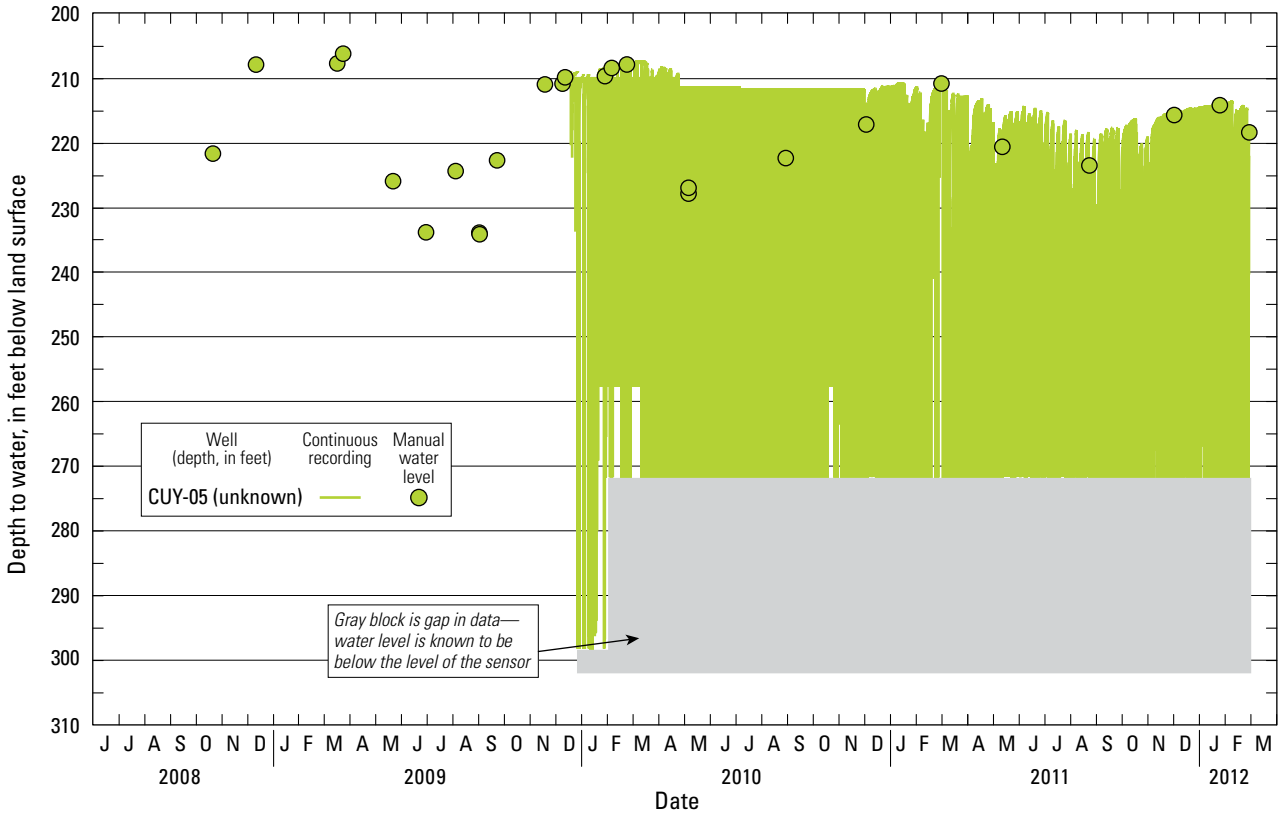

Figure 20. Water-level hydrograph from CUY-05, from January 1, 2008, to February 28, 2012, Cuyama Valley, California.

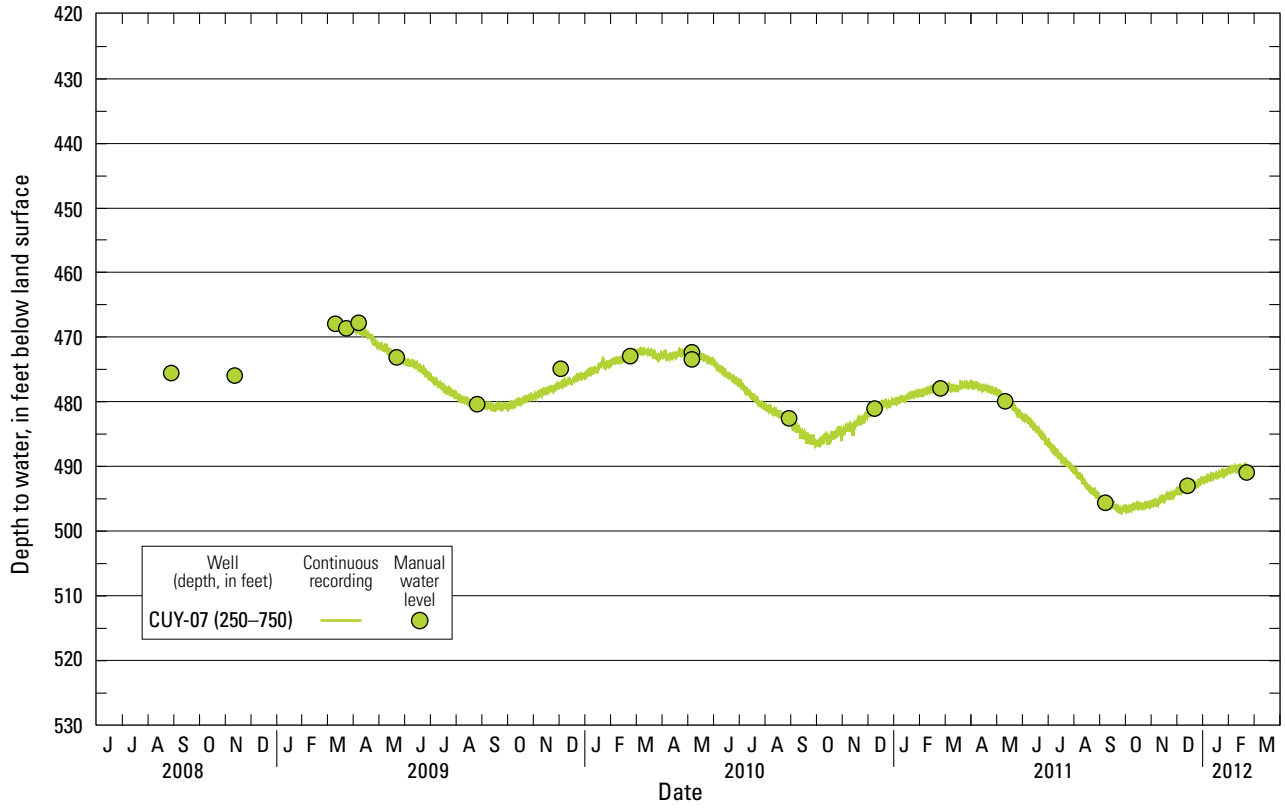

Figure 21. Water-level hydrograph from CUY-07, from January 1, 2008, to February 21, 2012, Cuyama Valley, California.

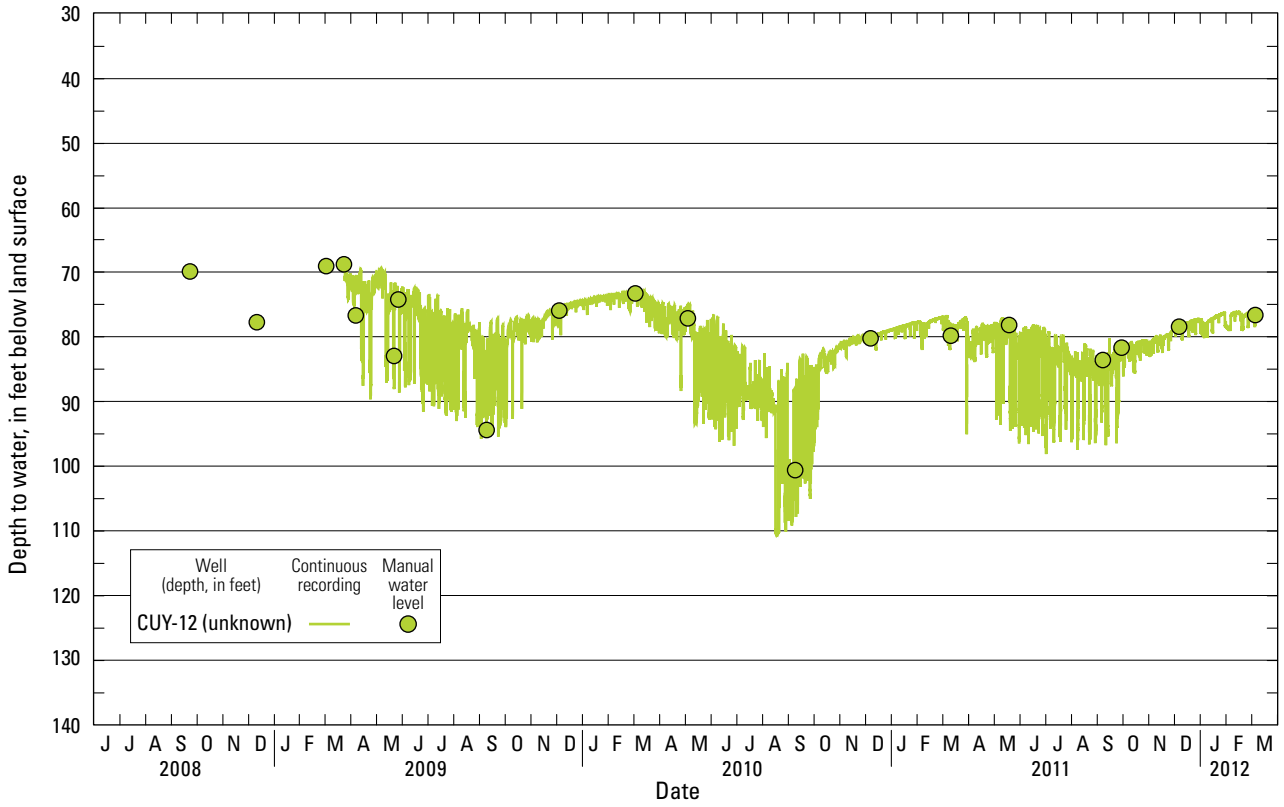

Figure 22. Water-level hydrograph from CUY-12, from January 1, 2008, to March 5, 2012, Cuyama Valley, California.

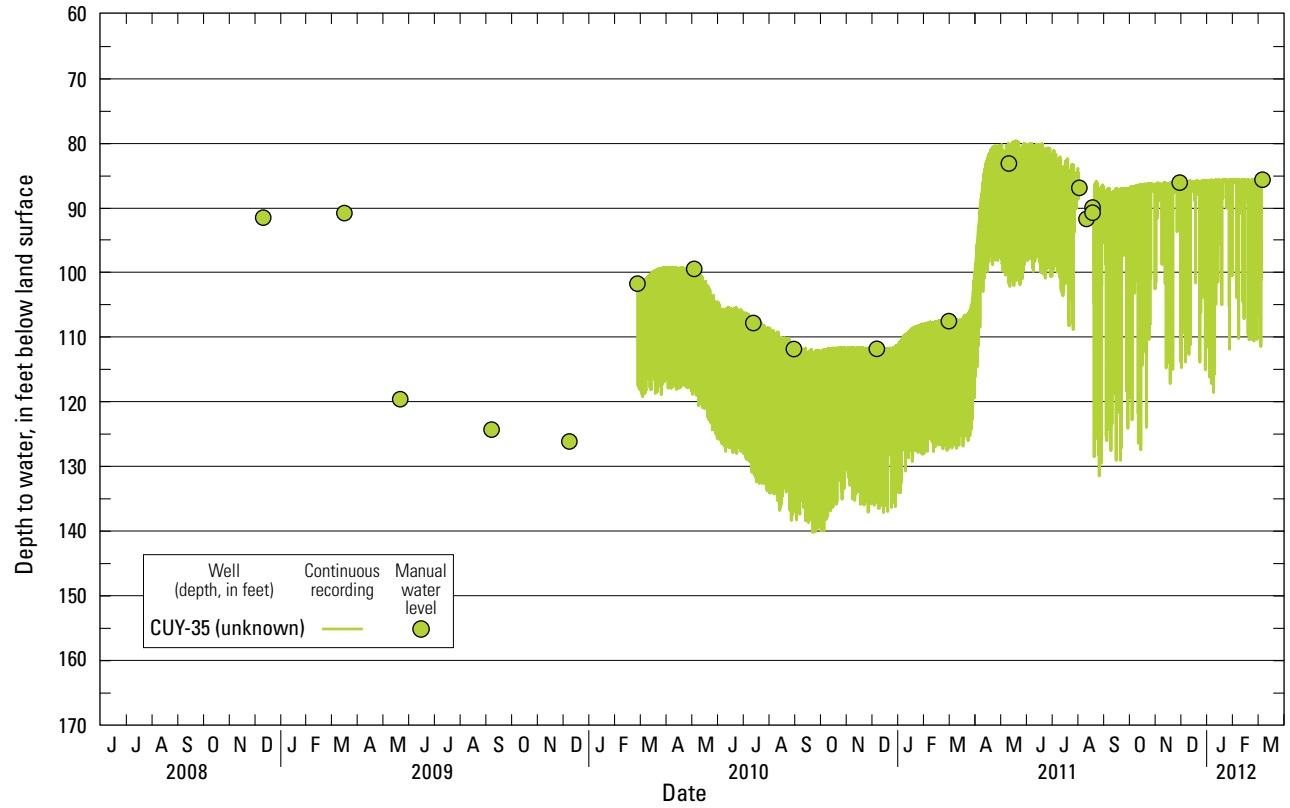

Figure 23. Water-level hydrograph from CUY-35, from January 1, 2008, to March 6, 2012, Valley, California.

Historic Water Levels

Historic water-level data, some dating back to the early 1940s, were compiled for 16 sites in the Cuyama Valley. Analysis of the long-term trends indicated that 10 wells showed a declining trend, 3 wells showed no trend, and 3 wells showed a rising trend (fig. 24).

All six wells in the South-Main zone showed declines over the period of record. Well CUY-04 showed the largest decline—over 300 feet between 1960 and 2001, for an average decline of over 7 ft per year. Well CUY-75 declined nearly 200 ft from 1954 to 2007, for an average decline of almost 4 ft per year. Wells CUY-27, -54, and -56 declined about 100 feet over the period of record, for an average decline of between 1 and 2 ft per year. Large water-level declines were not limited to the South-Main zone. Well CUY-62, in the Caliente Northern-Main zone, declined over 100 feet between 1947 and 2007, for an average decline of almost 2 ft per year. Well CUY-60, in the Western Basin zone, declined over 80 ft between 1945 and 2012, an average decline of over 1 ft per year. Well CUY-24, in the Central Sierra Madre foothills zone, declined approximately 30 feet between 1983 and 2012, for an average decline of about 1 ft per year.

Two of the wells that showed an increase in water levels, CUY-13 and -74, are in the Southern Ventucopa Uplands zone, which further indicated that this zone can respond quickly to periods of increased recharge. The third well that had an increase in water levels, well CUY-36, is in the Northeast Ventucopa Uplands zone. The record for well CUY-36 was limited, and it cannot be determined if the fluctuations in water levels that were observed in the Southern Ventucopa Uplands also occurred in this well.

Wells CUY-13, -30, -39, -46, and -74, in the Southern Ventucopa Uplands, showed cyclical fluctuations in water levels. Declines in water levels over a 5 to 12 year period were followed by a marked rise. Well CUY-74 showed an increase in water level of over 116 feet between December 1977 and May 1978. Other rapid increases in water levels over a short time included 58 feet over 3 months in 1958, 74 ft over 2 months in 1969, and 68 feet over 4 months in 1983. Well CUY-32, also in the Southern Ventucopa Uplands, did not show cyclical fluctuations in water levels.

Increases in water levels observed in the Southern Ventucopa Uplands corresponded to increased annual precipitation. The marked water-level rises in well CUY-74 observed in 1958, 1969, 1978, and 1983 correlated with above average rain-fall totals during the respective years. Although increases in water levels were associated with increased precipitation (fig. 11), all of the marked increases were associated with annual rainfall totals exceeding 20 in/yr at either Station 347 or 174A. The 25-ft rise in water level at CUY-35 (fig. 23) in late March 2011 correlated with an above average monthly rainfall of over 5 inches at Station 34 (fig. 12). A similar monthly rainfall in December 2010 also correlated to an increase in water level of 5 ft at CUY-35. This indicated that recharge to the aquifer system in the Southern Ventucopa Uplands is highly dependent on periods of increased annual rainfall and stream levels.

Aquifer Tests

Aquifer tests were performed on the monitoring wells and selected domestic and supply wells in the Cuyama Valley groundwater basin (fig. 25). Slug tests on the monitoring wells were done by using physical displacement. Historic pump test data for 51 wells were collected and analyzed to estimate the aquifer transmissivity.

Slug Tests

Hydraulic conductivity estimates for the aquifer materials proximate to the screened intervals of the three multiple-well monitoring sites (CVKR, CVBR, and CVFR) were obtained by using physical displacement “slug” tests. These tests are useful for determining aquifer properties around small-diameter wells that have short screened intervals. Unlike longer-term tests, the results are based on small changes in water level measured over short periods and, therefore, represent the hydraulic response from only a small volume of aquifer material next to the well screen.

The slug used for the displacement of volume was a 1.05-inch outer diameter PVC pipe 63 inches long. The pipe was filled with sand for weight and sealed at both ends with pointed capes. The slug displacement was 0.0327 cubic feet (ft^3), which resulted in an equivalent head displacement of approximately 1.50 ft in a 2-inch well. The initial head displacement observed for some tests differed from the calculated equivalent head displacement. The cause of the difference is uncertain. The observed initial head displacement was used for processing the results.

Computations were performed by using existing spreadsheet-based tools (Halford and Kuniansky, 2002). The selection of the most appropriate method to analyze the data was based on a preliminary analysis of the slug test data and comparison with predicted responses from different methods. Wells CVKR-1, -2, and -3 were analyzed by using methods developed by James Butler of the Kansas Geological Survey (Butler and others, 2003) for formations of high hydraulic conductivity. All other wells were analyzed by using methods developed by Green and Shapiro (1998), with the exception of CVFR-4 . The water level in CVFR-4 was below the top of the sand pack at the time of testing; therefore, it was considered unconfined and was analyzed by using methods developed by Bouwer and Rice (1976) for unconfined wells.

The following assumptions were made for the interpretation of slug test data: the volume of water is displaced instantaneously at t = 0, and the well is of finite diameter and

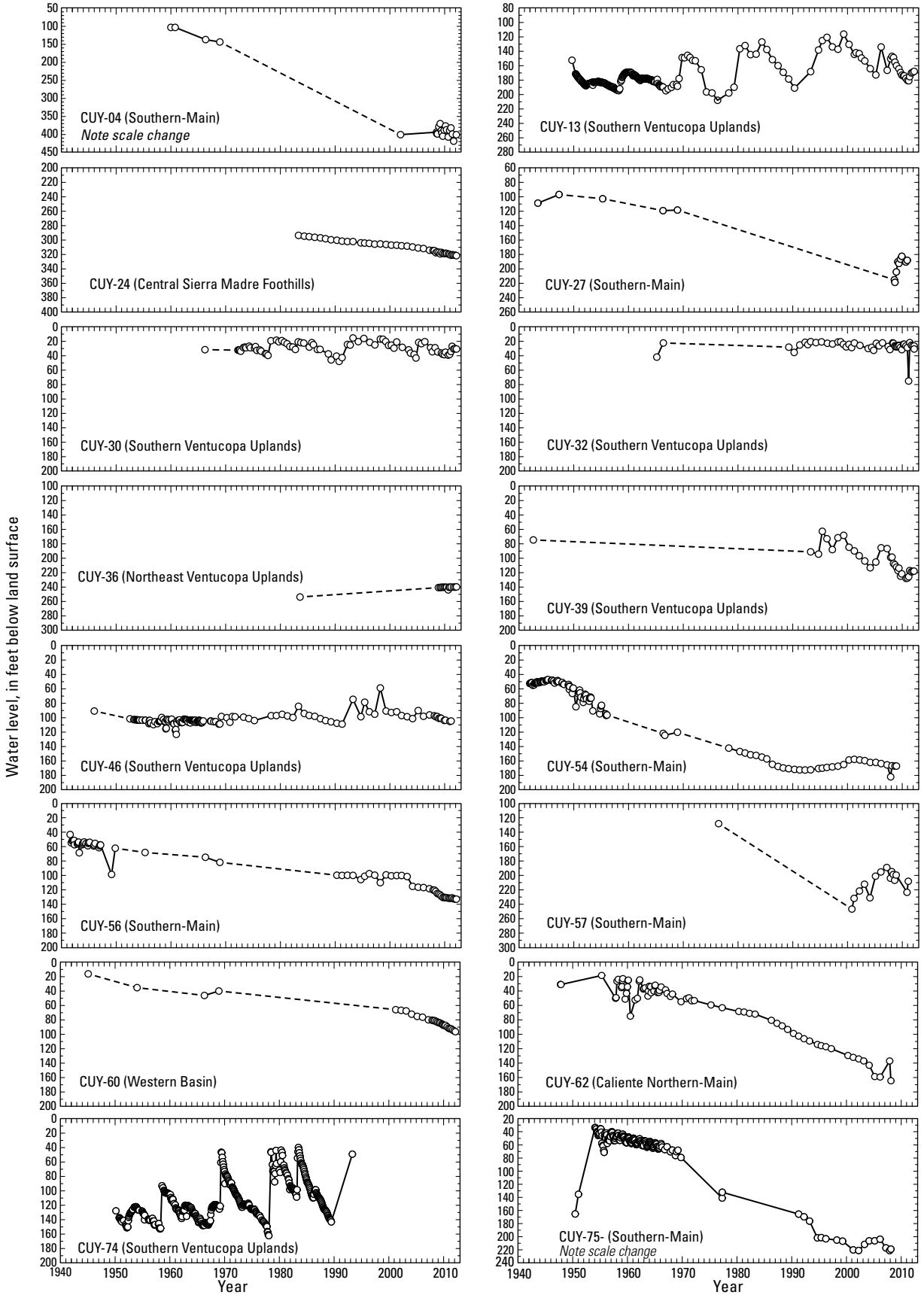

Figure 24. Historic water-level hydrographs from 16 selected domestic and supply wells, Cuyama Valley, Santa Barbara County, California.

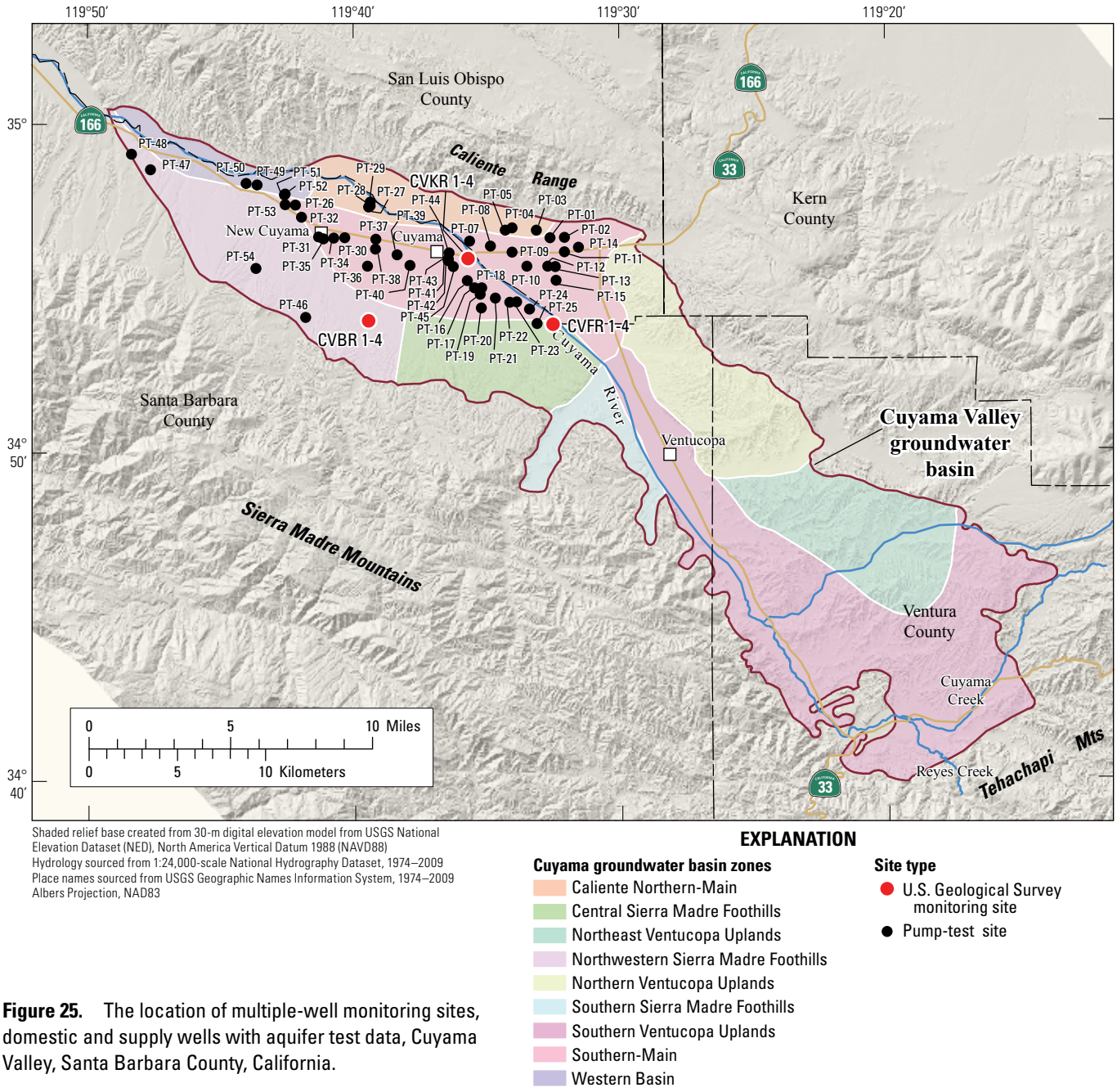

Figure 25. The location of multiple-well monitoring sites, domestic and supply wells with aquifer test data, Cuyama Valley, Santa Barbara County, California.

fully penetrates the aquifer. It is also assumed that the aquifer is confined, homogeneous, isotropic, and of uniform thickness; the flow within each aquifer is horizontal and radially symmetric; and that the response is influenced over the entire screened interval. Thus, for these calculations, the aquifer thickness is assumed to equal the length of the screened interval of the monitoring well.

For wells analyzed after Butler and others (2003), the type curve can be automatically or manually fit to match the observed response by using the spreadsheet tool to adjust the dimensionless dampening coefficient and the hydraulic conductivity. The accuracy of the fit between the match curve and the measured response curve is characterized best by the residual standard error. For wells analyzed after Green and Shapiro (1998), the type curve can be automatically or manually fit to match the observed response by adjusting the storage coefficient and the hydraulic conductivity. For wells analyzed after Bouwer and Rice (1976), the type curve can be automatically or manually fit to match the observed response by adjusting the hydraulic conductivity (K).

Slug tests from each well were analyzed and grouped on the basis of the shape of each type curve. Similarly shaped type curves were grouped together. For each approach, the individual tests were manually examined; tests that

contained errors were removed from the batch. For each well, the results from all valid tests were averaged to estimate K for the given well. Common errors included measured displacements varying greatly from the calculated equivalent head displacement, irregular recoveries, and tests containing anomalous readings.

Slug test results from the monitoring wells indicated that horizontal hydraulic conductivities ranged from about 1.5 feet per day (ft/d) for the CVBR-4 well to 28 ft/d for the CVKR-3 well (table 12). The median hydraulic conductivity of 15 ft/d observed for the wells in the older alluvium was almost five times greater than the median hydraulic conductivity observed in the Morales Formation (3.1 ft/d). The relatively low hydraulic conductivity values estimated in the Morales Formation probably reflect the greater degree of cementation and induration. None of the wells tested was screened in the younger alluvium.

Pump Tests

To better understand hydraulic properties of the local aquifer system, transmissivity (T) of the aquifer was estimated at 51 wells screened in the water-bearing units of the Cuyama Valley groundwater basin (table 13). The data used for the analysis were from historical pump efficiency tests performed on irrigation wells between 1941 and 1966. Data from these tests were analyzed by using the Jacob's equations to estimate T of the aquifer material around the well (Jacob, 1946). Most of the tests were done by Pacific Gas and Electric (PG&E) as a service to the customers for the purpose of maximizing the well efficiency and aiding in the protection of the electrical grid. Water pumping accounts for approximately 80 percent of the energy consumed by PG&E's agricultural customers and is a significant load to the electrical system (Pacific Gas and Electric, 2006). PG&E has performed free well-efficiency tests of water-pumping systems for their customers since 1911. The data—date and time, static and pumping water levels, total lift, discharge, specific capacity, kilowatt input, kilowatt-hour per acre-foot (ac-ft), and plant efficiency—were provided to the USGS for analysis. The overall condition of the well was not noted; it was assumed that wells were fully developed and in good working condition.

A common approach for analyzing short-term single-well pumping test data is the use of the Jacob's Method (Jacob, 1946) to estimate the transmissivity of the aquifer. Although this method makes various assumptions (including the aquifer is infinitely large, homogeneous, isotropic, confined, and unconsolidated), it still provides a reasonable first-order approximation of the transmissivity of the aquifer near the well. Because drawdown data seldom fall in a straight line when plotted on a linear time scale (Bear, 1979), the method assumes that steady-state conditions are eventually reached, and the time since pumping began is plotted on a log cycle. It is assumed from the PG&E data that the reported water level was measured after a static condition had been reached, and the pump was allowed to run for at least one log-time cycle (for example, 1, 10, 100; or 30, 300 min, and so on). This technique allows for an estimation of transmissivity from specific capacity by taking the flow rate and drawdown of a well, at one log cycle apart, and applying Jacob's Equation for straight-line drawdown, as shown (Roscoe Moss Company, 1990).

Table 13. Summary of pump-test estimates of hydraulic properties for selected well sites, Cuyama Valley, Santa Barbara County, California.

Table available separately as Microsoft Excel® at http://pubs.usgs.gov/sir/2013/5108.

Table 12. Summary of slug-test estimates of hydraulic properties for selected multiple-well monitoring sites, Cuyama Valley, Santa Barbara County, California.

[Depth in feet below land surface, see table 1 for definitions of common well names. **Abbreviations**: Qoa, Older alluvium; QTm, Morales Formation; ft/day, feet per day; USGS, U.S. Geological Survey]

Common well name	Tested by	Number of tests	Date of test (mm/dd/yyyy)	Top of screen	Bottom of screen	Formation at top of screen	Formation at bottom of screen	Method of analysis	Hydraulic conductivity (ft/d)
CVKR-1	USGS	17	3/22/2009	960	980	Qoa	Qoa	Butler, Garnett and Healey, 2003	18
CVKR-2	USGS	17	3/23/2009	760	780	Qoa	Qoa	Butler, Garnett and Healey, 2003	22
CVKR-3	USGS	14	3/23/2009	600	620	Qoa	Qoa	Butler, Garnett and Healey, 2003	28
CVKR-4	USGS	15	3/23/2009	440	460	Qoa	Qoa	Greene and Shapiro, 1998	9.3
CVBR-1	USGS	20	11/4/2009	830	850	QTm	QTm	Greene and Shapiro, 1998	3.3
CVBR-2	USGS	19	11/5/2009	730	750	QTm	QTm	Greene and Shapiro, 1998	2.6
CVBR-3	USGS	17	11/5/2009	540	560	Qoa	Qoa	Greene and Shapiro, 1998	12
CVBR-4	USGS	18	11/4/2009	360	380	Qoa	Qoa	Greene and Shapiro, 1998	1.5
CVFR-1	USGS	20	11/4/2009	960	980	QTm	QTm	Greene and Shapiro, 1998	9.9
CVFR-2	USGS	20	11/5/2009	810	830	QTm	QTm	Greene and Shapiro, 1998	3.0
CVFR-3	USGS	20	11/5/2009	680	700	QTm	QTm	Greene and Shapiro, 1998	6.8
CVFR-4	USGS	20	11/5/2009	590	610	QTm	QTm	Bouwer and Rice, 1976	1.6

$$T = \frac{2.303}{4\pi} x \frac{Q}{\Delta s}$$

where

T is transmissivity (gallons per day per foot or square meters per day),
Δs is drawdown (feet or meters),
Q is well discharge (gallons per minute or liters per second).

Adding the conversion from gallons per minute (gpm) to gallons per day (gpd) allows for the flow (Q) to be entered in the standard unit of gpm while transmissivity (T) is calculated in the conventional units of gallons per day per foot (gpd/ft). Simplifying the resulting equation yields the following:

$$T = \frac{264Q}{\Delta s}$$

The median transmissivity estimates from pump-test analyses of the supply wells ranged from 560 to 163,400 gallons per day per foot (gal/d/ft). The median transmissivity of 15,700 gal/d/ft for wells in the younger alluvium was three times that of the older alluvium (5,000 gal/d/ft). Wells screened in both the younger and older alluvium had a median transmissivity of 11,300 gal/d/ft. Data from wells screened solely in the Morales Formation were not available to be analyzed; however, transmissivity estimates from two wells screened in both the older alluvium and Morales Formation averaged 4,900 gal/d/ft.

Pump tests were repeated for some wells over a span of several years. Analysis of the results indicated that transmissivity typically decreased over time, with a few exceptions. These temporal changes in transmissivity are likely due to physical deterioration of the well, but could also be influenced by declines in water levels over time, the loss of storage due to land subsidence, or both.

Geomechanical Activity

Geomechanical data collected from the study area included continuously operating global positioning system (GPS) and interferometric synthetic aperture radar (InSAR) data. The geomechanical data were used to estimate the rate of vertical land movement in the Cuyama Valley groundwater basin to determine if it is subsiding. Data from 5 GPS stations and 133 unique interferograms were analyzed. Estimates of land subsidence for the Cuyama Valley provided insight into the response of the aquifer system to groundwater withdrawal.

GPS Data

The horizontal and vertical motion of the Earth's tectonic activity in California is monitored by a continuously operating network of GPS stations that are operated by various groups, including government agencies and education consortiums. Stations within the Cuyama study area were installed as part of Southern California Integrated GPS Network (SCIGN), which was designed to monitor plate boundary deformation and seismic hazards throughout Southern California (Hudnut and others, 2002). The GPS stations generally were constructed by using a stable monument embedded in the ground to a depth of approximately 10 meters to minimize signal noise and employ a standard choke ring antenna for the GPS receiver (Hudnut and others, 2002). The receiver detects signals transmitted by GPS satellites in orbit around the earth and determines the distance between the satellites to the receiver based on the travel time of the signal (U.S. Geological Survey Earthquakes Hazards Program, 2012). The station position (latitude, longitude, and elevation) is determined by triangulation of the distances to at least four GPS satellites (U.S. Geological Survey Earthquakes Hazards Program, 2012).

Variations in the position of a GPS station can result from tectonic motion and from deformation associated with fluid pumping from anthropogenic activities—in this case, groundwater withdrawal. A study of continuous GPS data from sites in southern California determined that measured seasonal horizontal and vertical motion across a basin were consistent with simple elastic movement of the basin material responding to aquifer pumping and recharge (Bawden and others, 2001). "GPS sites on the margin… undergo seasonal horizontal motion toward and away from the basin, while sites within the basin undergo seasonal uplift and subsidence." (Bawden and others, 2001, pg. 814). Seasonal motion showing fluctuating compression and expansion of the aquifer sediment is a result of elastic, or reversible, deformation and is the result of fluctuations in the pore-fluid pressure in the aquifer sediments that are less any previous maximum fluctuations (Galloway and others, 1999). Generally, elastic deformation is correlated with water-level changes and associated pumping. Inelastic, or irreversible, deformation occurs when the pore-fluid pressure is reduced to a value lower than the previous minimum pressure; in response, the aquifer sediments are permanently rearranged and the pore volume is reduced (Galloway and others, 1999). Generally, inelastic deformation is indicated by a multi-year trend of decline in the elevation of the land surface and does not correlate with water level recovery.

The GPS stations used for the study, shown in figure 2, were Cuyama Valley High School (CUHS), Ventucopa Station (VCST), McPherson_CS2008 (P521), Bitter Creek Wildlife Refuge (BCWR), and OZST_SCGN_CS2000 (OZST). GPS stations within the Cuyama Valley study area are maintained by the USGS, and the data are available online at *http://earthquake.usgs.gov/monitoring/gps/* (accessed July 12, 2012). Post-processing of data collected from the GPS network stations can include cleaning, filtering, and de-trending for each position component (north, east, and up for a local Cartesian coordinate system). The data were cleaned to remove outliers that deviate significantly relative

to an average position measurement, filtered to remove systemic errors that increase the signal noise, and de-trended to remove the regional tectonic signal (N. King, oral commun., 2012). Regionally, filtered data were the most appropriate for comparison with estimates of subsidence from InSAR (see next section, "InSAR Data").

Comparison of the annual velocity in the north and east directions for all GPS stations in the Cuyama study area indicated the land surface is moving northwest at an average rate of almost 36 millimeters per year (mm/yr; table 14). The stations in the valley (CUHS, VCST, and OZST) are moving northwest at nearly the same velocity (about 25 mm/yr). P521, in the mountains to the west of the basin, is moving at a slightly faster velocity (about 29 mm/yr) toward the northwest direction; BWCR, in the hills to the east of the basin, is moving at a slightly slower velocity (about 22 mm/yr) toward the northwest. This indicates that there is movement consistent with the San Andreas fault system, with regional compression still occurring around this "pull-apart" basin.

The annual velocity in the up direction for all GPS monitoring stations was positive, with the exception of CUHS, indicating a general net upward motion for the land surface in the region. The annual velocity at VCST, OZST, and BCWR was 0.7 mm/yr (table 14), indicating the valley is moving upward at the same rate as the area to the east and slightly slower than the mountains to the west (annual velocity at P521 was 1.3 mm/yr). The annual velocity at CUHS is −7.5 mm/yr, indicating significant downward motion at this location relative to the region. The daily land surface position in the up coordinate for CUHS (raw data from the USGS Earthquakes Hazard Program) showed a downward trend over the period of record and cyclic variability over shorter periods (fig. 26). The measured displacement at CUHS between December 5, 2002, and May 22, 2008, was −40 mm. It is likely that this downward trend, or subsidence, represents inelastic deformation and indicates compaction and reduced storage capacity of the aquifer sediments; a significant component of the seasonal fluctuations represented elastic deformation, as evidenced by various periods of partial recovery.

The cyclic variability in the daily land surface position in the north, east, and up directions for CUHS also indicated the aquifer sediments in the area had experienced elastic deformation. The variability in the north and east directions of the de-trended data correlated with the variability in the up direction (fig. 27). As noted by Bawden and others (2001), elastic deformation in a basin will result in horizontal motion near the edge of the basin as the surface is pulled inward toward the center of subsidence and pushed outward during expansion. Cyclic deformation at CUHS in the north and east direction indicated elastic deformation of the aquifer sediments. The cyclic variation in the position of the land surface at CUHS also correlated with water-level measurements in nearby wells, which supports the conclusion that elastic deformation was caused by groundwater withdrawals. Water levels at well CUY-57 from 2000 to 2008 followed the de-trended up data; higher water levels occurred close in time to surface expansion, and lower water levels occurred close in time to surface compression (fig. 27). In 2011, motion in all directions increased substantially and corresponded to compression of the aquifer sediments (fig. 27). Likewise, in 2011, water levels from CUY-05 and CUY-58 sharply declined, and the surface compressed at the highest rate during the period of record (fig. 27).

InSAR Data

Interferometric synthetic aperture radar (InSAR) is a satellite-based remote sensing technique that can detect centimeter-level land-surface deformation over hundreds of square kilometers at a spatial resolution (pixel size) of 90 meters or better and a height resolution of 5–10 mm (Bawden and others, 2003). Synthetic aperture radar (SAR) imagery is produced by reflecting radar signals off a target area and measuring the two-way travel time to the satellite. SAR imagery has two components: amplitude and phase. The amplitude is the measure of the RADAR signal intensity returned to the satellite and shows roads, mountains, and other features because of their varying reflective properties. The phase component is the percentage of the sine wavelength that intersects the land-surface and is proportional to the line-of-site distance from the land surface to the satellite (range).

There are two forms of interferometric processing: conventional and persistent scatterer (PS InSAR). The conventional InSAR technique uses two SAR scenes of the same area taken at different times and differences the

Table 14. Annual velocities and associated uncertainties for selected GPS monitoring stations in the Cuyama study area, reported from the regionally filtered data from the U.S. Geological Survey Earthquakes Hazard Program for the period of record, Cuyama Valley, Santa Barbara County, California.

[mm/yy; millimeters per year]

GPS monitoring station	P521 (McPherson_CS2008)		CUHS (Cuyama Valley High School)		VCST (Ventucopa Station)		OZST (OZST_SCGN_CS2000)		BCWR (Bitter Creek Wildlife Refuge)	
	Velocity (mm/yr)	Uncertainty (mm/yr)	Velocity (mm/yr)	Uncertainty (mm/yr)	Velocity (mm/yr)	Uncertainty (mm/yr)	Velocity (mm/yr)	Uncertainty (mm/yr)	Velocity (mm/yr)	Uncertainty (mm/yr)
North	29.10	0.50	24.70	0.30	24.50	0.30	24.60	0.30	21.50	0.30
East	–27.40	0.50	–28.00	0.30	–25.10	0.30	–26.80	0.30	–22.00	0.30
Up	1.30	0.50	–7.50	0.30	0.70	0.30	0.70	0.30	0.70	0.30

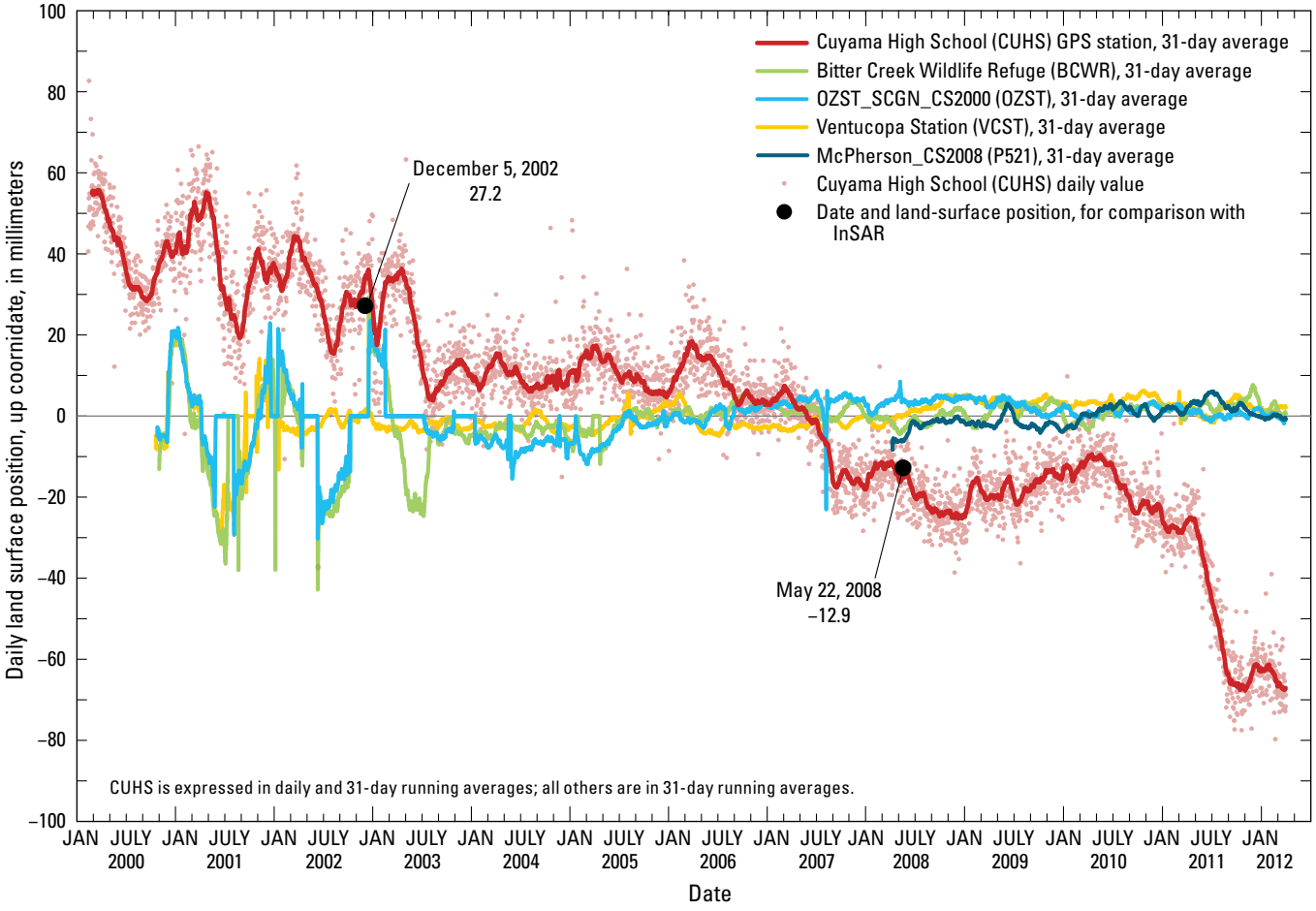

Figure 26. Land-surface position, up coordinate, in millimeters, for the GPS stations Cuyama High School (CUHS), Ventucopa Station (VCST), McPherson_CS2008 (P521), Bitter Creek Wildlife Refuge (BCWR), and OZST_SCGN_CS2000 (OZST), Cuyama Valley, Santa Barbara County, California.

phase portion of the SAR signal, resulting in maps called interferograms that show relative land-surface elevation change (range change) between the two SAR acquisition dates (Sneed and Brandt, 2007). If the land surface has moved away from the satellite (subsidence), a slightly longer portion of the wavelength is reflected back to the satellite. Conversely, if the land surface has moved closer to the satellite (uplift), a slightly shorter portion of the wavelength is reflected back to the satellite. The PS InSAR technique requires many more SAR —usually 20 or more—that are processed together to determine, in part, the amplitude variance across the entire data stack (all of the SAR images) for each pixel. Pixels with relatively high amplitude variance (in time) are filtered from the data set, resulting in a list of relatively "stable" points, or persistent scatterers (PS). The differential phase is then calculated in a manner identical to that of conventional InSAR, except that the differential phase is only calculated for each "stable" point, rather than across the entire image.

InSAR signal quality is dependent on topography, ground cover, land-use practices, atmospheric artifacts, time span of the interferogram, and orbit geometry, among other factors. Areas with high topographic relief can result in blocked radar signal in the line-of-sight (shadows). Densely forested areas are prone to poor signal quality because RADAR cannot effectively penetrate thick vegetation, and it either gets absorbed or reflects back to the satellite from random depths within the canopy, which leads to spatially incoherent signals. Certain land-use practices, such as farming, also cause spatially incoherent signal. The tilling, plowing, or flooding of farm fields causes large and non-uniform land-surface change that affect the amount of RADAR signal reflected back to the satellite and cannot be resolved with InSAR. Urban centers, however, generally have high signal quality because roads and buildings have high reflectivity (amplitude) and remain relatively uniform throughout the InSAR timescale. Non-uniform atmospheric water-vapor, such as clouds or fog, slows the radar signal, causing a phase shift that can lead to inappropriate deformation interpretations. Atmospheric artifacts can be identified by using multiple independent interferogram pairs, or by stacking interferograms.

Stacking interferograms involves adding together several back-to-back shorter term images into a longer term time series for either select points or for the entire image. Long time span interferograms (generally 2 years or more) usually

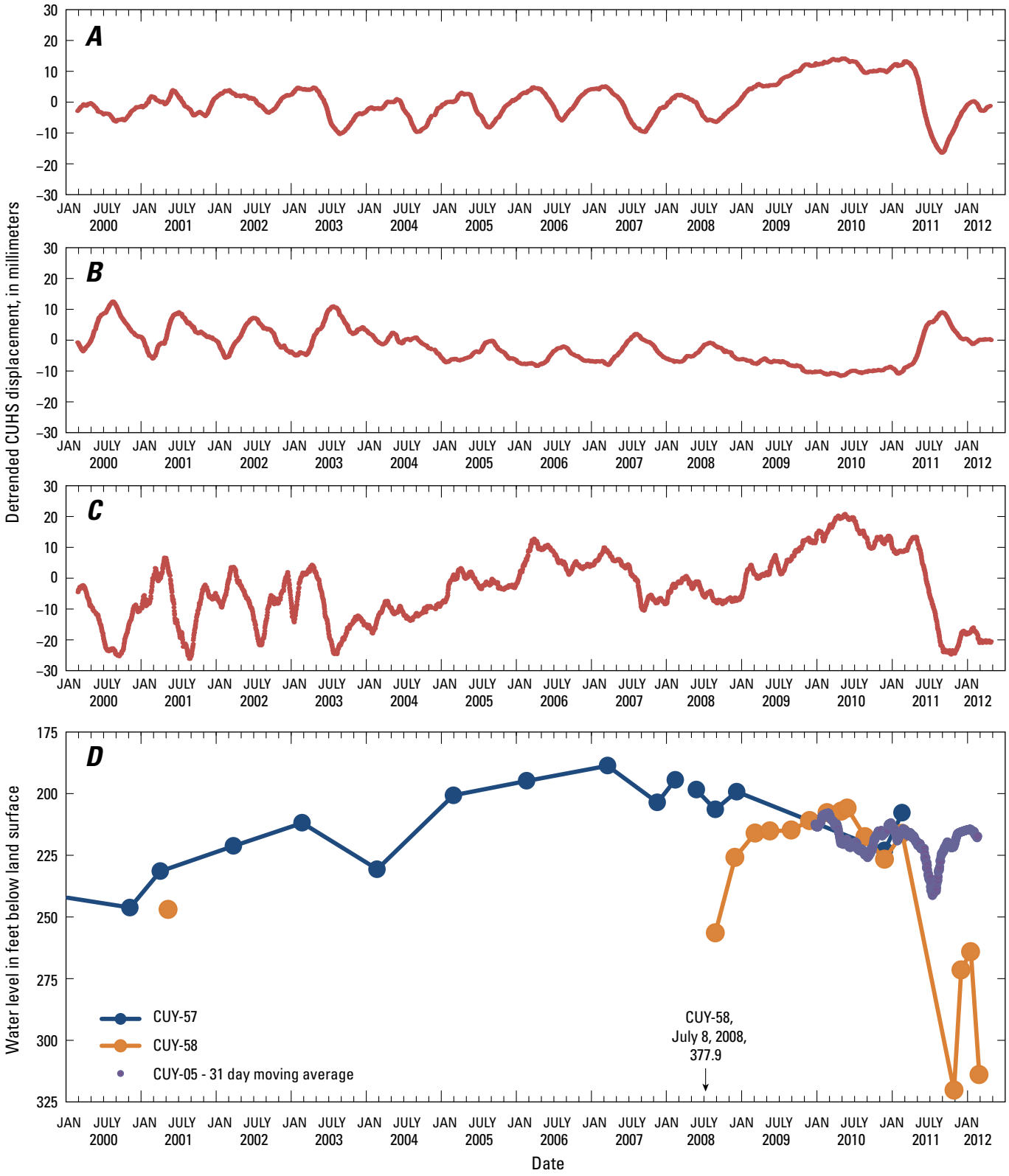

Figure 27. Daily detrended land-surface position, in millimeters, for the GPS station Cuyama High School (CUHS) for the *A*, north; *B*, east; and *C*, up direction; and *D*, water levels in selected wells near CUHS, in feet below land surface, Cuyama Valley, Santa Barbara County, California.

have poor signal quality because more non-uniform change is likely to have occurred in both urban and non-urban areas and are, therefore, generally not used (Sneed and Brandt, 2007). Stacking is very beneficial in reducing these time-dependent errors. The agricultural fields in the study area produce significant random noise across the imagery, which obscures good-quality points. The PS InSAR technique has the inherent ability to account for many of the anthropogenic effects because pixels with relatively high amplitude variance are removed early in the processing. The use of multiple, independent interferograms and stacking were used in the interpretation of both the conventional and PS InSAR imagery to account for atmospheric and time-dependent errors.

Strict orbital control is required to precisely control the look angle and position of the satellite. Successful application of the InSAR technique is contingent on looking at the same point on the land-surface from the same position in space, such that the horizontal distance between each satellite pass, or perpendicular baseline, is minimized. Perpendicular baselines generally greater than about 200 meters (m) usually produce excessive topographic effects (Sneed and Brandt, 2007). The relatively flat topography of the study area, however, allowed some images with perpendicular baselines of up to about 500 m to be successfully interpreted.

Understanding an interferogram image is not intuitive. An interferogram is a map that represents the change in the line-of-site distance between the land-surface and the satellite. This change is manifested as a set of repeating color fringes that indicate the magnitude and direction of deformation. In the case of ENVISAT (C-band), each complete color fringe (for example, purple, blue, cyan, green, yellow, red) represents 28.3 millimeters (mm) of deformation. The progression of colors indicates whether the change is uplift or subsidence. For example, a change resulting in a mound-shaped increase of 85 mm in height would appear as concentric rings alternating in color. Starting from outside the "bulls-eye" and working inward, there would be three complete color fringes; the colors would progress from red to yellow through purple, then the sequence would repeat twice more, indicating about 85 mm of uplift (three fringes times 28.3 mm is equal to 84.9 mm). If the shape were a depression, the color sequence would be reversed. One might think of the different colors as lines of topography, but instead of elevation, the changing colors represent the magnitude and direction of deformation. The more deformation there is, the larger number of color fringes are drawn.

For this study, data from the European Space Agency's (ESA) ENVISAT satellite were acquired through the InSAR and GeoEarthScope data archives. These archives are operated through UNAVCO, a consortium of educational, public, and non-profit institutions whose goal is to use various precision land- and space-based technologies to identify and understand land deformation across the United States. For the period of this study, the side-looking 5.6 centimeter (cm) wavelength satellite orbited the earth at an altitude of approximately 800 kilometer (km) and had a 35-day repeat cycle. Tight orbital control is required in order to precisely control the look angle and position of the satellite, which consumes relatively large quantities of fuel. In October 2010, however, ESA made adjustments to ENVISAT's orbit parameters in an attempt to extend its lifespan by 3 years, primarily by reducing fuel consumption. As a consequence, the satellite look angle is no longer controlled. Although the orbital changes did not affect the functionality of the SAR instruments, the lack of tight orbital control makes interferogram generation using post October 2010 data unlikely.

For this study, 30 SAR images were used to produce a total of 152 interferograms (77 conventional, and 75 PS InSAR), 42 of which (20 conventional, and 22 PS InSAR) were of sufficient quality for interpretation. Both the conventional and PS InSAR techniques were used to produce 19 interferogram pairs; in all, 133 unique interferograms were generated. The 133 interferograms spanned from December 5, 2002, to May 22, 2008, and each represented differences in time ranging from 35 to 665 days. No compatible SAR data were available from June 2008 to September 2010.

Data from the continuous GPS site CUHS (fig. 2) were used to calibrate InSAR interpretations. However, day-to-day GPS height solutions varied by as much as about plus or minus 13 mm likely because of variable atmospheric conditions, random walk noise, and other effects not directly related to land-surface-elevation change (Zerbini and others, 2001; Williams and others, 2004; Langbein, 2008). To minimize this high-frequency variability to allow better correlation of GPS heights to InSAR measurements, a correction was used: the height values for the 15 days prior to and following the observed date were combined into a 31-day running average. The relatively large day-to-day variations in GPS heights were thus minimized, while maintaining a height resolution similar to that of InSAR (within about 5 mm) and the long-term deformation magnitudes evident in the GPS data.

The construction of the InSAR time series involved selecting interferograms on the basis of image quality and the minimization of time gaps and overlaps and combining them to form longer-term time series. Various combinations of 28 of the previously mentioned 42 interferograms were combined into 8 different time series. Each time series contained between 8 and 11 interferograms. Gaps or overlaps were never more than 70 days and were accounted for by using simple linear interpolation (for example, if the subsidence rate before a 35-day gap was 50 mm/yr, and it was 30 mm/yr after the gap, a rate of 40 mm/yr (or approximately 4 mm) was added to the time series for that period). The resultant time series (fig. 28) was the average of these eight individually constructed time series.

Five points were selected from the Cuyama Valley on the basis of geographic distribution and proximity to wells. The resultant InSAR time series (fig. 28*B*) for these five points (fig. 29) showed a total maximum detected subsidence of about 65 mm between December 5, 2002, and May 22, 2008, at point five (which, if constant, would extrapolate to a rate about 12 mm/yr) compared to about 40 mm (about 8 mm/yr) at CUHS

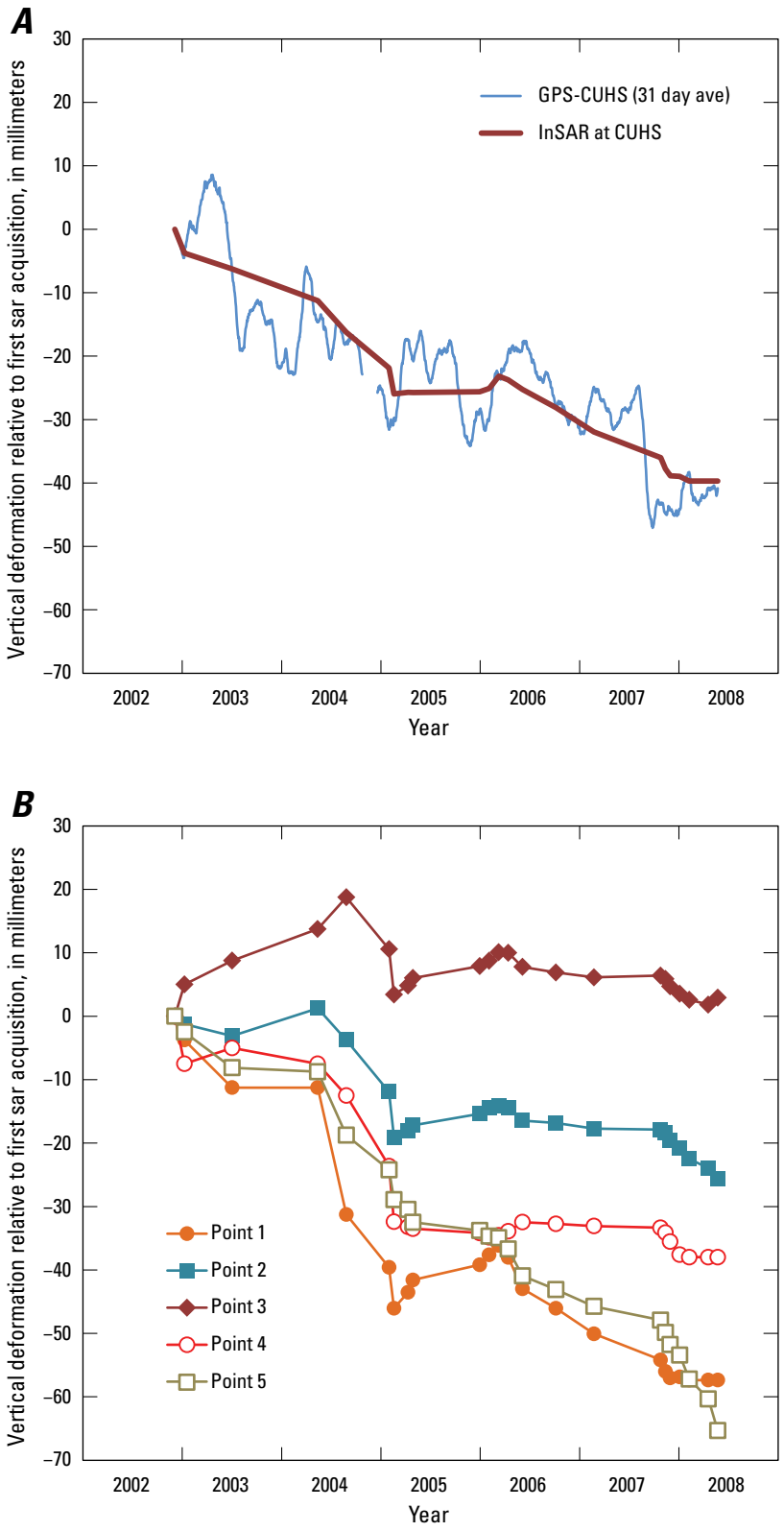

Figure 28. Vertical deformation in Cuyama Valley, Santa Barbara County, California, relative to *A*, first SAR acquisition for the Cuyama High School (CUHS) continuous GPS station; and *B*, selected reference points.

(fig. 28*A*), which is approximately 7 km to the east of point five. An interferogram spanning December 5, 2002–January 9, 2003, that was used in the construction of the averaged time series indicated a local short-term maximum subsidence magnitude of approximately 15 mm near point four. Two interferograms not used in the construction of the long-term time series spanning December 9, 2004–January 13, 2005, and December 29, 2005–February 2, 2006, (fig. 28*B*) indicated a local maximum uplift of approximately 10 mm (about 100 mm/yr) at points one and three, respectively. Interferograms between December 5, 2002, and May 22, 2008, showed the area of primary deformation approximately 3 kilometers to the southeast of the GPS site CUHS. The size and location of this feature appeared to be dependent, in part, on the timespan of the interferogram, which could reflect seasonal variations in pumping (figs. 29 and 30). Interferograms beginning in summer and ending in winter generally showed uplift (fig. 30*B*). Interferograms beginning in winter or spring and ending in summer or fall generally showed subsidence (figs. 29*A*–*B*, 30*A*, 31).

A qualitative analysis of the InSAR imagery, with respect to nearby faulting and oil-field production, was also completed (fig. 31). The primary faults in question were the Morales fault on the northern boundary of Cuyama Valley, the Russell fault to the west, the Rehoboth fault in the central portion of the basin, and the South Cuyama fault on the southern boundary of Cuyama Valley (fig. 31). In a few interferograms, there was an apparent deformation to the north of the range-front Morales fault, but this is more likely attributed to the parallax effect from relatively large perpendicular baselines than true land-surface elevation change because the signal mirrors that of the topography and is not consistent throughout the InSAR time span. The South Cuyama fault on the southern boundary of the basin showed no tendency to create sharp phase-change ramps (lineaments) in interferograms parallel to the fault itself. Both the Morales and South Cuyama faults are thrust faults, with older alluvium and the Morales Formation extending beneath exposed consolidated rocks in the range blocks. It is likely that these faults showed no INSAR response because the basin-fill units were not truncated below the map-view trace of the fault. The Santa Barbara Canyon fault is too far to the south and east of the primary deforming areas to show a fault-related

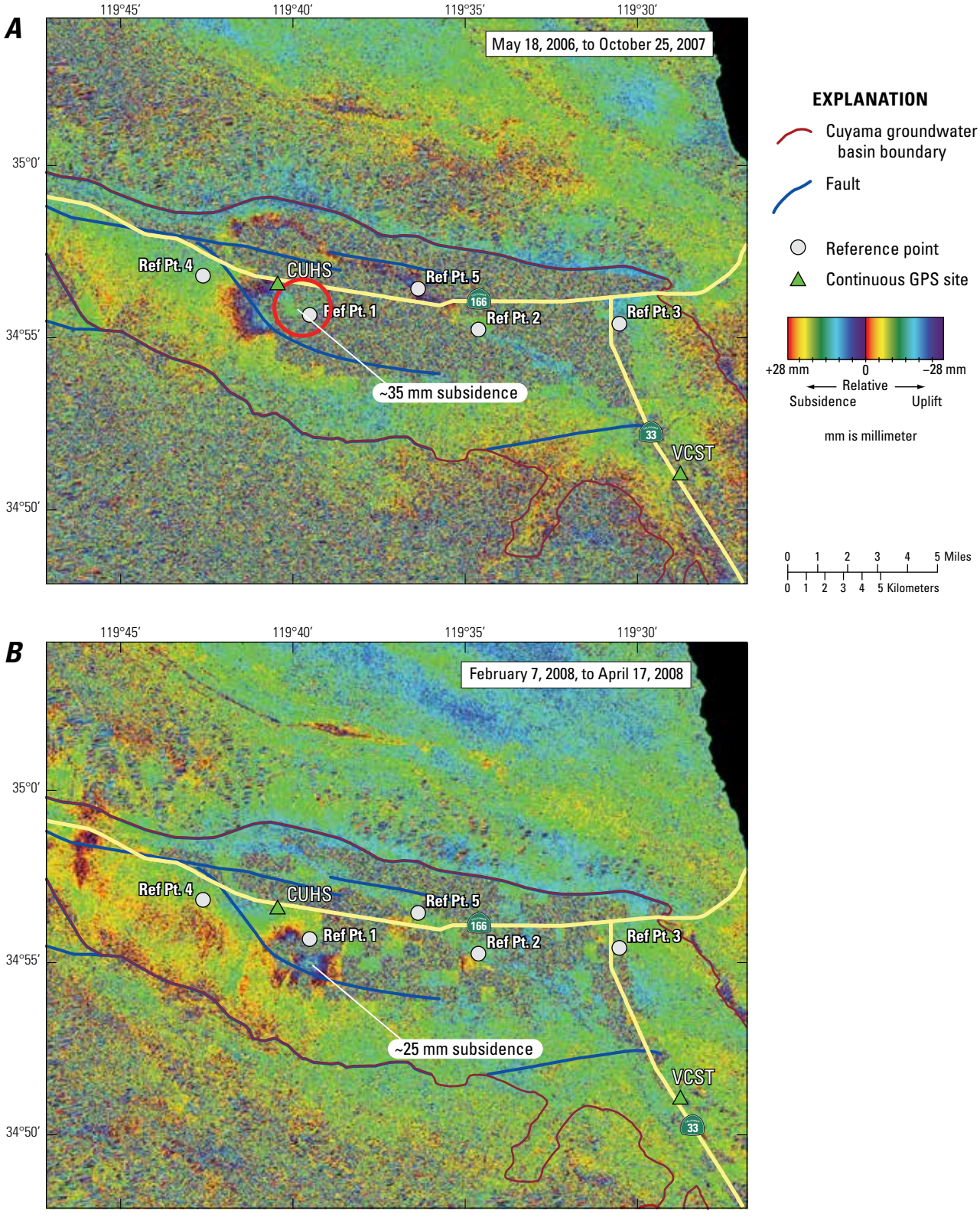

Figure 29. Conventional InSAR interferogram images for Cuyama Valley, Santa Barbara County, California, from *A*, May 18, 2006, to October 25, 2007; and *B*, February 7, 2008, to April 17, 2008.

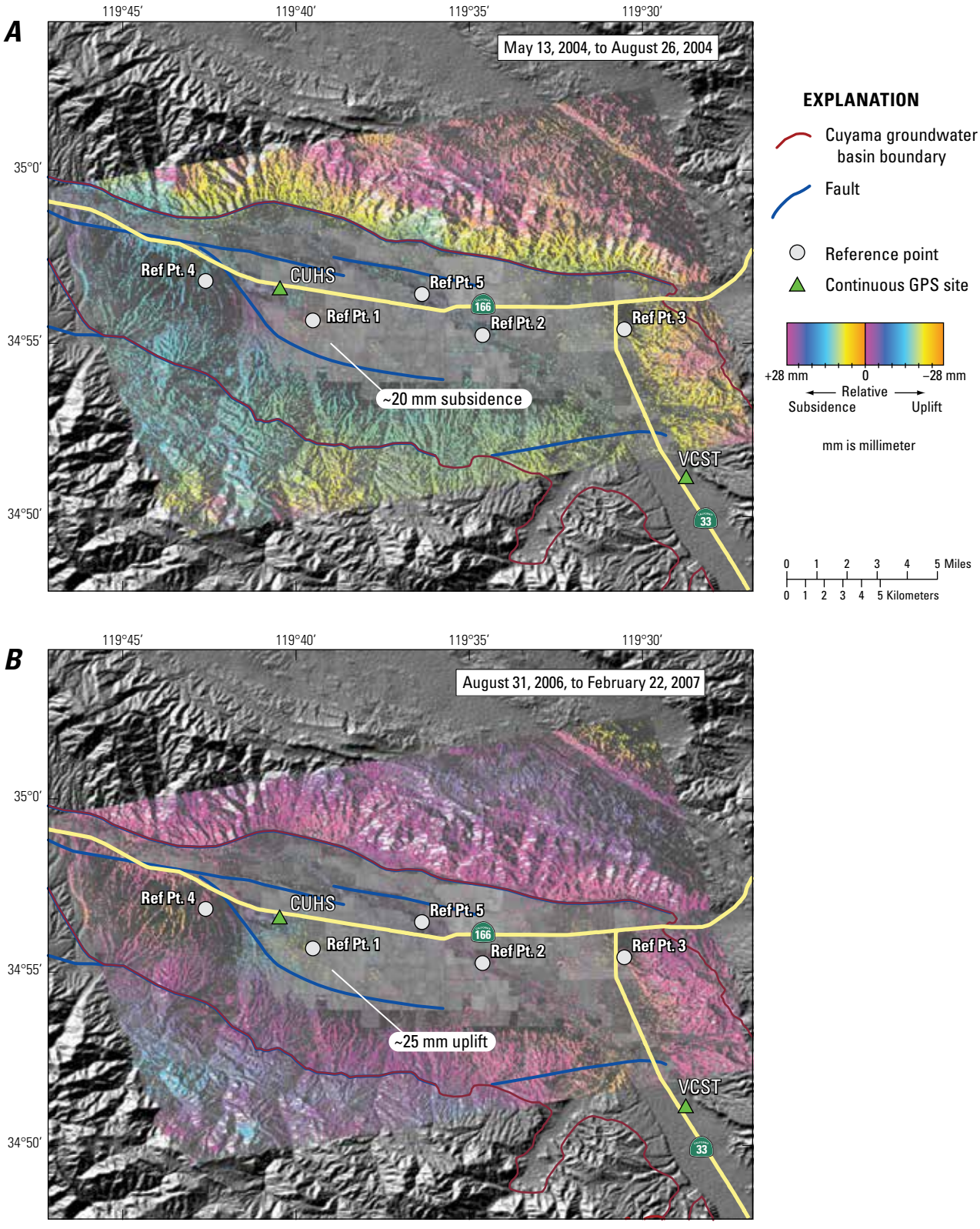

Figure 30. Persistent scatterer InSAR interferogram images for Cuyama Valley, Santa Barbara County, California, from *A*, May 13, 2004, to August 26, 2004; and *B*, August 31, 2006, to February 22, 2007.

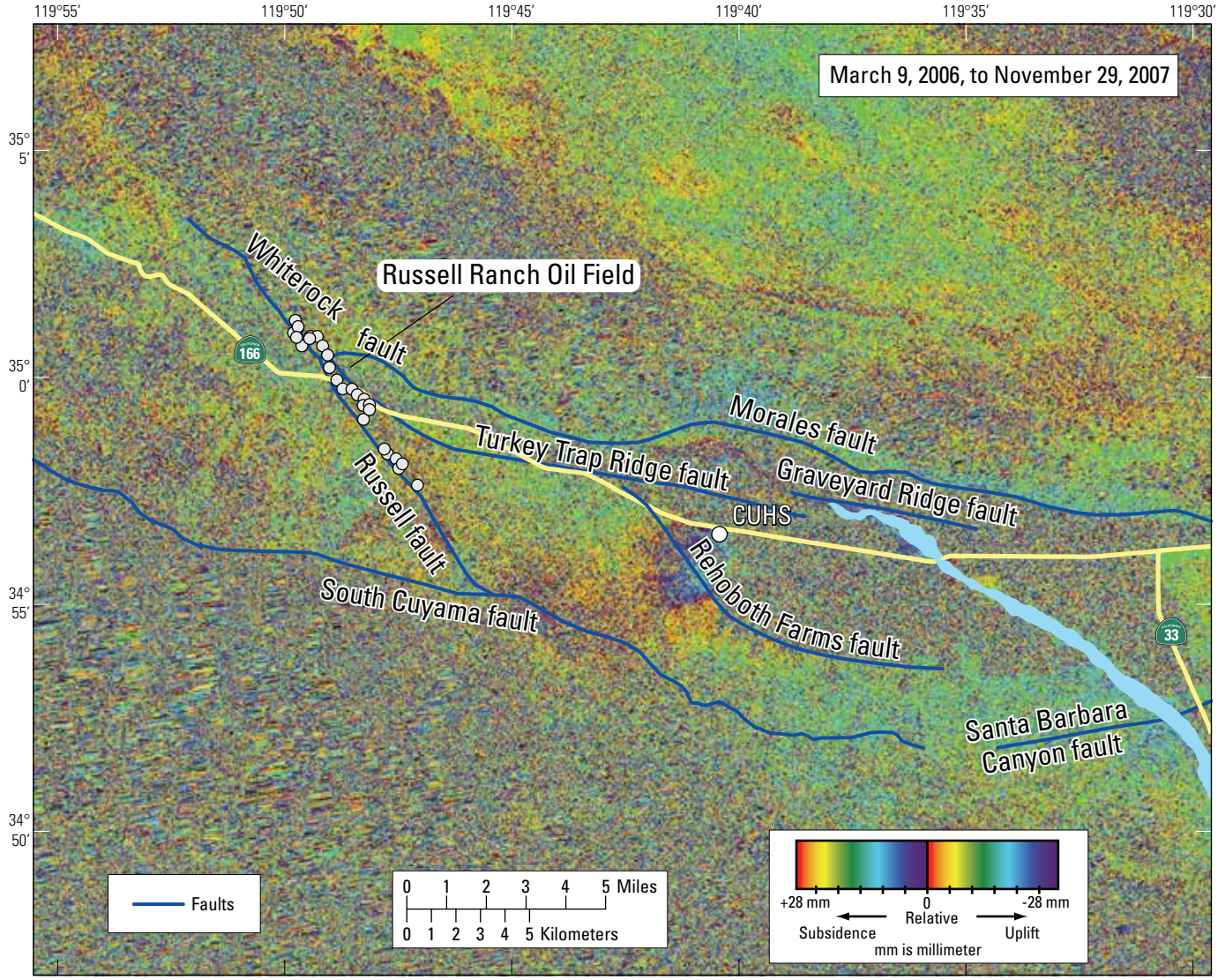

Figure 31. Persistent scatterer InSAR interferogram images for Cuyama Valley, Santa Barbara County, California, from March 9, 2006, to November 29, 2007.

response. The Rehoboth Farms fault trends northwest/southeast and approximately bisects Cuyama Valley. It is apparent from InSAR that this fault is not a significant barrier to groundwater flow because the majority of interferograms showed symmetrical subsidence or uplift on both sides of this fault. The last fault that is of concern in the study area is the Russell fault, which runs roughly parallel to the Russell Ranch oil field. Similar to the other faults, the Russell fault did not appear to be acting as a barrier to groundwater flow. As with the South Cuyama fault, the primary areas of deformation did not typically extend far enough to the west to be truncated by the Russell fault, if it were to act as a groundwater-flow barrier. Subsidence detected by InSAR did not appear to be caused by hydrocarbon extraction from the Russell Ranch oil field because the primary subsidence feature lies 10 kilometers or more to the east of the 8-km long by 1-km wide oil field. Subsidence caused by oil and gas extraction is largely restricted to the area of the oil field itself, as compared to the regional-scale subsidence that is typical of regional groundwater-extraction effects (Coplin and others, 1999).

Summary and Conclusions

To better assess the water resources of the Cuyama Valley groundwater basin, Santa Barbara County, California, geologic, lithologic, geophysical, water-quality, and hydraulic data were collected from three groundwater multiple-well monitoring sites constructed in Cuyama Valley. Additional water-quality and hydraulic data were collected and compiled from 2008 to 2012 from selected domestic and supply wells, springs, and surface-water sites. Geomechanical processes in the Cuyama Valley were also analyzed.

Three multiple-well monitoring sites, CVKR, CVBR, and CVFR, were installed in the study area to test specific conditions related to the geologic and hydrologic system. Data collected from multiple-well monitoring sites wells provided information on vertical differences in geology, water-quality, water levels, and hydraulic properties at the same location; these vertical profiles at multiple locations helped characterize the three-dimensional groundwater system.

Analysis of the generalized lithologic characterization and geophysical logs collected from the monitoring sites indicated the water-bearing units are composed of alternating layers of alluvial fan and stream deposits consisting of unconsolidated to partly consolidated sand, gravel, silt, clay, and occasional cobbles that range from less than 1 foot to more than 20 feet thick. At the CVKR site, the contact of younger and older alluvium is 365 ft bls; the contact of the older alluvium and the Morales Formation is deeper than 1,003 ft bls. At the CVBR site, the contact of recent and older alluvium is 30 ft bls; the contact of the older alluvium and the Morales Formation is 595 ft bls. At the CVFR site, the contact of younger and older alluvium is 75 ft bls; the contact of the older alluvium and the Morales Formation is 560 ft bls. Thus, structure, deposition, and erosion have resulted in considerable variation in the depth and thickness of these units in the valley.

Deviations in temperature-gradient logs indicated that the local geothermal gradient is influenced by the movement of groundwater. Changes in the temperature gradients were used to identify several flow zones at each site. At the CVKR and CVBR sites, flow generally decreased with depth, whereas at the CVFR site, a majority of the flow is in the deeper zones.

Water-quality samples indicated poor water quality, with respect to total dissolved solids and sulfate, throughout the Cuyama Valley, whereas poor water quality with respect to other constituents was less prevalent. Concentrations greater than the USEPA secondary drinking-water standard (SMCL) were observed for total dissolved solids in 97 percent of the samples and for sulfate in 95 percent of the samples. Concentrations greater than the USEPA primary drinking standard (MCL) were observed for nitrate in 13 percent the samples and for arsenic in 12 percent of the samples. Concentrations of total chromium [Cr(T)] were not greater than the MCL-CA of 50 µg/L in any of the samples; however, concentrations of hexavalent chromium [Cr(VI)] greater than the PHG were observed in 95 percent of the samples (the PHG is a non-regulatory threshold, and PHGs are typically orders of magnitude lower than MCLs). Nitrate concentrations decreased with depth at the CVKR site, indicating the source was near surface. Four of the five wells where nitrate levels were greater than the MCL were in the Southern-Main zone in center of the agricultural land-use area. Wells with the lowest nitrate levels were on the edges of the agricultural land-use areas, indicating the source of nitrate was likely from irrigation return flows. Low concentrations of nitrate (NO_3-N), less than 0.02 mg/L, in the surface-water samples indicated that natural surface-water recharge was not a source of high nitrate concentrations.

The isotope data indicated that groundwater does not move freely among the different flow-paths within the older alluvium or the Morales Formations, and that these units could have different sources of recharge. The range in isotope values observed at the different depths at the CVKR, CVBR, and CVBR indicated the water does not readily flow vertically between the water-bearing units. The relation between isotope values and depths also indicated that these units could have different sources of recharge. Variations in isotope values among the three monitoring sites indicated movement of water between different zones also could be restricted. The isotope samples from the four CVBR wells were, in general, lighter in deuterium than the CVKR wells, whereas isotope samples from the four CVFR wells were the heaviest collected in the basin. Comparison of values from other supply wells in the basin also supported restricted lateral flow between zones that could be controlled by the structural compartments of the basin.

Tritium concentrations and carbon activities showed a wide range in groundwater age for the basin. Concentrations of tritium in the samples ranged from 0.9 to 9.0 pCi/L, while time since recharge ranged between 600 and 38,000 years before present. The youngest water was collected in the Southern Ventucopa Uplands, and the oldest water was collected in the Northwestern Sierra Madre Foothills. Tritium concentrations in samples indicated the presence of some recent recharge in the CVKR-3, CVKR-4, and CVBR-3 wells and the absence of modern water in the CVKR-1, CVKR-2, and CVBR-3 wells. Tritium concentrations in samples from all four CVFR indicated a higher percentage of recent recharge. Tritium levels at the CVFR site increased with depth, indicating that the percentage of younger water at depth was most likely caused by local pumping. Estimated carbon-14 ages for the CVKR, CVBR, and CVFR sites ranged from 2,700 to 31,200 years before present. Samples from CVKR-3 and 4, CVBR-3, and CVFR-1, -2, -3, and -4 were all older than 2,700 years before present but also contained detectable levels of tritium, indicating that water from these wells is a mix of differently aged groundwater from different sources.

Arsenic concentrations ranged from less than 0.2 to 71.4 µg/l. The highest concentration sample was collected from a well in the Southern-Main zone that was screened in both the younger and older alluvium. A surface-water sample collected from the Cuyama River contained arsenic concentrations of 0.51 µg/l. Variation in the concentration of

arsenic across zones and formations was observed. Elevated arsenic concentrations were observed in water recharged more than 22,000 years before present, indicating that arsenic concentrations are higher in groundwater that has had more time to mobilize the arsenic.

Water-level data indicated water levels fluctuated seasonally by as much as 80 feet, and water-level differences between aquifers were as great as 40 feet during the peak of the pumping season. Hydrographs showed downward vertical hydraulic gradients during the peak of the pumping season. The water-level hydrographs indicated different water-level changes and relations between aquifers in different parts of the basin. A comparison of the highest level observed each year since January 2008 showed a variation in water-level trends, with some levels declining, some rising, and some reversing. Declines from 6 to over 30 feet were observed in the Southern-Main zone and Central Sierra Madre Foothills. Rises in water levels from less than 1 to about 8 feet were observed the Southern Ventucopa Uplands and Northeast Ventucopa Uplands. Reversal from declining to rising water levels was only observed in the Southern Ventucopa Uplands and indicated that this zone could have the only viable source of recharge (from the Cuyama River) for the Cuyama Valley under the current conditions.

Time-series water-level data showed a seasonal pattern of declining levels coinciding with the peak of the agricultural season and rising water levels when nearby irrigation and related pumping were at a minimum. The pumping of nearby irrigation wells directly influenced water levels in all of the CVKR and CVBR wells. Water-level data from all of the monitoring sites showed a decline in the seasonally high levels over the period of record and showed a vertical hydraulic gradient reversal from upward during the winter months to downward during the irrigation season. Observations at the CVKR site showed water levels in the three deeper wells varied by as much as 60 ft seasonally, while water levels in the shallowest well varied by about 25 ft. Water levels in all wells showed a decline of over 20 ft between 2009 and 2012. Observations at the CVBR site showed water levels in the three deeper wells varied by as much as 90 ft seasonally, while water levels in the shallowest well varied by about 40 ft. Water levels in all wells showed a decline of over 5 ft between 2010 and 2012. Observations at the CVFR site showed water levels in all wells varied by as much as 15 ft seasonally. Water levels in all wells showed a decline of over 20 ft between 2010 and 2012.

Water-level rises and declines observed in the Sierra Madre Foothills zone correlated to the duration of seasonal pumping of the wells. Increased pumping in 2011 resulted in a water-level decline of over 25 ft in 1 year. Changes in the pumping, and possible the recharge, conditions between 2010 and 2011 in Northwestern Sierra Madre Foothills zone can be the difference between static and overdraft conditions. Time-series data from two wells in the Southern Main Zone showed a detailed record of the steady decline in water level. The hydrographs showed the seasonal highs and lows that were expected; however, the year-to-year seasonal high showed a steady decline in water levels of approximately 2.5 and 7 ft per year. Time-series data from two wells showed a rise in water levels in the Southern Ventucopa Uplands zone during the spring of 2012. Observations showed the rise began in late March 2012 and rose over the 25 ft in one well in about 1 month. This marked rise in water level over a short period indicated that this zone responds quickly to periods of increased recharge, possibly from the Cuyama River.

Historic water level data, dating back to the early 1940s, showed long-term trends. Data indicated that nine wells had declining water levels, four wells had relatively static levels, and three wells had rising water levels. All of the wells in the wells in the South-Main zone had declines in water levels over the period of record. The largest decline of 300 ft, averaging 7.25 ft per year, was observed between 1960 and 2001. However, large declines in water levels were not limited to the Southern Main zone. In the Caliente Northern-Main zone, a decline of over 130 feet, for an average decline of 1.7 ft per year, was observed. In the Western Basin zone, a decline of over 80 ft, for an average decline of 1.2 ft per year, was observed. In the Southern Sierra Madre zone, a decline of over 30 ft, for an average decline of 0.9 ft per year, was observed. Declines were not observed in all zones of the basin. Two of the wells in the Southern Ventucopa Uplands zone showed an increase in water levels, while five others showed slow declines followed by a marked rise in water levels—over 100 ft in one case—indicating that this zone responds quickly to periods of increased recharge.

Slug-test data from the monitoring wells indicated that horizontal hydraulic conductivities range from 1.5 to 28 ft/day. The median hydraulic conductivity of 15 ft/day observed for the wells in the older alluvium was almost five times higher than the median hydraulic conductivity of 3.1 ft/day in the Morales formation. Pump-test data from supply wells indicated that transmissivities range from 560 to 163,400 gal/d/ft. The median transmissivity of 15,700 gal/d/ft for the wells in the younger alluvium was three times higher than the median transmissivity of 5,000 gal/d/ft in the older alluvium. Tests were repeated on some wells over a span of several years. Analysis of the results indicated that hydraulic conductivity typically decreased over time. These temporal changes in hydraulic conductivity are likely due to well performance, but also could be influenced by the declines in water levels over time.

Daily discharge data from stream-flow gaging stations in the Cuyama Valley drainage showed the stream flows vary seasonally. Records from the Cuyama River, where it enters and exits the basin, showed a higher flow, averaging between 2 and 200 cubic feet per second (cfs), through most of the winter months, while there was lower flow, below 2 cfs, during the summer months. Summer flow rates in 2011 were greater than in 2010. High flows of almost 900 cfs were observed in January and December of 2010. Changes in water levels in well CUY-35, in the Southern Ventucopa Uplands, correlated with high-flow events, while the extended-flow event

corresponded with the 25-foot increase in water level at this well. In general, surface water flowing into the valley from the Cuyama River was equal to the amount of water flowing out of the valley, indicating that all other sources of inflow to the Cuyama Valley would be sources of recharge. Starting in October 2011, there was a net increase of inflow into the valley along the Cuyama River compared to the outflow, indicating that surface water was recharging the groundwater system.

Data collected from continuously operating GPS stations indicated that the Cuyama study area is slowly moving northwest. Stations in the mountains to the west of the valley, in the hills to the east of the valley, and in the Southern Ventucopa uplands showed a net upward motion for the land surface in the region. The CUHS, in the Southern-Main zone showed an annual velocity of −7.5 mm/yr (downward), indicating significant downward motion at this location relative to the region. The cyclic variability in the daily land-surface position in the lateral and vertical directions for CUHS indicated the aquifer sediments in the area had experienced elastic deformation. However, a longer-term downward trend likely represents inelastic deformation and indicates reduced storage capacity in the aquifer sediments. In 2011, motion in all the directions increased substantially and corresponded to compression of the aquifer sediments. The cyclic variation in the position of the land surface at CUHS also correlated with water-level measurements in nearby wells, which supports the conclusion that elastic deformation was caused by groundwater withdrawals.

InSAR data showed local and regional changes that appeared to be dependent, in part, on both the time span of the interferogram, seasonal variations in pumping, and geological uplift. Long-term InSAR time series showed a total detected subsidence rate of approximately 12 mm per year at one location, while short InSAR time series showed uplift of approximately 10 mm per year at several locations. The resultant InSAR time series for five selected points showed a total maximum detected subsidence of about 40 mm (about 8 mm/yr) at CUHS. Interferograms showed that a local maximum deformation bowl typically forms approximately 3 kilometers to the southeast of the CUHS GPS site. The size and location of this feature appear to be dependent, in part, on both the timespan of the interferogram and seasonal variations in pumping. A qualitative analysis of the InSAR imagery with respect to nearby faulting production showed the Rehoboth Farms fault trend is not a significant barrier to groundwater flow because the majority of interferograms showed symmetrical subsidence or uplift on both sides of this fault. A qualitative analysis with respect to the local Russell Ranch oil field, which runs roughly parallel to the Russell fault, indicated that subsidence did not appear to be caused by hydrocarbon extraction and that the fault did not appear to be a contributing barrier to groundwater flow.

References Cited

Ball, J.W., and McCleskey, R.B., 2003a, A new cation-exchange method for accurate field speciation of hexavalent chromium: U.S. Geological Survey Water-Resources Investigations Report 03–4018, 17 p.

Ball, J.W., and McCleskey, R.B., 2003b, A new cation-exchange method for accurate field speciation of hexavalent chromium: Talanta, v. 61, p. 305–313.

Bawden, G.W., Sneed M., Stork S.V., and Galloway D.L., 2003, Measuring Human Induced Land Subsidence from Space: U.S. Geological Survey Fact Sheet 069–03, 4 p.

Bawden, G.W., Thatcher, W., Stein, R.S., Hudnut, K.W., and Peltzer, G., 2001, Tectonic contraction across Los Angeles after removal of groundwater pumping effects: Nature, v. 412, p. 812–815.

Bear, Jacob, 1979, Hydraulics of Groundwater: New York, McGraw-Hill, 569 p.

Bouwer, Herman and Rice, R.C., 1976, A slug test for determining hydraulic conductivity of unconfined aquifers with completely or partially penetrating wells: Water Resources Research v. 12 no. 3, p.423–428.

Butler, J.J., Jr., Garnett, E.J., and Healey,J.M., 2003, Analysis of slug tests in formations of high hydraulic conductivity: Ground Water, v. 41, no. 5, p. 620–630.

California Department of Public Health, 2012a, California drinking water-related laws—Drinking water-related regulations, Title 22: California Department of Public Health, accessed February 28, 2013, at *http://www.CDPH.ca.gov/certlic/drinkingwater/Pages/Lawbook.aspx*.

California Department of Public Health, 2012b, Drinking water notification levels—Notification levels: California Department of Public Health, accessed February 28, 2013, at *http://www.CDPH.ca.gov/certlic/drinkingwater/Pages/NotificationLevels.aspx*.

California Department of Water Resources—Southern District, 1998, Evaluation of Groundwater Overdraft in the Southern Central Coast Region, Technical Information Record SD-98-1.

California Department of Water Resources, 2003, California's Groundwater: Bulletin 118 Update 2003. Chapter 6: Basic Groundwater Concepts. Retrieved May 1, 2012, from *http://www.water.ca.gov/pubs/groundwater/bulletin_118/california%27s_groundwater__bulletin_118_-_update_2003_/bulletin118-chapter6.pdf.*

Clark, I.D., and Fritz, P., 1997, Environmental isotopes in hydrogeology: Boca Raton, Fla., CRC Press LLC, 328 p.

Coplen, T.B., 1994, Reporting of stable hydrogen, carbon, and oxygen isotopic abundances: Pure and Applied Chemistry, v. 66, p. 273–276.

Coplen, T.B., Wildman, J.D., and Chen, J., 1991, Improvements in the gaseous hydrogen-water equilibration technique for hydrogen isotope ratio analysis: Analytical Chemistry, v. 63, p. 910–912.

Coplin, L.S., and Galloway, D.L., 1999, Houston-Galveston, Texas—Managing coastal subsidence, in Land subsidence in the United States: U.S. Geological Survey Circular 1182, p. 35–48.

Craig, H., 1961, Isotopic variations in meteoric waters: Science, v. 133, p. 1702–1703.

Davis, T.L., Lagoe, M.B., Bazeley, W.J.M., Gordon, Stuart, Mcintosh, Kirk, and Namson, J.S., 1988, Structure of the Cuyama Valley, Caliente Range, and Carrizo Plain and its significance to the structural style of the southern Coast Ranges and western Transverse Ranges, in Bazeley, W.J.M., ed., Tertiary Tectonics and Sedimentation in the Cuyama Basin, San Louis Obispo, Santa Barbara, and Ventura Counties, California: Society of Economic Paleontologists and Mineralogists, Pacific Section, v. 59, p. 159–161.

DeLong, S.B., Pelletier, J.D., and Arnold, L.J., 2008, Climate change triggered sedimentation and progressive tectonic uplift in a coupled piedmont-axial system: Cuyama Valley, California, USA: Earth Surface Processes and Landforms, v. 33, no. 7, p. 1033–1046.

Dibblee, T.W., Jr., 1973, Regional geologic map of San Andreas and related faults in Carrizo Plain, Temblor, Caliente, and La Panza Ranges and vicinity, California: U.S. Geological Survey Miscellaneous Investigations Series Map I-757, scale 1:125,000.

Dibblee, T.W., Jr., 1982, Geology of the Alamo Mountain, Frazier Mountain, Lockwood Valley, Mount Pinos, and Cuyama badlands areas, southern California, in Fife, D.L., and Minch, J.A., eds., Geology and mineral wealth of the California Transverse Ranges (Mason Hill volume): Santa Ana, California, South Coast Geological Society, p. 57–77.

Dibblee, T.W., Jr., and Minch, J.A., ed., 2005, Geologic map of the New Cuyama quadrangle, San Luis Obispo and Santa Barbara Counties, California: Thomas W. Dibblee, Jr. Geological Foundation Map DF–179, scale 1:24,000.

Dibblee, T.W., Jr., and Minch, J.A., ed., 2006, Geologic map of the Cuyama Peak quadrangle, Santa Barbara and Ventura Counties, California: Thomas W. Dibblee, Jr. Geological Foundation Map DF–202, scale 1:24,000.

Dibblee, T.W., Jr., and Minch, J.A., ed., 2007, Geologic map of the Fox Mountain quadrangle, Santa Barbara County, California: Thomas W. Dibblee, Jr. Geological Foundation Map DF–260 , scale 1:24,000.

Ellis, B.J., 1994, Changing Tectonic Regimes in the Southern Salinian Block: Extension, Strike-Slip Faulting, Compression and Rotation in the Cuyama Valley, California: Corvallis, Oregon State University, Ph.D. dissertation, 141 p., 31 figs.

Ellis, B.J., Levi, Shaul, and Yeats, R.S., 1993, Magnetic stratigraphy of the Morales formation: Late Neogene clockwise rotation and compression in the Cuyama Basin, California Coast Ranges: Tectonics, v. 12, p. 1170–1179.

Fishman, M.J., 1993, Methods of analysis by the U.S. Geological Survey National Water Quality Laboratory—Determination of inorganic and organic constituents in water and fluvial sediments: U.S. Geological Survey Open-File Report 93–125, 217 p.

Fishman, M.J., and Friedman, L.C., 1989, Methods for determination of inorganic substances in water and fluvial sediments: U.S. Geological Survey Techniques of Water-Resources Investigations, book 5, chap. A1, 545 p.

Folk, R.L., 1954, The distinction between grain size and mineral composition in sedimentary-rocks: Journal of Geology, v. 62, no. 4, p. 344–359.

Galloway, D.L., Jones, D.R., and Ingebritsen, S.E., 1999, Land subsidence in the United States: U.S. Geological Survey Circular 1182, 175 p. *http://pubs.usgs.gov/circ/circ1182/*, accessed March 22, 2012

Garbarino, J.R., 1999, Methods of analysis by the U.S. Geological Survey National Water Quality Laboratory—Determination of dissolved arsenic, boron, lithium, selenium, strontium, thallium, and vanadium using inductively coupled plasma-mass spectrometry: U.S. Geological Survey Open-File Report 99–093, 31 p.

Garbarino, J.R., Kanagy, L.K., and Cree, M.E., 2006, Determination of elements in natural-water, biota, sediment and soil samples using collision/reaction cell inductively coupled plasma-mass spectrometry: U.S. Geological Survey Techniques and Methods, book 5, sec. B, chap.1, 88

Godwin, H, 1962, Half-life of radiocarbon: Nature ,v.195, p. 984.

Gonfiantini, R., 1978, Standards for stable isotope measurements in natural compounds: Nature, v. 271, p. 534–536.

Gonfiantini, R., 1984, Advisory group meeting on stable isotope reference samples for geochemical and hydrological investigations, Vienna, September 19–21, 1983: International Atomic Energy Agency, Vienna, 77 p.

Graham, S.E., Mahony, T.M., Blissenbach, J.L., Mariant, J.J., and Wentworth, C.M., 1999, Regional geologic map of San Andreas and related faults in Carrizo Plain, Temblor, Caliente and La Panza Ranges and vicinity, California—A digital database: U.S. Geological Survey Open-File Report 99–14, scale 1:125,000.

Greene, E.A. and Shapiro, A.M., 1998, AIRSLUG: A FORTRAN program for the computation of type curves to estimate transmissivity and storativity of prematurely terminated air-pressurized slug tests: Ground Water, v. 36, no.2, p. 373–376.

Halford, K. J., and Kuniansky, Eve L., 2002, Documentation of Spreadsheets for the Analysis of Aquifer-Test and Slug-Test Data: U.S. Geological Survey Open-File Report 02–197, 54 p.

Hem, J.D., 1992, Study and interpretation of the chemical characteristics of natural water, third edition: U.S. Geological Survey Water Supply Paper 2254, 264 p.

Hill, M.L., Carlson, S.A., and Dibblee, T.W., Jr., 1958, Stratigraphy of Cuyama Valley–Caliente Range area, California: American Association of Petroleum Geologists Bulletin, v. 42, no. 12, p. 2,973–3,000.

Hudnut, K. W., Bock, Y., Galetzka, J.E., Webb, F.H., and Young, W.H., 2002, The Southern California Integrated GPS Network (SCIGN), in Seismotectonics in Convergent Plate Boundary, edited by Y. Fujinawa and A. Yoshida: Toyko, Terra Scientific Publishing Company, p. 167–189. Ingebritsen, S.E., and Sanford, W.E., 1998, Groundwater in geologic processes: New York, New York, Cambridge University Press, 341 p.

Izbicki, J. A. and Michel, R. L., 2003, Movement and Age of Ground Water in the Western Part of the Mojave Desert, Southern California, USA: U.S. Geological Survey Water-Resources Investigations Report 03–4314, 35 p.

Jacob, C. E., 1946, Drawdown test to determine effective radius of artesian well: American Society of Civil Engineers Proceedings, v. 72, May.

Kayen, R.E., Edwards, B.D., and Lee, H.J., 1999, Nondestructive laboratory measurement of geotechnical and geoacoustic properties through intact core-liner, in Nondestructive and Automated Testing for Soil and Rock Properties, 1999: West Conshohocken, Pa., American Society for Testing and Materials, STP 1350, p. 83–94.

Kellogg, K.S., Minor, S.A., and Cossette, P.M., 2008, Geologic Map of the Eastern Three-Quarters of the Cuyama 30’ x 60’ Quadrangle, California: U.S. Geological Survey Scientific Investigations Map 3002, scale 1:100,000, 2 plates, 1 pamphlet, 23 p.

Keys, W.S., and MacCary, L.M., 1983, Application of borehole geophysics to water-resources investigations: U.S. Geological SurveyTechniques of Water-Resources Investigations, book 2, chap. E1, 126 p.

Lagoe, M.B., 1987, Middle Cenozoic basin development, Cuyama Basin, California, in Ingersoll, R.V. and Ernst, W.G., eds., Cenozoic basin development of coastal California, Rubey Volume VI : Englewood Cliffs, New Jersey, Prentice-Hall, p. 172–206.

Langbein, John, 2008, Noise in GPS displacement measurements from Southern California and Southern Nevada: Journal of Geophysical Research, v. 113, B05405, 12 p.

McCleskey, R.B., Nordstrom, D.K., and Ball, J.W., 2003, Metal interferences and their removal prior to the determination of As(T) and As(III) in acid mine waters by hydride generation atomic absorption spectrometry: U.S. Geological Survey Water-Resources Investigations Report 03–4117, 14 p. Available at *http://pubs.usgs.gov/wri/wri03-4117/WRI034117.pdf*

McNeill, J.D., 1986, Geonics EM39 borehole conductivity meter-theory of operation: Mississauga, Ontario, Geonics Ltd., Technical Note 20, 11 p.

Munsell Color, 1994, Munsell soil color charts: Baltimore, Md., Munsell Color, Inc.

National Research Council, 1947, Report of the Subcommittee on Sediment Terminology: American Geophysical Union Transactions, v. 28, no. 6, p. 936–938.

Ostlund, H.G., Craig, H., Broecker, W.S., and Spencer, D., 1987, Geosecs Atlantic, Pacific, and Indian Ocean Expeditions, Shorebased Data and Graphics, v. 7, p. 7–19.

Ostlund, H.G. and Dorsey, H.G., 1977, Rapid electrolytic enrichment and hydrogen gas proportional counting of tritium, in Low-Radioactivity Measurements and Applications: Proceedings of the International Conference on Low-Radioactivity Measurements and Application, October 6–10, 1975, The High Tatras, Czechoslovakia, p. 55–60.

Pacific Gas and Electric Company, 2006, PG&E's Energy Management Solutions for Pumps & Pumping Systems: C-0492 ver. September 2006, 2p.

Piper, A.M., 1944, A graphic procedure in the geochemical interpretation of water analyses: American Geophysical Union Transactions, v. 25, p. 914–923.

Plummer, L.N., Michel, R.L., Thurman, E.M., and Glynn, P.D., 1993, Environmental tracers for age dating young ground water, in Alley, W.M., ed., Regional ground-water quality: New York, Van Nostrand Reinhold, p. 255–294.

Roscoe Moss Company, 1990, Handbook of Groundwater Development, Wiley-Interscience, p. 493.

Santa Barbara County Planning and Development Department, 1994, Santa Barbara County Comprehensive Plan, 77 p.

Schlumberger, 1972, Log interpretation, volume I—principles: New York, Schlumberger Limited, 113 p.

Schwing, H.F., 1984, Subsurface geology of the South Cuyama oil field and adjacent areas, southern Coast Ranges, California: Corvallis, Oregon State University, M.S. thesis, 81 p., 19 pls., 10 figs.

Singer, J.A., and Swarzenski, W.V., 1970, Pumpage and ground-water storage depletion in Cuyama Valley California, 1947–66: U.S. Geological Survey Open-Rile Report 70–304, 24 p.

Spitz, H.M., 1986, Subsurface Geology of the southeastern Cuyama Valley, southern Coast Ranges, California: Corvallis, Oregon State University, M.S. thesis, 88 p., 20 pls., 12 figs.

Sneed, Michelle., Brandt, J.T., 2007, Detection and measurement of land subsidence using global positioning system surveying and interferometric synthetic aperture radar, Coachella Valley, California, 1996–2005: U.S. Geological Survey Scientific Investigations Report 2007–5251, 31 p.

Stookey, L.L., 1970, FerroZine—A new spectrophotometric reagent for iron: Analytical Chemistry, v. 42, p. 779–781.

Stuiver, M., and Polach, H.A., 1977, Reporting of 14C data: Radiocarbon, v. 19, p. 355–363.

Struzeski, T.M., DeGiacomo, W.J., and Zayhowski, E.J., 1996, Methods of analysis by the U.S. Geological Survey National Water Quality Laboratory— Determination of dissolved aluminum and boron in water by inductively coupled plasma-atomic emission spectrometry: U.S. Geological Survey Open-File Report 96–149, 17 p.

Sweetkind, D.S., Faunt, C.C., and Hanson, R.T., 2013, Construction of 3-D geologic framework and textural models for Cuyama Valley groundwater basin, California: U.S. Geological Survey Scientific Investigations Series Report 2013-5127, 46 p.

Upson, J.E. and Worts, G.F., Jr, 1951, Groundwater in the Cuyama Valley California: US Geological Survey Water-Supply Paper 1110-B, 81 p., 1 plate.

U.S. Environmental Protection Agency, 2012a, National Primary Drinking Water Regulations, accessed April 1, 2012, at *http://water.epa.gov/drink/contaminants/index.cfm*

U.S. Environmental Protection Agency, 2012b, Drinking water contaminants, accessed April 1, 2012, at *http://www.epa.gov/safewater/contaminants/index.html*

U.S. Geological Survey Earthquakes Hazards Program, 2012, About GPS: accessed May 2012 at *http://earthquake.usgs.gov/monitoring/gps/about.php*

U.S. Geological Survey, variously dated, National field manual for the collection of water-quality data: U.S. Geological Survey Techniques of Water-Resources Investigations, book 9, chap. A1–A9, accessed January 17, 2013, at *http://water.usgs.gov/owq/FieldManual/*

Vedder, J.G., 1968, Geologic map of the Fox Mountain quadrangle, Santa Barbara County, California: U.S. Geological Survey Miscellaneous Investigations Map I-547, scale 1:24,000.

Vedder, J.G., and Repenning, C.A., 1975, Geologic map of the Cuyama and New Cuyama quadrangles, San Luis Obispo and Santa Barbara Counties, California: U.S. Geological Survey Miscellaneous Investigations Map I–876, scale 1:24,000.

Wigley, T.M.L., and Muller, A.B., 1981, Fractionation corrections in radiocarbon dating: Radiocarbon, v. 23, p. 173–190.

Williams, J.H., Lapham, W.W., and Barringer, T.H., 1993, Application of electromagnetic logging to contamination investigations in glacial sand-and-gravel aquifers: Groundwater Monitoring Review, v. 13, no. 3, p. 129–138.

Williams, S.D.P., Bock, Yehuda, Fang, Peng, Jamason, Paul, Nikolaidis, R.M., Prawirodirdjo, Linette, Miller, Meghan, and Johnson, D.J., 2004, Error analysis of continuous GPS position time series: Journal of Geophysical Research, v. 109, B03412, 19 p.

Yeats, R.S., Calhoun, J.A., Nevins, B.B., Schwing, H.F., and Spitz, H. M., 1989, Russell Fault; early strike-slip fault of California Coast Ranges: American Association of Petroleum Geologists Bulletin, v. 73, p. 1089–1102.

Zerbini, Susanna, Richter, Bernd, Negusisi, Monia, Romagnoli, Claudia, Simon, Dietrich, Domenichini, Francesco, and Schwahn, Wolfgang, 2001, Height and gravity variations by continuous GPS, gravity and environmental parameter observations in the southern Po Plain, near Bologna, Italy: Earth and Planetary Science Letters, v. 192, no. 3, p. 267–279.

Prepared by the Sacramento Publishing Service Center.

For more information concerning this report, contact:

Director
U.S. Geological Survey
California Water Science Center
6000 J Street, Placer Hall
Sacramento, CA 95819
dc_ca@usgs.gov

or visit our Web site at:
http://ca.water.usgs.gov